The Messenger

No. 182 | 2021

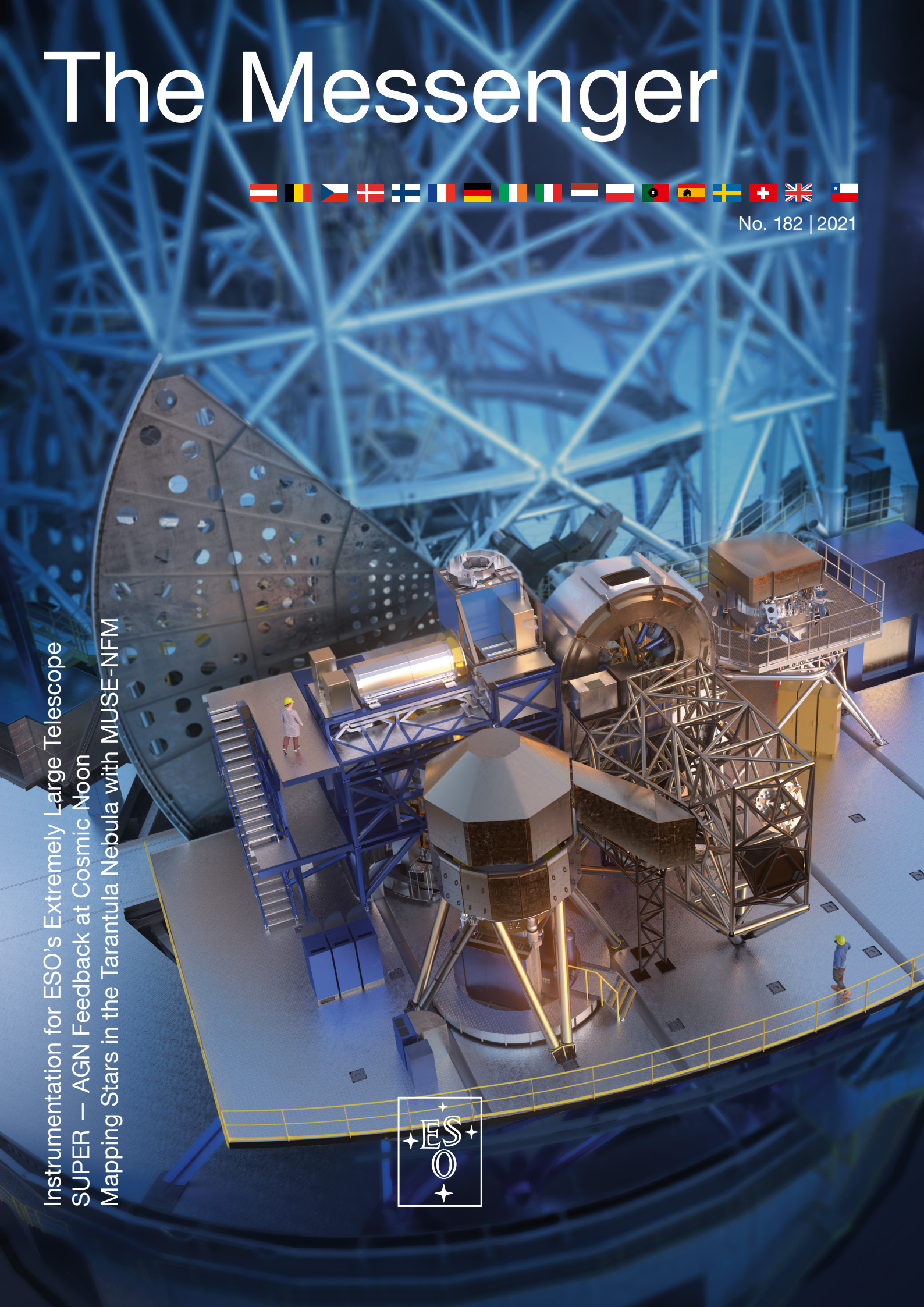

Instrumentation for ESO's Extremely Large Telescope
SUPER — AGN Feedback at Cosmic Noon
Mapping Stars in the Tarantula Nebula with MUSE-NFM

ESO, the European Southern Observatory, is the foremost intergovernmental astronomy organisation in Europe. It is supported by 16 Member States: Austria, Belgium, the Czech Republic, Denmark, France, Finland, Germany, Ireland, Italy, the Netherlands, Poland, Portugal, Spain, Sweden, Switzerland and the United Kingdom, along with the host country of Chile and with Australia as a Strategic Partner. ESO's programme is focused on the design, construction and operation of powerful ground-based observing facilities. ESO operates three observatories in Chile: at La Silla, at Paranal, site of the Very Large Telescope, and at Llano de Chajnantor. ESO is the European partner in the Atacama Large Millimeter/submillimeter Array (ALMA). Currently ESO is engaged in the construction of the Extremely Large Telescope.

The Messenger is published, in hardcopy and electronic form, four times a year. ESO produces and distributes a wide variety of media connected to its activities. For further information, including postal subscription to The Messenger, contact the ESO Department of Communication at:

ESO Headquarters
Karl-Schwarzschild-Straße 2
85748 Garching bei München, Germany
Phone +498932006-0
information@eso.org

The Messenger
Editors: Mariya Lyubenova, Gaitee A. J. Hussain
Editorial assistant: Isolde Kreutle
Copy-editing: Peter Grimley
Layout, Typesetting, Graphics: Lorenzo Benassi
Graphics: Mafalda Martins
Design, Production: Jutta Boxheimer
www.eso.org/messenger/

Printed by omb2 Print GmbH, Lindberghstraße 17, 80939 Munich, Germany

ISSN 0722-6691

Contents

Front cover: Artist rendering of the instruments HARMONI, MICADO, MAORY and METIS, together with the prefocal station A, sitting on one of the Nasmyth platforms of ESO's Extremely Large Telescope.

DOI: 10.18727/0722-6691/5214

Instrumentation for ESO's Extremely Large Telescope

Suzanne Ramsay[1]
Michele Cirasuolo[1]
Paola Amico[1]
Nagaraja Naidu Bezawada[1]
Patrick Caillier[1]
Frédéric Derie[1]
Reinhold Dorn[1]
Sebastian Egner[1]
Elizabeth George[1]
Frédéric Gonté[1]
Peter Hammersley[1]
Christoph Haupt[1]
Derek Ives[1]
Gerd Jakob[1]
Florian Kerber[1]
Vincenzo Mainieri[1]
Antonio Manescau[1]
Sylvain Oberti[1]
Celine Peroux[1]
Oliver Pfuhl[1]
Ulf Seemann[1]
Ralf Siebenmorgen[1]
Christian Schmid[1]
Joël Vernet[1]
and the ESO ELT Programme
and follow-up team

[1] ESO

Design and construction of the instruments for ESO's Extremely Large Telescope (ELT) began in 2015. We present here a brief overview of the status of the ELT Instrumentation Plan. Dedicated articles on each instrument are presented elsewhere in this volume.

Instruments planned for ESO's ELT

When, in December 2014, the ESO Council gave the green light for the construction of the 39-m Extremely Large Telescope[1] in two phases (de Zeeuw, Tamai & Liske, 2014), this triggered the final preparations to launch the design and construction of the powerful instrument suite for this telescope. The ELT Instrumentation Plan, to provide the instruments to meet the science case for the telescope, had already been defined in consultation with ESO's science community and scientific and technical advisory committees. The instruments were selected following a set of Phase A conceptual design studies that have been described previously (see papers in The Messenger 140, 2010). While ESO is ultimately responsible for delivering the instruments to the scientific community on time and with the expected performance, an important feature of the Instrumentation Plan is that the instruments are being developed in collaboration between ESO and consortia made up of universities and institutes in the Member States and beyond. This model has worked very successfully for the delivery of instruments to the Very Large Telescope (VLT) and is a key aspect of the interaction between ESO as an organisation and the astronomical community. Figure 1 shows a timeline for instrument development as it stands at the time of writing.

A pair of instruments was selected by the ELT Science Working Group to be delivered for first light: the High Angular Resolution Monolithic Optical and Near-infrared Integral field spectrograph (HARMONI) and the Multi-adaptive optics Imaging CamerA for Deep Observations (MICADO), a near-infrared camera. Adaptive optics systems tailored to meet the scientific goals of each of these instruments are also being developed. The HARMONI Consortium is building a laser tomographic adaptive optics (LTAO) module. A multi-conjugate adaptive optics (MCAO) module, the Multi-conjugate Adaptive Optics RelaY (MAORY), is being developed as a facility adaptive optics system with two "clients" — MICADO and a future multi-object spectrograph. Together this first light pair of workhorse instruments will immediately exploit both the enormous collecting area and the superb spatial resolution of the new telescope, enabling a wide range of scientific projects to be executed at first light. The next instrument in the Instrumentation Plan is the Mid-infrared ELT Imager and Spectrograph (METIS), working in the mid-infrared (3–14 μm) with single-conjugate adaptive optics (SCAO). All of these instruments are formally part of ESO's ELT Construction Programme. Agreements for the design, construction and commissioning of the three instruments plus MAORY were signed in 2015. The LTAO module for HARMONI was one of the Phase 2 items whose funding was initially deferred (de Zeeuw, Tamai & Liske, 2014) and so only the work to carry out the preliminary design was included in the agreement for HARMONI. Formal approval of the next design phases and the construction of the LTAO module was signed in 2019 when funds for this module became available. It will now be delivered along with HARMONI for first light with the spectrograph, ensuring optimised performance and increased sky coverage.

The instruments under construction have now completed the important preliminary design phase, during which the basic concept for the instrument is refined and compliance with the scientific and technical requirements is confirmed. The first Preliminary Design Review (PDR) meeting, for HARMONI, was held in November 2017, those for MICADO and METIS followed in October 2018 and May 2019, respectively. Everything about these projects is on a very large scale, as befits the extreme size of the telescope. The effort that goes into the PDRs is no exception. The document package for each instrument amounts to more than one hundred documents and many thousands of pages. The design concepts have been reviewed by tens of engineers from ESO with support from external experts from industry and from other extremely large telescope projects, such as the Thirty Meter Telescope (TMT)[2] and the Giant Magellan Telescope (GMT)[3]. Each of these instruments is now formally in the final design phase during which the design is detailed to the level that manufacturing of the key components can start after the Final Design Review (FDR) is concluded. The design for MAORY has undergone significant revision since the Phase A study; it has been optimised for manufacturability and ease of alignment, compliance with the available volume and mass, and also to ensure that it provides a good interface for the two client instruments. The PDR for MAORY is planned for the second quarter of 2021.

As the instrument designs have progressed, much has been learnt about the real resource requirements of these huge systems with their challenging performance specifications. Mass and power budgets, space envelopes, vibration control and maintenance requirements are major topics of discussion. Careful follow-up and management of these items has allowed MICADO, HARMONI and METIS to move into their FDR phases without any loss of functionality or performance,

Instrument	Main specifications			Schedule				
	Field of view/slit length/ pixel scale	Spectral resolution	Wavelength coverage (μm)	Phase A	Project start	PDR	FDR	First light
MICADO	Imager (with coronagraph) 50.5′ × 50.5′ at 4 mas/pix 19′ × 19′ at 1.5 mas/pix	*I*, *Z*, *Y*, *J*, *H*, *K* + narrowbands	0.8–2.45	2010	2015	2019		
	Single slit	*R* ~ 20 000						
MAORY	AO Module SCAO – MCAO		0.8–2.45	2010	2015			
HARMONI + LTAO	IFU 4 spaxel scales from: 0.8″ × 0.6″ at 4 mas/pix to 6.1″ × 9.1″ at 30 × 60 mas/pix (with coronagraph)	*R* ~ 3200 *R* ~ 7100 *R* ~ 17 000	0.47–2.45	2010	2015	2018		
METIS	Imager (with coronagraph) 10.5″ × 10.5″ at 5 mas/pix in *L*, *M* 13.5″ × 13.5″ at 7 mas/pix in *N*	*L*, *M*, *N* + narrowbands	3–13	2010	2015	2019		
	Single slit	*R* ~ 1400 in *L* *R* ~ 1900 in *M* *R* ~ 400 in *N*						
	IFU 0.6″ × 0.9″ at 8 mas/pix (with coronagraph)	*L*, *M* bands *R* ~ 100 000						
HIRES	Single object	*R* ~ 100 000	0.4–1.8 simultaneously	2018				
	IFU (SCAO)							
	Multi object (TBC)	*R* ~ 10 000						
MOSAIC	~ 7-arcminute FoV ~ 200 objects (TBC)	*R* ~ 5000–20 000	0.45–1.8 (TBC)	2018				
	~ 8 IFUs (TBC)	*R* ~ 5000–20 000	0.8–1.8 (TBC)					
PCS	Extreme AO camera and spectrograph	TBC	TBC					

1 milliarcsecond (mas) = 0.001″

Figure 1. The ELT Instrumentation roadmap and timeline.

despite some greatly increased demands on the telescope and the observatory. MAORY is also on track to meet its requirements as the PDR approaches. The lessons learnt from these pioneering instruments are being applied to the development of future instruments.

In addition to the first three instruments and their adaptive optics modules, the ELT Construction Programme included two Phase A studies, for a multi-object spectrograph (named MOSAIC), and a high spectral resolving power, high-stability spectrograph (named HIRES). The original Phase A design studies carried out from 2007 to 2010 included three separate concepts for a multi-object spectrograph (OPTIMOS-EVE, Hammer, Kaper & Dalton, 2010; OPTIMOS-DIORAMAS, Le Fèvre et al., 2010; and EAGLE, Morris & Cuby, 2010) and two for a high resolving power spectrograph (CODEX, Pasquini et al., 2010 and SIMPLE, Origlia, Oliva & Maiolino, 2010). In 2016 ESO issued a call for two Phase A studies for HIRES and MOSAIC in order to update and optimise the scientific scope and specifications of these instruments, taking into account how best to complement the observing capabilities offered by the first-light instruments. These instrument studies concluded in 2018.

The next stage of construction of HIRES and MOSAIC, and the funding of the future ELT Planetary Camera and Spectrograph (ELT-PCS), fall outside the ELT Construction Programme and within the Armazones Instrumentation Programme (AIP). The AIP will manage all future instrument development during the lifetime of the ELT. The agreements for the construction phase of MOSAIC and HIRES, including the detailed scientific requirements, are being finalised now. ESO's committees support the start of the construction of these instruments once the resources (funding, effort and Guaranteed Time) needed to complete the first instruments are well understood and secured. This milestone is expected when the last of the PDRs for the first instruments is complete. An important step towards the launch of the MOSAIC and HIRES construction phases was the recent approval by the ESO Council for the procurement of the second prefocal station for the Nasmyth B platform that will host MOSAIC and HIRES. Taken together, the instruments so far planned for the ELT offer excellent coverage of the observing parameter space, allowing astronomers to tackle a very broad range of science cases that will fully exploit the collecting power and diffraction limit of the ELT. As shown in Figure 2, users will have access to imaging and spectroscopy, across a wide range of wavelengths and spectral resolving powers, in a variety of observing modes, and including high-contrast, precision astrometry and non-sidereal tracking.

ELT-PCS is the planet hunter that will deliver one of the highest priority and most challenging science goals of the telescope — the detection and characterisation of exo-Earths. Given the rapidly changing understanding of the population of exoplanets and the many new facilities that are being developed to study them, it was decided in 2010 that ELT-PCS should start later in the overall timeline in order to allow for developments in the science case. Furthermore, achieving the extreme contrast ratios required for these observations requires research and development in the field of adaptive optics and coronagraphy. Prototyping of components that are needed for ELT-PCS is part of ESO's ongoing Technology Development programme.

The development of this instrument is linked to both the level of technical readiness of these prototypes and the availability of funding and effort.

In other articles in this issue details of the science case, operational modes and instrument concepts are given for each of the instruments.

Activities at ESO

The activities at ESO that support the development of the instruments for the ELT take a number of different forms. To ensure that ESO meets its commitments for the delivery of the instruments, a dedicated follow-up team of scientists, managers and engineers across all disciplines is assigned to work with each instrument team. The role of this follow-up team is to support the consortia with their expertise and also with understanding the interface to and performance of the telescope. This team also provides each instrument consortium with guidance on the application of the ESO standards. Standardisation of hardware and software across the observatories is crucial for cost- and time-effective operation and maintenance of the telescope(s) and instruments and is a significant development activity for ESO. The ELT standards include cryogenic components, control and dataflow software, instrument control electronics, real-time computing and wavefront sensor cameras. The standards have been either adopted or extended from the Paranal Observatory standards, or are new developments that may also be adopted by new instruments for Paranal when that is technically feasible.

Engineers and scientists also work within the consortia to deliver specific components or expertise and so ESO is also an associate member of each instrument consortium. ESO has world-leading expertise in detector technology and traditionally delivers the science detectors with standard detector controllers to the instruments on the VLT, and the same concept has been adopted for the ELT instruments. For its optical mode, HARMONI will use the Teledyne-e2V CCD231-84 deep-depletion silicon CCDs already used in the Multi Unit Spectroscopic Explorer (MUSE). Both MICADO and HARMONI will use the Hawaii 4RG detector from Teledyne-e2V for their near-infrared modules. METIS will use near-infrared detectors from the Hawaii "family", the Hawaii 2RG, for its *LM*-band imager and spectrometer. A particularly exciting development for METIS is that it will use a new detector for the *N*-band observations. The initial plan was to use the Aquarius detector that has been used on-sky with the VLT Imager and Spectrometer for mid-InfraRed (VISIR). However, the technology of the new GeoSNAP detector from Teledyne-E2V is now sufficiently ready that the decision to switch to this detector was taken after the METIS PDR. Simplifications to the instrument design come from this change but, most importantly, the observing efficiency in the *N*-band imaging mode, where many of the important science cases in exoplanets will be tackled, is expected to be many orders of magnitude higher than with the design using the Aquarius detector. ESO leads the work package for the GeoSNAP detector that will be tested at the METIS consortium partners the Max Planck Institute for Astronomy and the University of Michigan. Finally, an update of the standard detector controller, the Next Generation Controller (NGC), to a new edition (NGCII) with enhanced performance and matching the interface requirements of the new telescope is being carried out under the Technology Development Programme.

Expertise in adaptive optics is also an important input to the instrument consortia. In this regard, ESO engineers and physicists work within the instrument consortia, fully integrated into the teams, providing backup for simulating the telescope behaviour and instrument performance, developing the calibration strategies for the adaptive optics and contributing to the engineering design of the adaptive optics modules based on their knowledge of the ELT and experience from the Adaptive Optics Facility upgrade programme. ESO is also leading an effort to coordinate the expertise of all the groups working on SCAO for the ELT, including for the telescope, to explore common solutions for the calibration of these systems.

ESO maintains an overview of all of the systems on the telescope to ensure a fully working system and is responsible for the interface from all instruments to the observatory and between MAORY and its client instruments. One of the challenges facing both the instrument consortia and ESO is the parallel development of the telescope and the instrumentation. The agreements that have been signed with the instrument consortia include formal documentation describing the interface to the telescope systems and the requirements for the instruments. Progress with the construction of the telescope is continuing at our industrial partners in Europe and in Chile. With over

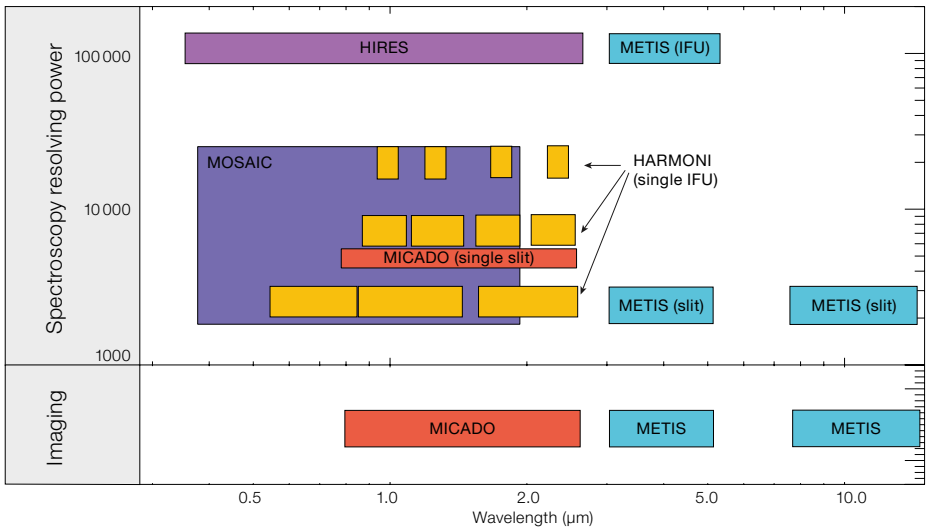

Figure 2. Parameter space for astronomical observations provided by the first-light and planned instruments on the Extremely Large Telescope.

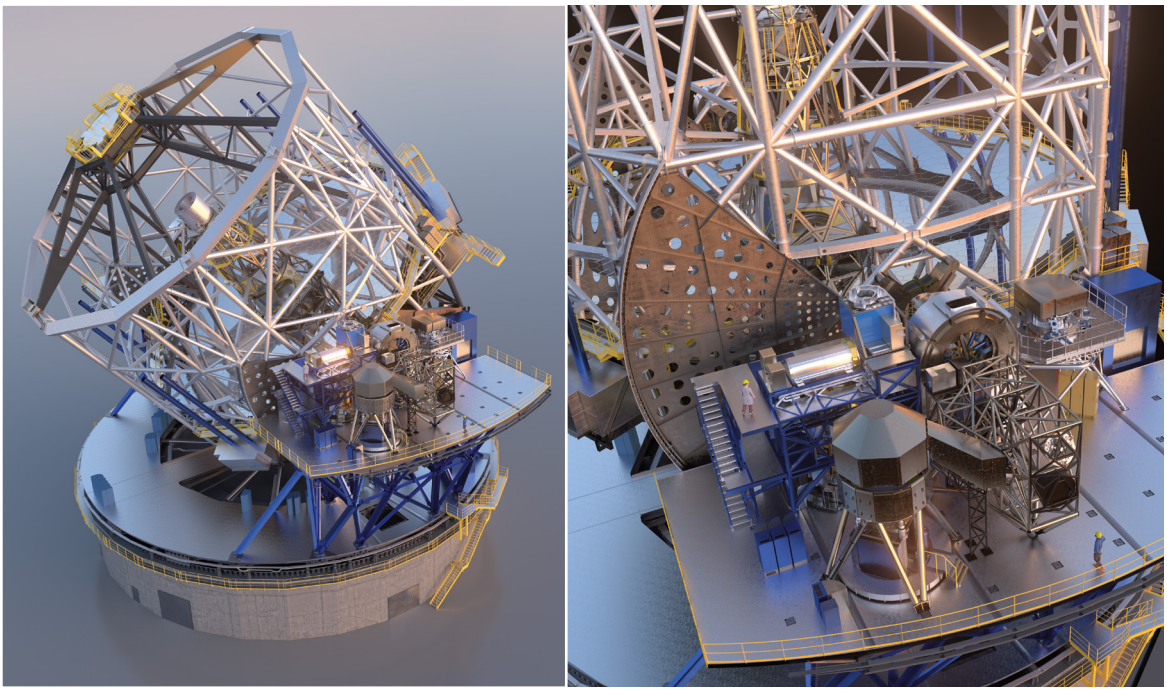

Figure 3. The instruments on the Nasmyth platform.

95% of the material budget spent, many components are in the manufacturing phases, including the many mirror segments and their mechanical supports for the main mirror, the remaining opto-mechanical components and parts of the dome and main structure. Significant work has been carried out on site, including the dome foundations on Cerro Armazones and a new technical facility as part of the Paranal observatory. As the telescope design evolves, a balance is sought between updating the interface information and maintaining the commitment to the numbers in the formal documentation. An informal, but controlled, exchange of information underpins the collaborative style that both ESO and the consortia wish to maintain while developing the most complex and costly instruments yet built for the most ambitious ground-based telescope ever. Workshops at ESO on the telescope and instrument operations concepts, on the alignment and verification of the instruments and on instrument software (pipeline, control and real-time control) have offered great opportunities for the exchange of the most up-to-date information between experts on the ESO and instrument teams.

Part of the system-level activity at ESO is keeping an up-to-date model of the instruments on the Nasmyth platform, as the instruments themselves and the telescope main structure and prefocal station designs evolve. This model allows ESO and the instrument consortia to explore how to access various parts of the system during installation and maintenance, permits the dynamical modelling of the system under earthquake conditions and provides an all-important check that the instruments and other items on the Nasmyth platform do not occupy the same physical space or attachment points to the Nasmyth floor. The latest version of this layout is shown in Figure 3.

Looking towards the future operation of the ELT, a number of working groups[4] on specific topics have been set up. Membership of the working groups is open to anyone with an interest in contributing to the future scientific success of the ELT, whether from ESO, from the instrument consortia or from the community in general. The topics so far under discussion are: preparing for ELT observations (from observation preparation to execution); calibrations (including standard stars and astro-weather); calibration improvements and post-processing (including point spread function reconstruction and detector effect characterisation); and end-to-end modelling.

Acknowledgements

Many more people than those listed as authors on this paper contribute to the development of the instruments for ESO's ELT. In particular, the importance of the work of the > 50 members of the follow-up team at ESO should not be underestimated. The authors would like to acknowledge the contribution of all those at ESO and in the community who are participating directly and indirectly in this exciting endeavour.

References

De Zeeuw, T., Tamai, R. & Liske, J. 2014, The Messenger, 158, 3
Hammer, F., Kaper, L. & Dalton, G. 2010, The Messenger, 140, 36
Le Fèvre, O. et al. 2010, The Messenger, 140, 34
Morris, S. & Cuby, J.-G. 2010, The Messenger, 140, 22
Origlia, L., Oliva, E. & Maiolino, R. 2010, The Messenger, 140, 38
Pasquini, L. et al. 2010, The Messenger, 140, 20

Links

[1] ESO's Extremely Large Telescope (ELT): elt.eso.org
[2] The Thirty Meter Telescope (TMT): www.tmt.org
[3] The Giant Magellan Telescope (GMT): www.gmto.org
[4] ELT Working Groups: elt.eso.org/about/workinggroups/

DOI: 10.18727/0722-6691/5215

HARMONI: the ELT's First-Light Near-infrared and Visible Integral Field Spectrograph

Niranjan Thatte[1]
Matthias Tecza[1]
Hermine Schnetler[2]
Benoit Neichel[3]
Dave Melotte[2]
Thierry Fusco[3,4]
Vanessa Ferraro-Wood[1]
Fraser Clarke[1]
Ian Bryson[2]
Kieran O'Brien[5]
Mario Mateo[6]
Begoña Garcia Lorenzo[7]
Chris Evans[2]
Nicolas Bouché[8]
Santiago Arribas[9]
and the HARMONI Consortium[a]

[1] Department of Physics, University of Oxford, UK
[2] United Kingdom Astronomy Technology Centre (UKATC), Edinburgh, UK
[3] Laboratoire d'Astrophysique de Marseille (LAM), France
[4] Département d'Optique et Techniques Avancées (DOTA), Office National d'Etudes et de Recherches Aérospatial (ONERA), Paris, France
[5] Physics Department, Durham University, UK
[6] Department of Astronomy, University of Michigan, USA
[7] Instituto de Astrofísica de Canarias (IAC) and Departamento de Astrofísica, Universidad de La Laguna, Tenerife, Spain
[8] Centre de Recherche Astrophysique de Lyon (CRAL), France
[9] Centro de Astrobiología – Instituto Nacional de Técnica Aeroespacial, Consejo Superior de Investigaciones Científicas (CAB-INTA/CSIC), Madrid, Spain

The High Angular Resolution Monolithic Optical and Near-infrared Integral field spectrograph (HARMONI) is the visible and near-infrared (NIR), adaptive-optics-assisted, integral field spectrograph for ESO's Extremely Large Telescope (ELT). It will have both a single-conjugate adaptive optics (SCAO) mode (using a single bright natural guide star) and a laser tomographic adaptive optics (LTAO) mode (using multiple laser guide stars), providing near diffraction-limited hyper-spectral imaging. A unique high-contrast adaptive optics with high performance and good sky coverage, respectively (AO) capability has recently been added for exoplanet characterisation. A large detector complement of eight HAWAII-4RG arrays, four choices of spaxel scale, and 11 grating choices with resolving powers ranging from R ~ 3000 to R ~ 17 000 make HARMONI a very versatile instrument that can cater to a wide range of observing programmes.

About HARMONI

HARMONI will provide the ELT's workhorse spectroscopic capability at first light. A visible and near-infrared integral field spectrograph (IFS), it provides a "point-and-shoot" capability to simultaneously obtain a spectrum of every spaxel[b] over a modest field of view. Several different flavours of adaptive optics ensure (near) diffraction-limited spatial resolution of ~ 10 milliarcseconds over most of the sky. ELT+HARMONI will transform the landscape of observational astronomy by providing a big leap in sensitivity and resolution — a combination of the ELT's huge collecting area, the exquisite spatial resolution provided by the AO, and large instantaneous wavelength coverage coupled with a range of spectral resolving powers (R ~ 3000 to 17 000).

Over the last couple of years, HARMONI has added substantially to the core instrument. The LTAO capability is part of the baseline, as is a high-contrast AO (HCAO) mode that aims to enable direct spectroscopy of extra-solar planetary companions. The University of Michigan has joined as a new partner, providing a much needed cash injection, while the Institut de Planétologie et d'Astrophysique de Grenoble (IPAG) is funding the hardware for HCAO.

HARMONI is equally suited to spatially resolved spectroscopy of extended targets and of point sources, particularly if their positions are not precisely known (for example, transients), or if they are located in crowded fields. The data cube obtained from a single integral field exposure can yield information about the source morphology (via broad- or narrow-band images), spatially resolved kinematics and dynamics (via Doppler shifts and widths), chemical abundances and composition (via emission and absorption line ratios) and the physical conditions (temperature, density, presence of shocks) of the emitting region (via line diagnostics). In addition, specialist capabilities such as molecular mapping for high contrast observations, or the use of deconvolution with knowledge of the point spread function (PSF) from AO telemetry extend the areas where HARMONI will make a huge impact. Some examples are showcased in the last section of this article.

Spatial and spectral grasp

Figure 1a shows the spatial layout of the HARMONI field of view (FoV) at its four different spaxel scales, one of which may be selected *on the fly*. At any spaxel scale, HARMONI simultaneously observes spectra of ~ 31 000 spaxels in a contiguous rectangular field. The common wavelength range in each data cube is ~ 3700 pixels long, after accounting for the stagger between adjacent slitlets and slit curvature. The spaxel scales range from 0.06 × 0.03 arcseconds per spaxel, limited by the focal ratios achievable in the spectrograph cameras, to 4 × 4 milliarcseconds per spaxel, set to Nyquist sample the ELT's diffraction limit in the NIR H band. Two other intermediate scales of 10 × 10 milliarcseconds per spaxel and 20 × 20 milliarcseconds per spaxel allow the user to optimise for sensitivity, spatial resolution or FoV, as required. A larger FoV is particularly desirable when using the "nod-on-IFU" technique to achieve accurate sky background subtraction, as it involves positioning the object alternately in each half of the FoV.

The versatility in choice of plate scale is complemented by a large choice of wavelength ranges and spectral resolving powers, as shown in Figure 1b. HARMONI uses Volume Phase Holographic (VPH) gratings for high efficiency. Each grating has a fixed wavelength range, so needs to be physically exchanged to change observing band. One of eleven different gratings can be chosen, which between them provide three different resolving powers (R ~ 3000, 7000 and 17 000) spanning the various atmospheric windows in the NIR (atmospheric transmission is shown in grey in Figure 1b).

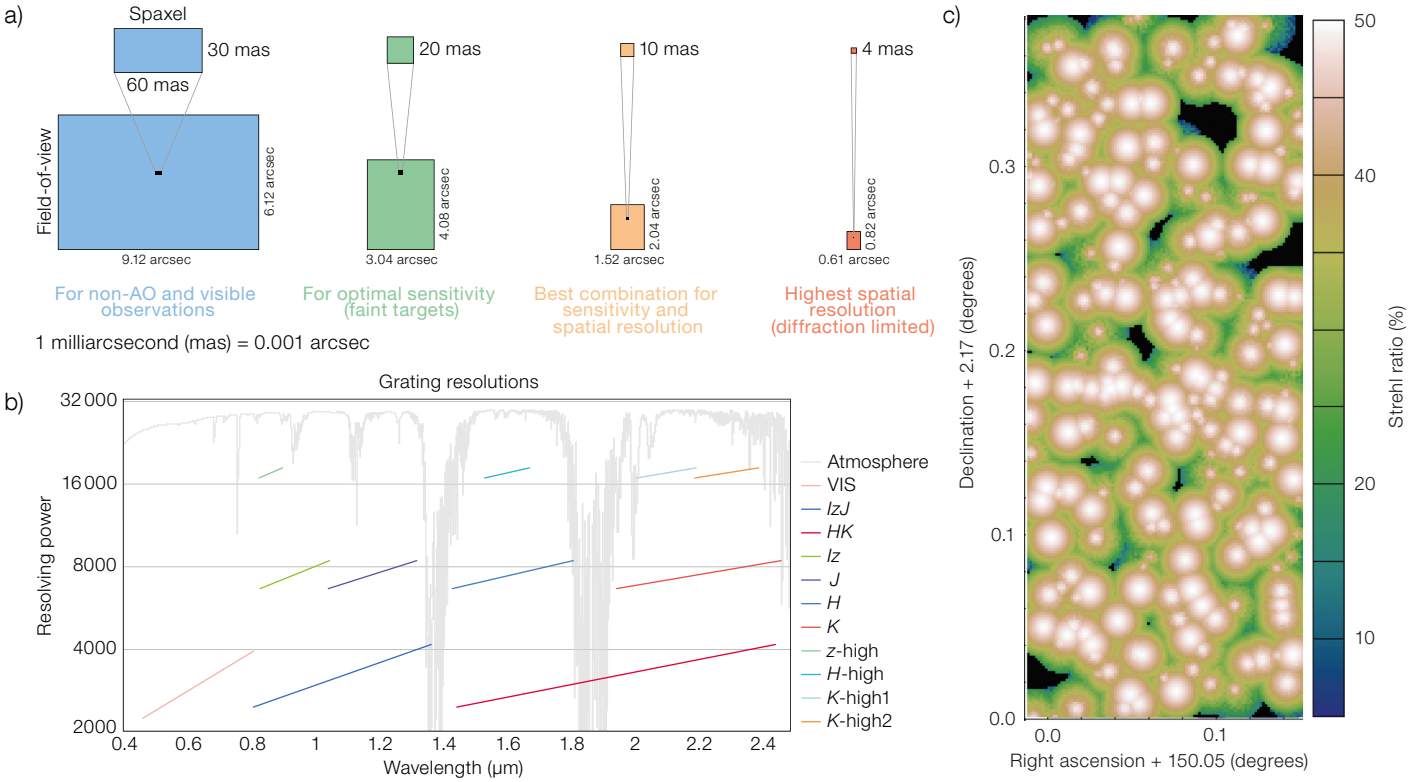

Figure 1. a) Spatial layout of the HARMONI science field, showing the spaxel sizes and fields of view at the four different spaxel scales. b) Spectral coverage and resolving power ranges for each of the 11 HARMONI grating choices. The atmospheric transmission is shown in grey. c) Expected AO performance (Strehl ratio) for the COSMOS deep field, observed with HARMONI LTAO in good seeing conditions (0.43 arcseconds), illustrating the sky coverage achieved for a typical patch of sky.

A fixed-length spectrum implies a natural compromise between instantaneous wavelength coverage and resolving power. One grating provides coverage at visible wavelengths (*V* and *R* bands), requiring a different set of detectors (CCDs instead of the HgCdTe arrays used in the NIR). However, as AO correction works well only at longer NIR wavelengths, the spatial resolution achieved at visible wavelengths is close to seeing-limited, making the large spaxel count somewhat superfluous. Consequently, only half the FoV is offered at visible wavelengths, at all spaxel scales.

Adaptive optics flavours

The ELT is an adaptive telescope, with M4 (a deformable mirror with over 5000 actuators) and M5 (a fast tip-tilt mirror) providing active correction of atmospheric turbulence. The sensing of the wavefront aberrations is done by the science instruments — better rejection of common-mode disturbances such as flexure and vibrations is achieved by splitting the wavefront sensing light as close to the science focal plane as possible. The scheme used for wavefront sensing leads to HARMONI's four distinct operating modes: LTAO, SCAO, HCAO, and noAO — the last providing no adaptive optics correction of atmospheric turbulence.

In LTAO operation, six laser guide star (LGS) sensors, each with 78 × 78 subapertures, measure the wavefront aberrations at 500 Hz from six sodium laser stars. The laser stars are located in an asterism with a diameter of ~ 1 arcminute, which provides the best compromise between peak performance and robustness to changing atmospheric parameters. HARMONI's AO Control System (AOCS) stitches together the wavefront information from the six lines of sight to reconstruct the wavefront aberration for the on-axis path, and commands M4 and M5 to the appropriate shapes to eliminate the effect of the turbulence, providing a near diffraction-limited corrected wavefront to the IFS.

It is not possible to measure the image motion with LGS, so a separate natural guide star (NGS) is needed to sense tip-tilt and focus. A single off-axis NGS is sensed by HARMONI's NGS System (NGSS), with a probe arm that patrols a 1-arcminute-radius field centred on the IFS FoV. The NGS position and focus are sensed at several hundred Hz in the *H* and *K* bands, while a slow "Truth Sensor" uses the *J*-band light from the same star to eliminate any low-order wavefront errors introduced by the LGS. The NGSS is able to operate with stars as faint as H_{AB} = 19, so that HARMONI's LTAO system can provide excellent sky coverage — 75% of the sky at the south Galactic pole (SGP) with Strehl exceeding 30% in the *K* band under median conditions of atmospheric turbulence (see Figure 1c for an example of LTAO sky coverage).

Even better performance may be obtained by using HARMONI's SCAO system, provided a single, bright, natural guide star is present within 15 arcseconds of the science target of interest. SCAO can also deal with extended objects as AO reference "stars", with slightly degraded performance, as long as the reference is less than 2.5 arcseconds in diameter. Unlike the LTAO system (which uses an off-axis NGS), SCAO uses a dichroic that sends light in the 700–1000 nm range to a pyramid wavefront sensor operating at 500 Hz, with longer wavelengths (1000–2450 nm) available for spectroscopy with the IFS. Both on-axis and off-axis NGS may be used. Optimal performance is achieved for stars down to $V = 12$, with a limiting magnitude of $V \sim 17$. A second SCAO dichroic is available, albeit with a reduced patrol field of 4 arcseconds in diameter, with a cut-in wavelength of 800 nm for spectroscopy, allowing observations that use *z*-band stellar absorption features as diagnostics.

The HCAO mode adds a high-contrast capability to HARMONI, using a combination of a pupil-plane apodiser and a focal-plane mask. Because of uncorrected atmospheric differential refraction (chromatic beam shift), it is not possible to use classical coronagraphs to improve contrast. The novel design by Carlotti et al. (2018) achieves good rejection of starlight — the goal being (post-processed) contrasts of $> 10^6$ at separations < 0.2 arcseconds — whilst enabling inner working angles (IWA) of less than 100 milliarcseconds for IFS spectroscopy. HCAO works only with an on-axis NGS. It uses the pyramid wavefront sensor of the SCAO system for sensing wavefront aberrations, with a second ZELDA wavefront sensor (N'Diaye et al., 2016) for improved sensitivity in the high-Strehl regime. Angular Differential Imaging (ADI) will also be employed to reduce the impact of quasi-static speckles. Consequently, the HCAO mode drives the IFS rotator to track the pupil, rather than field tracking as employed in all other modes.

At wavelengths where AO correction is expected to be poor, or when AO cannot be used owing to weather or technical constraints, HARMONI's noAO mode can provide "seeing-limited" performance. The noAO mode utilises a faint ($I < 23$) natural star for slow (~ 0.1 Hz) secondary guiding, eliminating slow drifts of the instrument focal plane and ensuring accurate pointing. This mode is typically expected to be used with the visible grating and the coarsest spaxel scale, as all scales heavily oversample the full width at half maximum (FWHM) of the seeing. 2 × 1 and 4 × 1 binning along the spatial axis can be used to reduce readout times for the CCD detectors, creating effective spaxels of 0.06 × 0.06 arcseconds and 0.06 × 0.12 arcseconds, respectively, that are a better match to the seeing FWHM.

Instrument description

Figure 2b shows an overview CAD model of the HARMONI instrument. The instrument is ~ 8 m tall, and has a footprint of 5 × 6 m and a total weight of approximately 36 tonnes. The opto-mechanics of the IFS consists of the pre-optics scale changer, the integral field unit (IFU) and four spectrograph units. The IFU rearranges the light from the field into four 500-mm pseudo long slits, which form the input to the four spectrograph units. The IFS opto-mechanics resides in a large cryostat, about 3.26 m in diameter and 4 m tall (a cutaway view is shown in Figure 2a), at a constant operating temperature of 130 K to minimise thermal background. The NIR detectors (eight 4096 × 4096-pixel HAWAII 4RG arrays) are operated at the lower temperature of 40 K. The instrument rotator and cable wrap (IRW) allow the entire cryostat to rotate about a vertical axis to follow field rotation at the ELT's Nasmyth focus. The vertical rotation axis guarantees an invariant gravity vector, improving the instrument's stability by minimising flexure.

Figure 2. a) Cutaway CAD model of the HARMONI cryostat (ICR), situated on the instrument rotator and cable wrap (IRW). The view shows the main opto-mechanical components of the integral field spectrograph (IFS), namely the IFS pre-optics (IPO), the integral field unit (IFU), and the spectrographs (ISP). b) overall CAD assembly of HARMONI, with the various systems comprising the instrument coloured differently. The LSS is the LGSS Support Structure. Other acronyms are explained in the text.

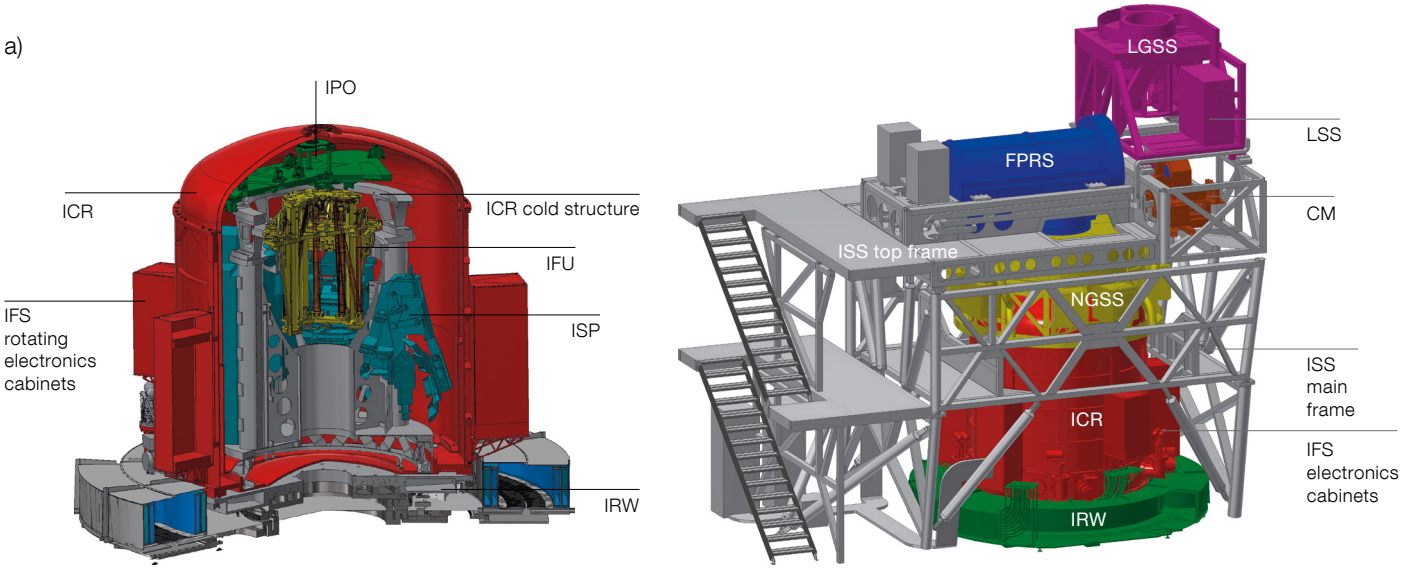

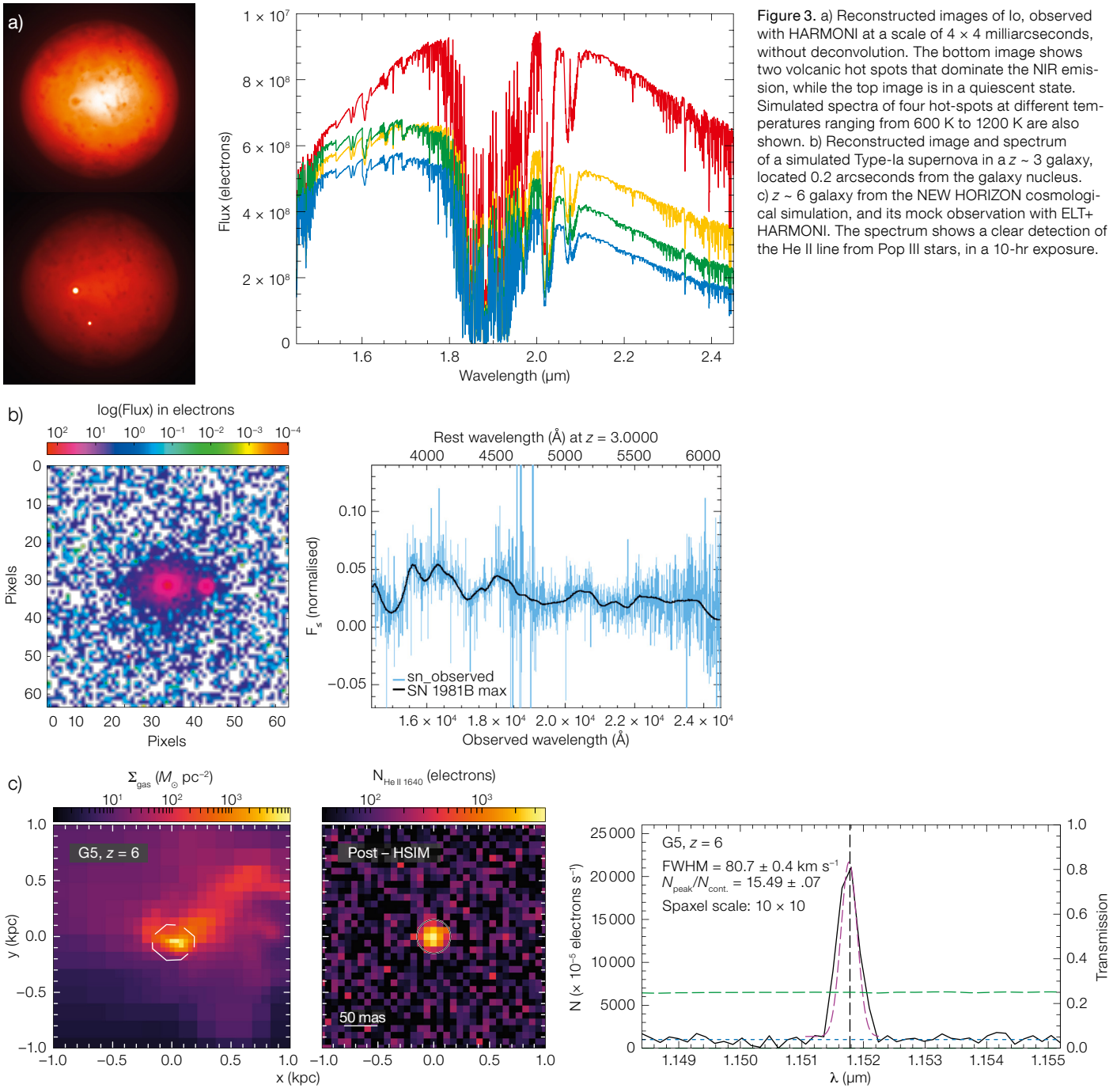

Figure 3. a) Reconstructed images of Io, observed with HARMONI at a scale of 4 × 4 milliarcseconds, without deconvolution. The bottom image shows two volcanic hot spots that dominate the NIR emission, while the top image is in a quiescent state. Simulated spectra of four hot-spots at different temperatures ranging from 600 K to 1200 K are also shown. b) Reconstructed image and spectrum of a simulated Type-Ia supernova in a $z \sim 3$ galaxy, located 0.2 arcseconds from the galaxy nucleus. c) $z \sim 6$ galaxy from the NEW HORIZON cosmological simulation, and its mock observation with ELT+HARMONI. The spectrum shows a clear detection of the He II line from Pop III stars, in a 10-hr exposure.

The NGSS is located on top of the IFS cryostat and co-rotates with it. It houses the natural guide star sensors for all four operating modes. As the telescope's back focal distance is insufficient to relay the telescope light directly into the upward-looking cryostat, a focal-plane relay system (FPRS) re-images 2 arcminutes of the telescope focal plane to the top of the cryostat and the NGSS. Both the FPRS and NGSS are maintained in a dry gas environment at a constant temperature of –15 degrees C, reducing thermal background for improved *K*-band sensitivity and minimising thermal drifts.

The LGS System (LGSS) and the Calibration Module (CM) are located just past the instrument slow shutter, close to where telescope light enters the instrument, at a beam height of 6 m above the Nasmyth platform. The first element in the instrument light path is the LGS dichroic, which sends light at 589 nm from the ELT's six LGS to the LGSS. As the LGS asterism is projected from the periphery of the ELT primary

mirror (M1), it co-rotates with the telescope pupil, and the LGSS needs its own de-rotator to compensate. The CM can insert light from calibration lamps via fold mirrors into the beam path, mimicking the telescope f-ratio and pupil location. It provides line and continuum sources for all science and technical calibrations. The Instrument Static Structure (ISS) provides a robust mechanical structure and access to all instrument systems.

Operation and calibration

HARMONI is conceptually simple to operate, as it provides a "point-and-shoot" capability. The user selects one of four operating modes: noAO, SCAO, HCAO or LTAO. In addition, the user must choose a setting that specifies a choice of spaxel scale, grating and, optionally, other user-selectable items (for example, SCAO dichroic, or apodiser) and the instrument is configured accordingly. Accurate pointing is assured by specifying offsets of the science field centre from the natural guide star. As a consequence, the default acquisition sequence does not require an acquisition exposure with the IFS — once the guide star is acquired and all control loops are closed, the first science exposure can commence straight away. Thanks to the unprecedented spatial resolution of the ELT, the accuracy of information needed for guide stars (proper motion, colour, etc.) is much higher than for the Very Large Telescope (VLT). With the faint guide stars which can be used by HARMONI, catalogues may not suffice and pre-imaging of the field might be needed in some cases.

Observing templates will have a similar look and feel to those of other VLT NIR IFS, and will include a variety of sky-subtraction strategies such as "offset to blank sky", "nod-on-IFU" or "stare", together with small jitters to work around bad or hot pixels. Mosaicking will also be supported in the usual way, as will non-sidereal tracking in LTAO and noAO modes (in SCAO and HCAO mode, the only non-sidereal observation possible is when the AO reference "star" is itself non-sidereal). NIR long exposures (typical for spectroscopy of faint targets) will use Sample-Up-The-Ramp (SUTR) readout to minimise readout noise, with every non-destructive readout saved in the archive. AO telemetry data, useful for reconstructing the PSF during the exposure, will also be archived.

Science calibrations needed by the data reduction pipeline, such as arc lamp exposures for wavelength calibration, detector bias and dark frames, flat fields and vertical line and pinhole masks, will be carried out the morning after the observations, as is typical for VLT instruments. ELT instruments are required to be light-tight, so calibrations can happen in parallel for all instruments. With four observing modes, 4 choices of spaxel scale, and 11 grating settings, the number of distinct configurations needing calibration exceeds 100. Consequently, only the configurations used during the night will be calibrated the following morning. Science calibrations and additional monitoring calibrations will be used for "health-checks" (to monitor trends in instrument performance). Efforts will be made to minimise night-time calibrations (telluric or flux standards) wherever possible. Methods that use model-based calibrations instead are being actively investigated by a number of ESO working groups.

Performance

We have developed a python simulator, HSIM[1], to provide prospective users with the ability to quantitatively assess the efficacy of their proposed observing programme. HSIM (Zieleniewski et al., 2015) is a "cube-in, cube-out" simulator that mimics the effects of atmosphere, telescope, instrument and detector, including the strongly wavelength-dependent, non-axisymmetric AO PSF. The user can analyse the output cube as if it were the output of the instrument pipeline for a real observation, as it incorporates noise from all sources, including shot noise from thermal background and night-sky emission, detector readout noise and dark current. Detector systematics and the impact of sky subtraction can also be included if desired. Through detailed analysis of the output cube, the astronomer can derive uncertainties and confidence levels for the derived physical parameters from the observation, rather than just the signal-to-noise ratio per spaxel (or pixel), thus quantifying the required exposure time or even the feasibility of the planned observation. It also allows the user to develop and test the analysis tools required. The HSIM code is publicly available[2].

HSIM predicts point source sensitivities (5σ, 5 hr, 2 × 2-spaxel extraction aperture) of J_{AB} = 25.6, H_{AB} = 26.8, K_{AB} = 25.9 in LTAO mode, with SCAO performance of J_{AB} = 26.2, H_{AB} = 27.0, K_{AB} = 26.0 at R ~ 3000. The point source sensitivities do not convey the full picture, so we have used HSIM to carry out detailed simulations showcasing a few planned observations with HARMONI. These range from objects in our own Solar System to the most distant galaxies at z ~ 6–10.

Jupiter's moon Io is the most volcanically active body in the Solar System. Groussin et al. (in preparation) have simulated ELT observations of Io's hotspots. They show that it is possible to distinguish between sulphurous and ultra-mafic composition of the ejecta by measuring the ejecta's temperature (see Figure 3a) from their NIR spectra, using HARMONI's SCAO mode providing near diffraction-limited spatial resolution.

Bounissou et al. (2018) have shown that HARMONI LTAO can provide direct spectroscopic classification of a supernova in a galaxy at z ~ 3 in a 3-hr observation, up to 2 months past maximum light (see Figure 3b), using the Si II feature (at 400 nm in the rest frame). Confirming type Ia supernovae spectroscopically for a small sub-sample will allow studies of cosmic expansion rates to be pushed to substantially higher redshifts.

We have used the adaptive mesh refinement cosmological simulations from the NEW HORIZON suite (Dubois et al., 2020) to simulate studies of high-z galaxies with HARMONI in a spatially resolved manner. Using cosmological simulations that create galaxies at high spatial resolution commensurate with HARMONI's observational capabilities (~ 100 pc at z ~ 2–10) is preferred because the objects have morphologies and kinematic and dynamical properties consistent with the observed ensemble population at high redshifts, and have well understood input physics consistent with known laws and cosmological evolution (Richardson et al., 2020).

Grisdale et al. (2020) have used NEW HORIZON simulations, post-processed using the CLOUDY radiative transfer code (Ferland et al., 2017) to show that HARMONI LTAO could detect the presence of the first stars (Pop III stars) in galaxies at very high redshifts (z = 3–10). The existence of Pop III stars has not been observationally confirmed up to now, although several attempts have been made and some excellent candidates have been identified. Given their primordial composition with no heavy elements, Pop III stars are expected to be substantially more massive than their metal-rich cousins. Consequently, they should burn much hotter, and have a much higher ultraviolet flux, capable of ionising not only hydrogen but also helium in the surrounding gas (H II region). The strength of the He II 164 nm line is thus a good observational diagnostic for the presence of Pop III stars. Despite the large luminosity distance of these very high-redshift star forming regions, the ELT's huge collecting area, coupled with the exquisite spatial resolution provided by HARMONI LTAO, would detect the He II feature with good signal-to-noise from a substantial fraction of the mock galaxies in a 10-hr exposure (Figure 3c). However, to be certain that the line indicates the presence of Pop III stars would require ancillary observations of the H-alpha line from these objects to measure the He II to H-alpha ratio, probably using the James Webb Space Telescope, given the high redshifts involved.

Acknowledgements

HARMONI work in the UK is supported by the Science and Technology Facilities Council (STFC) at the UK Astronomy Technology Centre (UKATC), Rutherford Appleton Laboratory (RAL), University of Oxford (grants ST/N002717/1 and ST/S001409/1) and Durham University (grant ST/S001360/1), as part of the UK ELT Programme. In France, the HARMONI Project is supported by the CSAA-CNRS/INSU, ONERA, A*MIDEX, LABEX LIO, and Université Grenoble Alpes. The IAC and CAB (CSIC-INTA) acknowledge support from the Spanish MCIU/AEI/FEDER UE (grants AYA2105-68217-P, SEV-2015-0548, AYA2017-85170-R, PID2019-107010GB-100, CSIC-PIE201750E006, and PID2019-105423GA-I00) and from the Comunidad de Madrid (grant 2018-T1/TIC-11035).

The authors would like to acknowledge contributions from Sophie Bounissou (supernova simulations), Olivier Groussin (Io simulations) and Kearn Grisdale (Pop III simulations). We are also grateful to James Carruthers, Neil Campbell, and David Montgomery for CAD views. Miguel Pereira-Santaella is the author of HSIM and we thank him for the sensitivity computations.

References

Bounissou, S. et al. 2018, MNRAS, 478, 3189
Carlotti, A. et al. 2018, Proc. SPIE, 10702, 107029N
Dubois, Y. et al. 2020, arXiv:2009.10578
Ferland, G. J. et al. 2017, Revista Mexicana de Astronomía y Astrofísica, 53, 385
Grisdale, K. et al. 2021, MNRAS, 501, 5517
N'Diaye, M. et al. 2016, Proc. SPIE, 9909, 99096S
Richardson, M. et al. 2020, MNRAS, 498, 1891
Zieleniewski, S. et al. 2015, MNRAS, 453, 3754

Links

[1] HSIM simulator: https://harmoni-elt.physics.ox.ac.uk/Hsim.html
[2] HSIM code: https://github.com/HARMONI-ELT/HSIM

Notes

[a] The full list of HARMONI Consortium members can be found at https://harmoni-elt.physics.ox.ac.uk/consortium.html
[b] Spaxel stands for SPAtial piXEL, to distinguish it from a pixel of the spectrograph detector.

ESO/SPECULOOS Team/E. Jehin

If you had a brand new state-of-the-art telescope facility, what would you look at first? Researchers at the SPECULOOS Southern Observatory — which comprises four small telescopes, each with a 1-metre primary mirror — chose to view the Lagoon Nebula. This magnificent picture is the result, and is one of the SPECULOOS' first ever observations.

DOI: 10.18727/0722-6691/5216

MAORY: A Multi-conjugate Adaptive Optics RelaY for ELT

Paolo Ciliegi[1]
Guido Agapito[1]
Matteo Aliverti[1]
Francesca Annibali[1]
Carmelo Arcidiacono[1]
Andrea Balestra[1]
Andrea Baruffolo[1]
Maria Bergomi[1]
Andrea Bianco[1]
Marco Bonaglia[1]
Lorenzo Busoni[1]
Michele Cantiello[1]
Enrico Cascone[1]
Gaël Chauvin[3]
Simonetta Chinellato[1]
Vincenzo Cianniello[1]
Jean-Jacques Correia[3]
Giuseppe Cosentino[1]
Massimo Dall'Ora[1]
Vincenzo De Caprio[1]
Nicholas Devaney[2]
Ivan Di Antonio[1]
Amico Di Cianno[1]
Ugo Di Giammatteo[1]
Valentina D'Orazi[1]
Gianluca Di Rico[1]
Mauro Dolci[1]
Sylvain Doutè[3]
Cristian Eredia[1]
Jacopo Farinato[1]
Simone Esposito[1]
Daniela Fantinel[1]
Philippe Feautrier[3]
Italo Foppiani[1]
Enrico Giro[1]
Laurance Gluck[3]
Aaron Golden[2]
Alexander Goncharov[2]
Paolo Grani[1]
Marco Gullieuszik[1]
Pierre Haguenauer[4]
François Hénault[3]
Zoltan Hubert[3]
Miska Le Louran[4]
Demetrio Magrin[1]
Elisabetta Maiorano[1]
Filippo Mannucci[1]
Deborah Malone[2]
Luca Marafatto[1]
Estelle Moraux[3]
Matteo Munari[1]
Sylvan Oberti[4]
Giorgio Pariani[1]
Lorenzo Pettazzi[4]
Cédric Plantet[1]
Linda Podio[1]
Elisa Portaluri[1]
Alfio Puglisi[1]
Roberto Ragazzoni[1]
Andrew Rakich[1]
Patrick Rabou[3]
Edoardo Redaelli[1]
Matt Redman[2]
Marco Riva[1]
Sylvain Rochat[3]
Gabriele Rodeghiero[1]
Bernardo Salasnich[1]
Paolo Saracco[1]
Rosanna Sordo[1]
Marilena Spavone[1]
Marie-Hélène Sztefek[3]
Angelo Valentini[1]
Eros Vanzella[1]
Christophe Verinaud[4]
Marco Xompero[1]
Simone Zaggia[1]

[1] INAF, Italy
[2] NUIG, Galway, Ireland
[3] CNRS/INSU, Grenoble, France
[4] ESO

The Multi-conjugate Adaptive Optics RelaY (MAORY) is the adaptive optics (AO) module for the Extremely Large Telescope (ELT) that will provide two gravity-invariant ports with the same optical quality for two different client instruments. It will enable high-angular-resolution observations in the near-infrared over a large field of view (~ 1 arcminute^2) by real-time compensation of the wavefront distortions caused by atmospheric turbulence. Wavefront sensing is performed using laser and natural guide stars while the wavefront sensor compensation is performed by an adaptive deformable mirror (DM) in MAORY which works together with the telescope's adaptive and tip-tilt mirrors M4 and M5 respectively.

Introduction

MAORY will provide the ELT with two adaptive optics modes: the single-conjugate adaptive optics (SCAO) mode, which provides a very high correction over a field of view (FoV) of diameter ~ 10 arcseconds, with performance rapidly degrading with distance from the bright natural star used to probe the wavefront, and a multi-conjugate adaptive optics (MCAO) mode, which provides a moderate correction over a FoV of diameter ~ 60 arcseconds, with pretty homogeneous performance over the whole FoV.

MAORY is designed to support two different instruments, each with the same optical quality and with a gravity-invariant port. One of these two instruments will be the Multi-adaptive optics Imaging CamerA for Deep Observations (MICADO) near-infrared camera (Davies et al., 2018), while the second one is as yet undefined. The SCAO module is being developed within the MICADO consortium with contributions from MAORY and is described in Davies et al. (p. 17). The MAORY project is now in its Phase B stage and is progressing towards its Preliminary Design Review in early 2021.

Science drivers

The scientific application of the SCAO mode will be limited by the need for a bright (approximately $V \leq 16$ magnitudes) star within few arcseconds of the scientific target, while the MCAO mode will make use of three natural guide stars (NGS) (with $H \leq 21.0$ magnitudes) to be found within an annular patrol field with an inner radius of ~ 40 arcseconds and an outer radius of ~ 160 arcseconds. The three NGS will allow us to correct low-order modes of the wavefront distortions, while the six laser guide stars (LGS) will be used to correct for high-order modes. This will make it possible to get AO-assisted observations over a large fraction of the sky, meeting the system specification for sky coverage (≥ 50% over the whole sky).

Coupled with MICADO, MAORY will enable the ELT to perform diffraction-limited observations in the near-infrared. In imaging mode MAORY + MICADO will provide an option with a wide FoV (50.5 × 50.5 arcseconds) at pixel scale of 4 milliarcseconds and a high-resolution option with a 1.5-milliarcsecond pixel scale over 19 × 19 arcseconds. This will represent a major step forward, with a significantly better spatial resolution than that of the Hubble Space Telescope (HST) and even the James Webb Space Telescope (which has a pixel scale ~ 30 milliarcseconds pixel^{-1}). Long-slit spectroscopy will be covered with two settings: a short slit

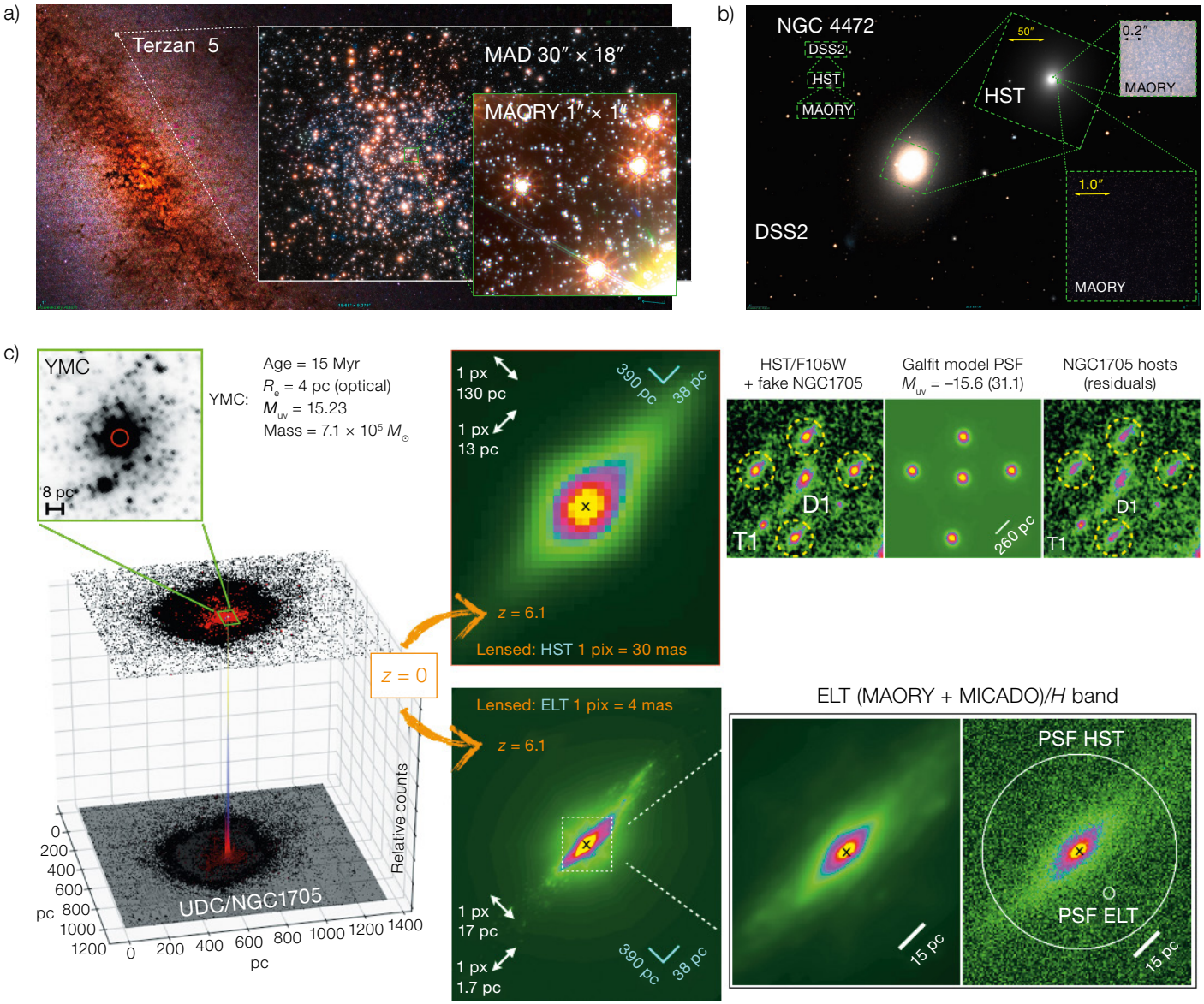

Figure 1. Combination of real and simulated images from the MAORY science cases White Book. a) Terzan 5 as imaged by MAD at VLT and by MAORY + MICADO. b) NGC 4470 as imaged by HST and MAORY + MICADO. c) 2D and 3D HST images of NGC 1705 and simulations at HST and MAORY + MICADO resolution lensed at z = 6.1.

of 0.84–1.48 μm, and a long slit of 1.48–2.46 μm (see Davies et al., p. 17 for a detailed description of the MICADO observing modes).

The science cases for MAORY + MICADO have been widely explored by the MAORY science team. A preliminary collection of the cases studied is reported in the MAORY science cases White Book available on the MAORY website[1].

Together the science cases address many of the major questions in astrophysics:

– Planetary systems, including cases in our own Solar System, exoplanets and the formation of planetary systems;
– Nearby stellar systems, comprising stars and stellar systems within our own Galaxy and its satellites;
– The local Universe, with science cases aimed at studying the stellar content and the structure of distant stellar systems that can be at least partially resolved into individual stars. In many cases they will fall within the range of resolved systems only thanks to the advent of MAORY + MICADO;
– The high-redshift Universe, with the science cases addressing the formation of structures and cosmology using the formidable sensitivity and resolution of MAORY + MICADO to probe the very distant Universe and consequently the earliest phases of galaxy formation, as well as high-energy phenomena over the range of cosmic distance and time made accessible by the ELT.

In Figure 1 we show a collection of real and simulated images selected from the MAORY White Book to illustrate the extreme capability and versatility of the MAORY + MICADO combination. The top left panel shows a zoom-in on a candidate building block of the Galactic bulge, the globular cluster Terzan 5, as imaged by the Multi-conjugate Adaptive optics Demonstrator (MAD) at the VLT (real image) and by MAORY + MICADO. Thanks to its unprecedented angular resolution, MAORY + MICADO will make it possible to study the dynamics of stars very close to the centre of a globular cluster and to reveal the presence of an intermediate-mass black hole (IMBH) with a mass in the range 10^2–10^4 $M_\odot$), shedding light on the origin of supermassive black holes (with masses larger than 10^6 $M_\odot$). The top right panel shows a zoom-in on the giant elliptical galaxy NGC 4470 in Virgo, as imaged by a 2.5-m ground-based telescope, by the HST, and by MAORY + MICADO. Making use of spectroscopic and high-angular-resolution observations, we will be able to study the chemical composition of globular clusters from the Local Group to the VIRGO/Fornax galaxy cluster and the metallicity gradients in giant elliptical galaxies, and to resolve individual stars in nearby nuclear star clusters. The bottom panel illustrates a simulation of the ultra-compact dwarf galaxy NGC 1705 hosting its Super Star Cluster (SSC) (from Vanzella et al., 2019). On the left hand side is the HST image in 2D and 3D. To the right of that, the upper panel shows the modelled noiseless simulation at HST resolution lensed at z = 6.1, and in the lower panel is the same simulation with MAORY + MICADO in the MCAO narrow-field mode, alongside a zoomed-in region in which the physical scale and the two point spread functions (HST and MAORY + MICADO) are indicated. This figure shows that, depending on the local magnification, a SSC at z ~ 6 will likely be resolved, and with a proper point spread function deconvolution we will resolve the light profile of the star cluster down to a resolution of 4–8 pc, allowing a proper photometric and spectroscopic analysis of SSCs. These kinds of studies will be fundamental tools with which to characterise star clusters at cosmological distances and their influence on the surrounding medium (for example, feedback and ionisation).

Instrument design

Optical design

The original optical design was altered in early 2020 in order to provide each supported instrument with a gravity-invariant port. The new MAORY main-path optical layout is envisaged to have eight reflections: two aspheric concave mirrors, two spherical DM, one convex and one concave, one dichroic and three fold mirrors. This optical layout (side and top view) is shown in Figure 2, where the right panel also shows the second port focal plane, the LGS module area envelope and the MICADO envelope. However, under the current technical specification, the MAORY baseline includes only one DM (with a convex shape and a diameter of about 900 mm) while the second, concave, DM is replaced by a rigid mirror that can itself be replaced with a DM in future.

An aspheric correcting plate near the telescope focal surface (Rakich & Rogers, 2020a,b) allows the optical relay to simultaneously produce stigmatic images of the telescope focus and of laser guide stars over the full range of object distances. The plate correction also improves the image quality of system pupils and meta-pupils. In the presented optical configurations, the plates are at about 350 mm after the focal plane.

Mechanical design

Starting from the new optical design, developed in 3D (not in a single plane as before; see Figure 2), the mechanical design has been completely revised. The main structure is now based on a lattice-work tower made of standard structural steel truss-beam-shaped pipes (welded and bolted) with different section properties. The instrument is completed by an LGS wavefront sensor (WFS) module with 6 beacons (upgradable to 8) arranged to form a 45-arcsecond asterism, an NGS WFS module with 3 low-order sensors and 3 references patrolling a technical field of 160 arcseconds, a real-time computer (RTC) sized for 8 LGS and 2 post-focal DM with 1500 actuators and a calibration and test unit.

A general overview of the design adopted as baseline is shown in Figure 3.

Performance

The expected performance of the MAORY instruments is summarised in Figure 4. In the left panel we show the Strehl Ratio (SR) value as a function of

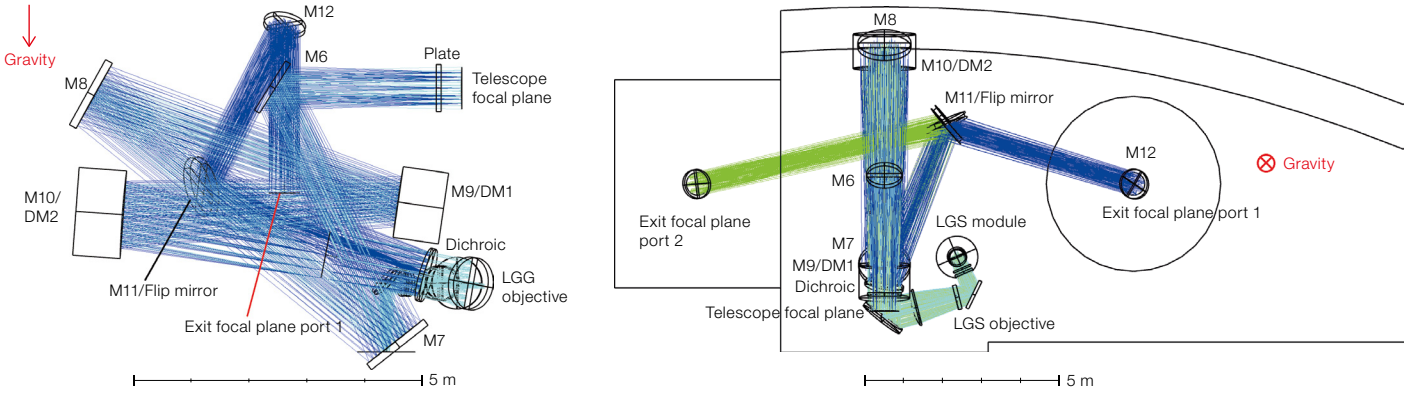

Figure 2. MAORY optical baseline side view layout (left) and top view layout (right).

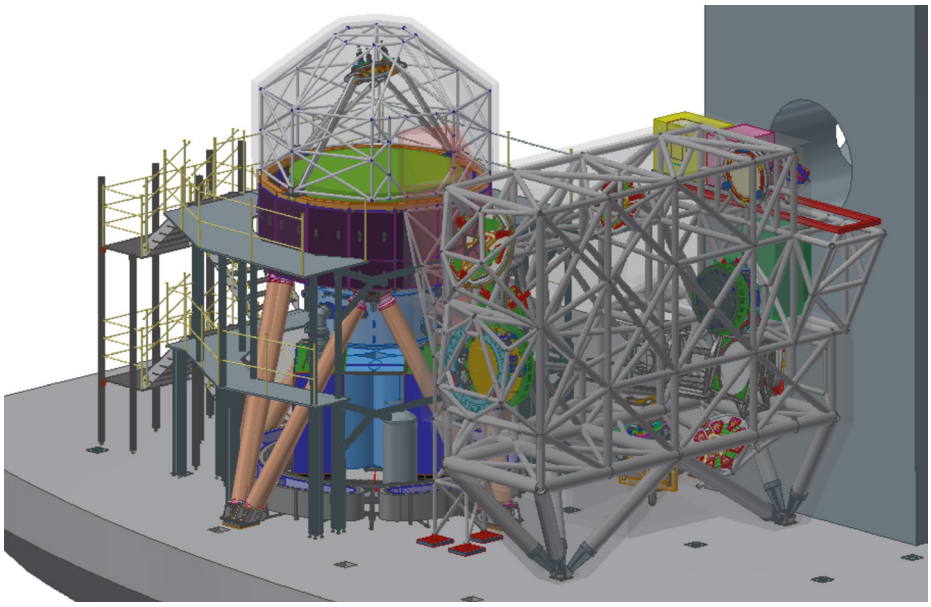

Figure 3. General overview of the MAORY instrument (with thermal cover shown transparent) installed on the Nasmyth platform with MICADO.

the radial distance (in arcseconds) from the field centre for different atmospheric conditions, in the case of only one post-focal DM (as it is in the baseline configuration, solid lines) and in the case of two post-focal DM (dashed lines). In the right panel we show the sky coverage as a function of the SR value, again for different atmospheric conditions and with one DM (solid lines) and two DM (dashed lines). To calculate the sky coverage we make use of a statistical approach to calculate the number of times that a given performance is obtained on a simulated field at the south Galactic pole (SGP). The performance figures that we quote at 50% sky coverage are hence to be seen as the median performance obtained for a large set of random pointing at SGP which is indeed conservative with respect to the MAORY requirement to reach a SR of 30% on 50% of the observable sky (the goal being a SR of 50% with 2 DM).

As shown in Figure 4, a system with a single DM is capable of delivering a SR above 40% at 50% of sky coverage — well above the requirement — while the presence of the second DM is fundamental to pushing the system towards maximal performance and higher robustness to varying atmospheric and observing condition.

Finally we would like to stress that a single set of performance figures cannot be fully representative of the real performance achievable on a specific target since many variable factors (like the atmospheric conditions, NGS asterism, sodium layer variability) play a role in the determination of the final result. As outlined also by Davies et al. (p. 17), potential users are encouraged to use the instrument data simulator ScopeSim[2] to familiarise themselves with the MAORY + MICADO instrument and to obtain a more accurate estimate of the performance on their own targets.

Acknowledgements

MAORY is a consortium involving more than 70 people from institutes in Italy, France, Ireland and Germany working together with ESO[a]. The authors are grateful to their own institutes for financial support.

References

Davies, R. et al. 2018, Proc. SPIE, 10702, 107021S
Vanzella, E. et al. 2019, MNRAS, 483, 3618
Rakich, A. & Rogers, R. J. 2020a, Proc. SPIE, 11548, 115480M
Rakich, A. & Rogers, R. J. 2020b, Proc. SPIE, 11451, 114514J

Links

[1] MAORY web pages with the science cases White Book, a summary of the project and a list of people and partners involved: http://wwwmaory.oabo.inaf.it/
[2] ScopeSim is available at https://scopesim.readthedocs.io/

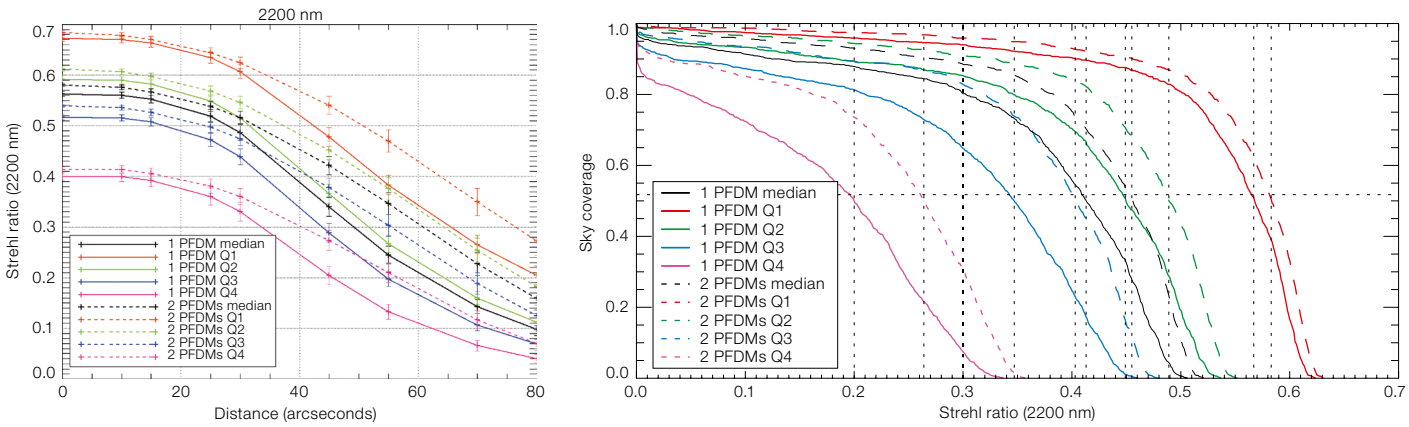

Figure 4. Summary of MAORY performance. Left: Strehl ratio (SR) as function of the radial distance from the field centre for different atmospheric conditions and 1 or 2 post-focal DM. Right: Sky coverage as function of the SR value for different atmospheric conditions and 1 or 2 post-focal DM.

DOI: 10.18727/0722-6691/5217

MICADO: The Multi-Adaptive Optics Camera for Deep Observations

Richard Davies[1]
Veronika Hörmann[1]
Sebastian Rabien[1]
Eckhard Sturm[1]
João Alves[2]
Yann Clénet[3]
Jari Kotilainen[4]
Florian Lang-Bardl[5]
Harald Nicklas[6]
Jörg-Uwe Pott[7]
Eline Tolstoy[8]
Benedetta Vulcani[9]
and the MICADO Consortium[a]

[1] Max Planck Institute for Extraterrestrial Physics, Garching, Germany
[2] University of Vienna, Austria
[3] LESIA, Université PSL, CNRS, Sorbonne Université, Université de Paris, Observatoire de Paris, France
[4] FINCA, University of Turku, Finland
[5] Universitäts-Sternwarte, Munich, Germany
[6] Georg-August-Universität, Göttingen, Germany
[7] Max Planck Institute for Astronomy, Heidelberg, Germany
[8] Kapteyn Institute, Groningen, the Netherlands
[9] INAF – Osservatorio di Padova, Italy

The Multi-adaptive optics Imaging CamerA for Deep Observations (MICADO) will image a field of view of nearly 1 arcminute at the diffraction limit of the Extremely Large Telescope (ELT), making use of the adaptive optics correction provided by single-conjugate adaptive optics (SCAO) and multi-conjugate adaptive optics (MCAO). Its simple and robust design will yield an unprecedented combination of sensitivity and resolution across the field. This article outlines the characteristics of the observing modes offered and illustrates each of them with an astrophysical application. Potential users can explore their own ideas using the data simulator ScopeSim.

Introduction

MICADO will provide the ELT with a diffraction-limited capability for imaging, coronagraphy, and slit spectroscopy at near-infrared wavelengths. The instrument is optimised to work with the laser-guide-star MCAO system developed by the Multi-conjugate Adaptive Optics RelaY (MAORY) consortium. It will also have a SCAO mode that uses just a single natural guide star. Following the start of Phase B in October 2015, MICADO had its Preliminary Design Review in November 2018, and is ready for its Final Design Review in 2021. The current plan is that, after an initial phase of operations at the ELT's first light, during which MICADO will be available only with the SCAO system, it will move to its final configuration where it interfaces to MAORY and will benefit from both a SCAO and a MCAO correction.

MICADO will be able to address many science topics relevant to modern astrophysics, and has clear synergies with other instruments and facilities. The science cases that have driven the design focus on five main themes: (i) galaxy evolution at high redshift, (ii) black holes in galaxy centres, including the centre of the Milky Way, (iii) resolved stellar populations, including photometry in galaxy nuclei, the initial mass function in young star clusters, and intermediate-mass black holes in globular clusters, (iv) characterisation of exoplanets and circumnuclear discs at small angular scales, and (v) the Solar System. To address these, MICADO will exploit its sensitivity and resolution in four observing modes: standard imaging, astrometric imaging, coronagraphic imaging, and spectroscopy. Both SCAO and MCAO can be used with all observing modes, albeit with some limitations, and the choice depends on the specific scientific goals as well as the target itself. Details about the MCAO system, and some further science applications, are given in the accompanying article on MAORY (Ciliegi et al., p. 13).

Observing modes

Standard imaging

Standard imaging is the simplest observing mode, designed to obtain images at the diffraction-limited resolution of 4–12 milliarcseconds at wavelengths of

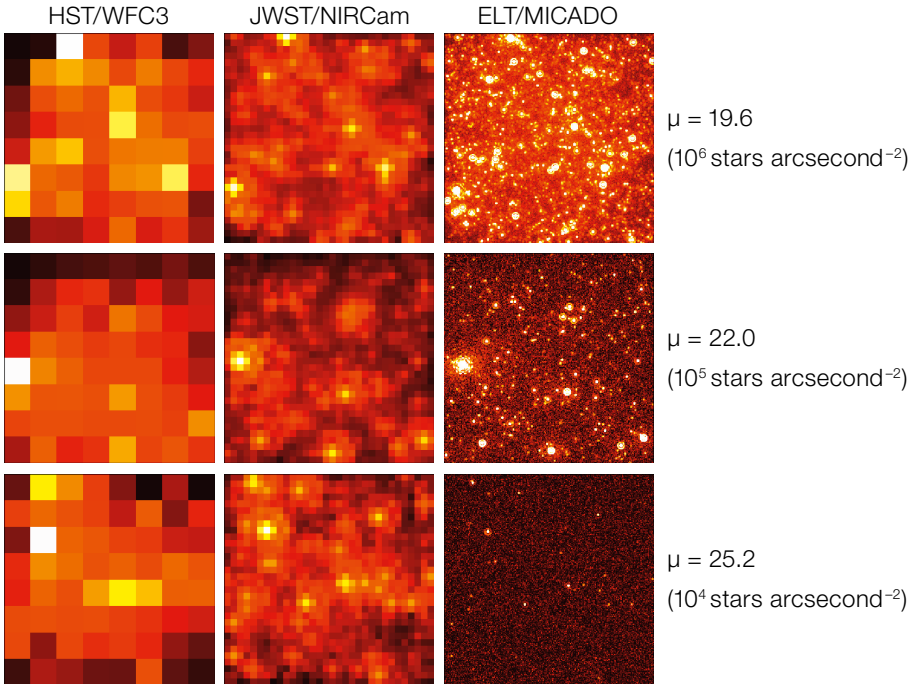

Figure 1. Comparison of how crowded stellar fields would appear when observed by the HST (left), the JWST (centre), and MICADO (right). The bottom row matches the stellar density at a radius of 4–5 R_{eff} for NGC 4472 in the Virgo Cluster and represents the limit of JWST resolution. The top row corresponds to 2 R_{eff} in the same galaxy and many individual stars can still be measured by MICADO. Each panel is 1 arcsecond across. These simulations were performed with ScopeSim.

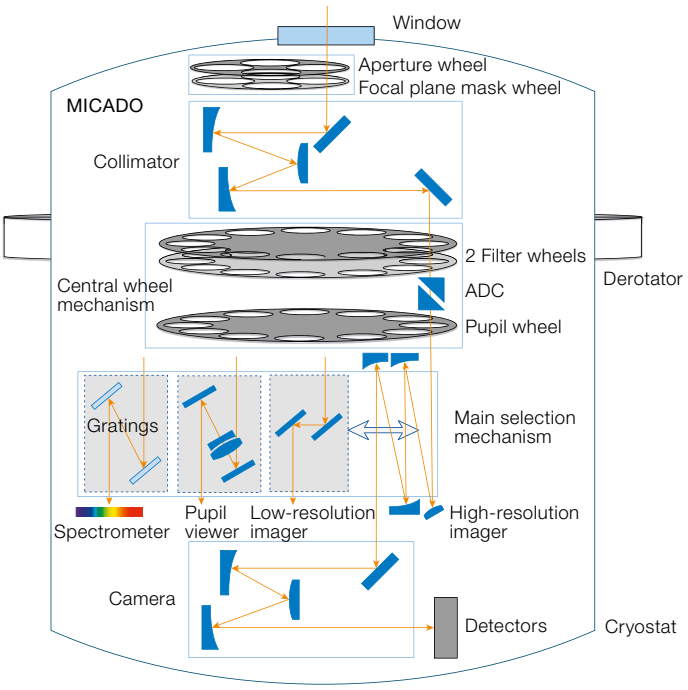

Figure 2. Schematic view of the MICADO design concept, illustrating how the cold optics and mechanisms are assigned to separate modules that can be tested separately and then integrated together in the cryostat.

0.8–2.4 μm. It can be used with SCAO, but will benefit enormously from the MCAO capability, which provides a uniform point spread function (PSF) over the field as well as high sky coverage. An array of 3 × 3 H4RG detectors (150 million pixels) provides a field of view of 50.5 × 50.5 arcseconds at a pixel scale of 4 milliarcseconds with the low-resolution imager. Complementing the multiplex advantage of this configuration is the high-resolution imager with a 1.5-milliarcsecond pixel scale over a 19 × 19 arcsecond field of view. This fully samples the diffraction-limited PSF from 0.8 μm to 1.5 μm, and provides the fine sampling at the longer wavelengths needed for PSF de-blending in very crowded fields. An atmospheric dispersion corrector ensures that the PSF remains compact (indeed, the chromatic dispersion is large enough that, even for isolated point sources, the gain in sensitivity over most of the sky outweighs the loss in throughput due to the additional optics). And, while in typical observatories more than 90% of observations are performed with no more than 10 filters, MICADO offers considerable flexibility with its large filter wheels which are able to hold more than 30 filters.

With a point-source sensitivity comparable to that of the James Webb Space Telescope (JWST) and a resolution about a factor of 6 better, this mode is well suited to numerous science cases. For the specific topic of galaxy evolution over cosmic time, we now have a fairly robust outline, in terms of global properties, of how galaxies assembled and transformed into the present-day Hubble sequence. The next step is to resolve faint distant galaxies on sufficiently small scales, to assess their sub-galactic components (disc structures, nascent bulges, clumps, and globular cluster progenitors) at spatial scales < 100 pc — equivalent to the seeing limit for the nearby Virgo Cluster galaxies. Relatively unexplored regimes include lower-mass galaxies, comprising the bulk (by number) of the galaxy population, and galaxies at early cosmic times when they were building their first stars.

An alternative probe of galaxy evolution is via relic populations in local galaxies, performing photometry on individual stars to generate colour-magnitude diagrams. Detecting stars on the horizontal branch enables one to trace the star formation history of local galaxies to the reionisation epoch at redshift $z > 6$. The ultimate goal for resolved stellar populations is to measure individual stars in the central regions of elliptical galaxies in the Virgo Cluster. As can be seen in Figure 1, the extreme stellar crowding makes this very challenging. The JWST will be most effective in the outskirts of these galaxies, while the higher resolution of MICADO will enable it to probe within the central effective radius.

Astrometric imaging

One of the most challenging requirements for MICADO is to perform astrometry over the full field at a precision better than 50 microarcseconds, with a goal of 10 microarcseconds — which is comparable to that achieved by the GRAVITY instrument at ESO's Very Large Telescope Interferometer (VLTI) and dedicated space missions such as Gaia, but with much fainter stars. To understand what that requirement means, we must distinguish between absolute and relative astrometry. Absolute astrometry is needed when comparing the positions of objects observed with different instruments, often in different wavebands. Because it relies on an external reference frame, which is dependent on the target field, it can only be done on a best effort basis. On the other hand, in the case of the MICADO instrument, the requirement refers to relative (or differential) astrometry, which is about changes in position between epochs and focuses on proper motion rather than position.

In this context, an obvious astrophysical rationale is the use of stellar proper motions to probe the existence and masses of black holes in stellar clusters and nearby low-mass dwarf galaxies. Studies of globular clusters have yielded a variety of tantalising results, but without robust detections. One key question concerns the relation between the mass of the central black hole and the velocity dispersion of the stellar spheroid around it. Intriguingly, a compilation of black hole mass limits for globular clusters concluded that the slope of the relation for those is rather shallower than that for galaxy bulges and elliptical galaxies. This implies a different regulation process in the star clusters, perhaps suggesting that many of those systems may be the stripped nuclei of dwarf galaxies. Again, current facilities are limited by the extreme crowding that occurs in the centres of

the star clusters, exactly where the key measurements have to be made. In particular, proper motions, rather than just line-of-sight velocity dispersions, are essential to measure the anisotropy, which can have a significant impact on the black hole mass derived. Suitable measurements that overcome the crowding will only become possible with the spatial resolution of the ELT.

Meeting this requirement is a major challenge (Pott et al., 2018). To do so, stability and calibration are more important than solely minimising the geometric distortion, which is < 0.4% and < 1.2% for the low- and high-resolution imagers, respectively. And it is necessary to distinguish between linear distortions over the full field, low-order distortions that affect ~ 10-arcsecond scales, and high-order distortions which dominate at < 1-arcsecond scales. These are handled in different ways most appropriate for each case, whether via instrument design (minimising mechanical and thermal flexure), operational scenario (use of calibration masks, and if needed, observational constraints), or post-processing (correcting low-order drifts between individual frames). The relative uniformity of the PSF enabled by MCAO is clearly an important factor in achieving the most precise astrometry.

Coronagraphic imaging

The study of planets around other stars is one of the fundamental science drivers for the ELT. Now that a large number of exoplanets are known, we are entering a phase driven by the need to characterise these planets, in particular the atmospheres of giant exoplanets. Direct imaging of exoplanets provides an opportunity to do this through the use of intermediate band filters that cover molecular absorption bands, enabling one to distinguish models with different temperatures, surface gravities, and clouds. Comparing observations with the Spectro-Polarimetric High-contrast Exoplanet REsearch instrument (SPHERE) to MICADO simulations for the planetary system around HR 8799 provides a glimpse of what it may be possible to achieve. Even in raw images, the inner two known planets are visible. And after basic processing it becomes possible to identify and characterise simulated fainter planets closer in. It opens up the very exciting potential to image planets for which a mass estimation is available from Gaia.

By exploiting the large aperture of the ELT, MICADO will achieve a meaningful contrast at very small inner working angles, and hence serve also as a pathfinder for future dedicated instrumentation. It will improve on a similar system on the VLT in a number of aspects: probing a factor of 5 closer to the primary star, increasing by a factor of 25 the contrast between the exoplanet PSF and the speckle noise that dominates in these locations, and elongation of the speckles which provides better discrimination between those and a compact exoplanet. The focus for MICADO will therefore be in terms of exoplanets at small orbital separations (~ 1 au) around nearby stars (< 20 pc), exoplanets at larger separations (> 10 au) around more distant stars (> 100 pc), and the circumstellar discs from which they form.

High-contrast imaging is an important driver for the SCAO system. The coronagraphy itself can make use of pupil tracking to enable angular differential imaging, and will be achieved via focal-plane and pupil-plane phase masks (in the former case, the centring of the star is actively maintained during the observation). Only basic post-processing is provided since algorithms evolve fast and the best one to use depends on the specific application. MICADO includes a pupil imager to ensure there is a detailed record of how the pupil appears, since the ELT pupil can change between nights, owing to “missing” segments and because the maintenance schedule leads to changing individual segment transmissions.

Spectroscopy

The rationale for spectroscopy in MICADO is to emulate the success of X-shooter while addressing a role complementary to the integral field spectroscopic capability of the High Angular Resolution Monolithic Optical and Near-infrared Integral field spectrograph (HARMONI, Thatte et al., p. 7). With a focus on faint compact or unresolved objects, MICADO uses a slit and provides a resolution of R ~ 20 000, corresponding to 15 km s^{-1} in the H band. The full bandpass is covered in just two settings: a short slit for 0.84–1.48 μm, and a long slit for 1.48–2.46 μm (and also 1.16–1.35 μm) that enables extraction of the sky background further off-axis. This is realised with a fixed configuration cross-dispersing spectrograph module. The wavelength range is defined solely by choice of slit and order-sorting filter. Since the focus is on compact objects, the role of MCAO here is to maximise the Strehl ratio in the centre of the field with a higher sky coverage than can be reached with SCAO.

There are a wide range of applications for this capability. At high redshift, one can measure the emission-line spectra of early supernovae or continuum absorption features in early-type galaxies to measure stellar populations and dynamics. More locally, one can use the line-of-sight velocity dispersions of nearby galaxies to constrain orbit-based models and hence derive black hole masses in galaxy nuclei, extending the currently accessible parameter space to lower black hole masses as well as more distant galaxies. In the Galactic centre, an exciting opportunity is to measure the spin of the black hole, a goal that is more tractable via spectroscopy than astrometry. This can be achieved by tracking a late-type star whose entire orbit lies within ~ 10 milliarcseconds (0.5 light days, about 1/10 of the S2 orbit) so that it is spatially indistinguishable from Sgr A* itself. Spectrally, determining the relative velocity of the star to a precision of < 1 km s^{-1} enables one to discern the impact on its orbit of the black hole’s quadrupole moment, which according to general relativity is fully determined by the spin. Even though in practice it is difficult to completely stabilise a source in the slit, sufficient precision can be reached via internal referencing between the stellar absorption features and the atmospheric absorption features imprinted into the observed continuum. Lastly, in terms of exoplanets, MICADO offers the potential for obtaining detailed spectra — with applications in both chemical and dynamical analyses — simply by exploiting the enhanced contrast due to the higher angular resolution of the ELT, without the need for simultaneous

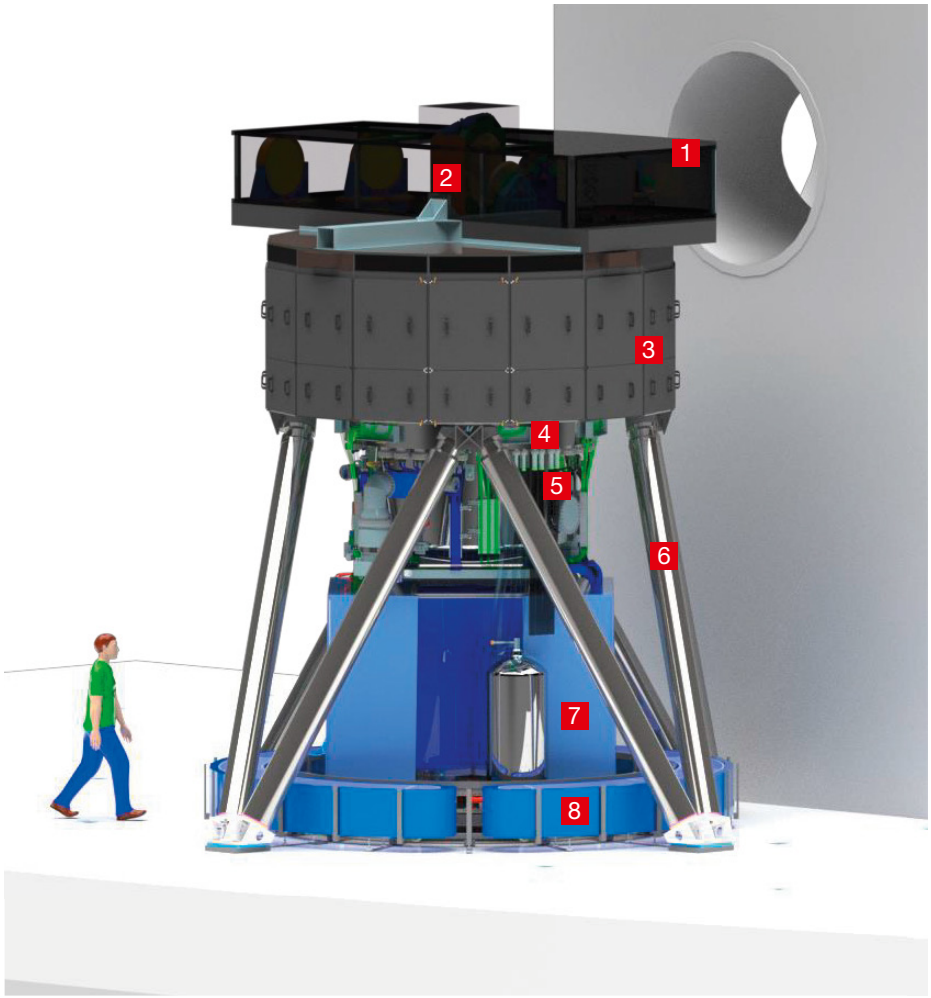

Figure 3. Rendering of MICADO in a stand-alone phase before it is integrated next to MAORY. The pre-focal station, which transfers the optical axis horizontally at a height of 6 m above the Nasmyth Platform, is indicated by the grey block. The key components of MICADO are labelled, and a person is shown for scale. For a view of MICADO in its final location next to MAORY, see the accompanying article on the MAORY system (Ciliegi et al., p. 13).

1. Calibration assembly, mounted next to relay optics, replicates ELT focal plane (later moves to MAORY bench)
2. Relay optics – transfers ELT focal plane downwards into MICADO (later exchanged for last MAORY mirror)
3. NGS WFS module, rotates under fixed cover – contains SCAO on top bench & MAORY NGS WFS on lower bench
4. Derotator
5. Cryostat, surrounded by peripheral devices
6. Support structure, for rotating mass (cryostat & NGS WFS module) as well as fixed upper platform
7. Co-rotating platform with electronics cabinets (due to cable length limitations)
8. Cable wrap for connection to external cabinets and services

coronagraphy. As an example, for HR8799e the flux from the halo of the star (type A5 with K ~ 5.2 magnitudes) within a 12-milliarcsecond aperture at an offset of 0.37 arcseconds is expected to be only about twice that in the PSF core of the exoplanet (K ~ 16.5 magnitudes). At this level, direct spectroscopy of the exoplanet is achievable within a reasonable integration time.

Instrument design concept

As a first-light instrument, MICADO has been designed to be as simple and robust as possible. Despite this, it contains a large number of mechanisms and control systems, and requires a huge amount of software and electronics. Although one might consider these as the brain and nervous system of the instrument, we do not discuss them in detail here. Instead we focus on the opto-mechanical concept; Figure 2 provides an outline of the key modules and functions. We refer the reader to Davies et al. (2016, 2018) for technical details and additional references, with the caveat that the instrument design has evolved considerably over the last few years.

The location of the 2-m diameter cryostat, the core of the instrument, within the global architecture is illustrated in Figure 3, which shows MICADO in its stand-alone configuration. The top platform, at a height of 6 m to match the optical axis of the ELT, hosts the calibration unit which is later moved to the MAORY bench, as well as the optics that relay the ELT focal plane down into the cryostat. On the way, the optical path passes through the natural guide star wavefront sensor (NGS WFS) module which has a lower level for the MCAO low-order wavefront sensors of MAORY and an upper level containing the SCAO system. When the SCAO system is used, a dichroic is moved into the optical path to reflect out the visible light. A natural guide star can then be picked off anywhere within an offset 6 × 20 arcsecond patrol field, enabling both on-axis and off-axis correction. This versatile system makes use of a modulated pyramid wavefront sensor, providing both the very good correction needed by high-contrast imaging and partial correction on stars fainter than V = 16 magnitude. A calibration unit in the same volume provides the ability to measure non-common path aberrations so that they can be corrected during science observations. The NGS WFS module is mounted rigidly onto the derotator together with the cryostat, to minimise differential flexure between them while tracking. This is all held up by an octopod support structure that provides space underneath for a co-rotating platform containing much of the electronics. This both keeps some cable lengths short and reduces the volume needed by the cable-wrap that provides connections to the observatory services and to the remaining electronics.

Following a light ray entering the cryostat through the entrance window, the first mechanism it encounters contains the focal plane masks (field stops, slits, coronagraphs, calibration mask).

The aperture wheel allows those masks to be mounted closer to each other, at the same time, providing an option for rapidly blocking the light path, which is needed for mitigating persistence on the detectors. After this, the collimator, the high-resolution imager and the camera below are designed and built as complete units out of AlSi alloy, so that the coefficient of thermal expansion of the mirrors is the same as their polished NiP coating. This avoids warping of the 20–30-cm mirrors when the optics are cooled with liquid nitrogen to 80 K. The central wheel mechanism contains the two filter wheels (1.25 m in diameter, each containing 16 slots of 140-mm diameter filters), the atmospheric dispersion corrector, and the pupil wheel (where the nominal cold stop diameter is 82 mm). These are mounted into a single pre-aligned unit that can then be easily integrated into the system. The main selection mechanism, which also has a diameter of 1.3 m, enables the choice of observing mode by rotating to different positions. In the open slot, the optical path is reflected through the zoom optics, a set of fixed mirrors that comprise the high-resolution imager. When switching to the low-resolution image, the mechanism rotates in a pair of fold mirrors that bypass these.

Similarly, by inserting suitable lenses one can instead re-image the pupil for calibration. And for spectroscopy one moves in the pair of cross-dispersed gratings. After the camera, the last unit is the focal plane array in which the detectors are mounted.

Performance

MICADO has a high throughput and a challenging wavefront error budget, both of which serve to maximise its sensitivity. The SCAO system will provide a Strehl ratio of ~ 65% in the *K* band on-axis using a bright NGS, while the MCAO system is expected to deliver a 30–50% Strehl ratio in the *K* band under moderate observing conditions and with a reasonable natural guide star asterism. From this we estimate the 5-hr, 5σ limiting point source magnitudes for imaging as approximately J_{AB} ~ 28.6, H_{AB} ~ 29.5, and K_{AB} ~ 29.1 magnitudes. In doing so, we caution that a single set of performance numbers does not reflect how well one might be able to make a specific set of measurements on a realistic source, that is perhaps extended or complex. And so we emphasise that the strength of MICADO is in combining this sensitivity with a resolution 5 times better than that of the VLT. It is for this reason that we encourage potential users to try out the instrument data simulator ScopeSim[1] (recently upgraded and expanded from the original SimCADO), and to test out their own ideas about how they might use MICADO.

Acknowledgements

The authors are grateful for the enormous effort invested into the project by the consortium and its various funding agencies. MICADO is a collaboration involving more than 100 people in Germany, France, the Netherlands, Austria, Italy, and Finland, working together with ESO.

References

Davies, R. et al. 2016, Proc. SPIE, 9908, 99081Z
Davies, R. et al. 2018, Proc. SPIE, 10702, 107021S
Pott, J.-U. et al. 2018, Proc. SPIE, 10702, 1070290

Links

[1] ScopeSim is available at https://scopesim.readthedocs.io/

Notes

[a] The MICADO partners and team members can be found at http://www.mpe.mpg.de/ir/micado

A huge structure is required to protect ESO's Extremely Large Telescope (ELT) from the elements. The telescope's structure and optical elements, including its giant 39-metre main mirror, will be housed in the largest telescope dome in the world, about 88 meters across, which is shown in this 3D rendering, along with the auxiliary building.

DOI: 10.18727/0722-6691/5218

METIS: The Mid-infrared ELT Imager and Spectrograph

Bernhard Brandl[1, 2]
Felix Bettonvil[1]
Roy van Boekel[3]
Adrian Glauser[4]
Sascha Quanz[4]
Olivier Absil[5]
António Amorim[6]
Markus Feldt[3]
Alistair Glasse[7]
Manuel Güdel[8]
Paul Ho[9]
Lucas Labadie[10]
Michael Meyer[11]
Eric Pantin[12]
Hans van Winckel[13]
and the METIS Consortium[a]

[1] Leiden University, the Netherlands
[2] Faculty of Aerospace Engineering, TU Delft, the Netherlands
[3] Max Planck Institute for Astronomy, Heidelberg, Germany
[4] Department of Physics, ETH Zürich, Switzerland
[5] STAR Institute, Université de Liège, Belgium
[6] Faculdade de Ciencias da Universidade de Lisboa, Portugal
[7] UK Astronomy Technology Centre, Edinburgh, UK
[8] Department of Astrophysics, University of Vienna, Austria
[9] Institute of Astronomy and Astrophysics, Academia Sinica, Taipei, Taiwan
[10] I. Physikalisches Institut, Universität zu Köln, Germany
[11] Department of Astronomy, University of Michigan, Ann Arbor, USA
[12] CEA Saclay, IRFU, Gif-sur-Yvette, France
[13] Instituut voor Sterrenkunde, KU Leuven, Belgium

The Mid-infrared ELT Imager and Spectrograph (METIS) will provide the Extremely Large Telescope (ELT) with a unique window to the thermal- and mid-infrared (3–13 µm). Its single-conjugate adaptive optics (SCAO) system will enable high contrast imaging and integral field unit (IFU) spectroscopy (*R* ~ 100 000) at the diffraction limit of the ELT. This article describes the science drivers, conceptual design, observing modes, and expected performance of METIS.

Introduction

METIS will be a versatile instrument serving a wide range of science applications that target the cool and dusty Universe. Its main science drivers are studies of exoplanets and proto-planetary discs. To that end, METIS will offer a combination of high angular resolution — six times that of the James Webb Space Telescope (JWST) — high-contrast imaging (HCI) with coronagraphy, and high spectral resolution (up to *R* ~ 100 000). Thanks to the ELT's 39-m aperture, METIS will have a sensitivity to spectrally unresolved emission lines similar to that of the JWST, and a point source sensitivity to continuum emission similar to that of Spitzer-IRAC. In terms of instruments at ESO's Very Large Telescope (VLT), METIS can be thought of as a combination of the Enhanced Resolution Imager and Spectrograph (ERIS), the Cryogenic high-resolution InfraRed Echelle Spectrograph (CRIRES), and the VLT Imager and Spectrometer for mid-InfraRed (VISIR), but enhanced with the spatial resolution and collecting area of the 39-m ELT aperture.

METIS is being designed and built by a consortium of 12 partner institutes from 10 countries[a]. The Principal Investigator is Bernhard Brandl and the project office is located at Leiden University. More information on the project, as well as the full list with names of the METIS team members, can be found on the METIS website[1].

While the origin of METIS dates back to its Phase A study in 2008/09, the instrument concept has evolved quite considerably since then; most notably streamlining the instrument modes and strengthening its high-contrast imaging performance. Phase B started in September 2015 and was concluded with a successful Preliminary Design Review in May 2019, aiming for a Final Design Review in 2022.

METIS science

METIS will address a broad range of science cases. These include investigations of Solar System objects, young stellar clusters and massive star formation, active galactic nuclei (AGN), evolved stars, the centre of our Milky Way, and star formation in other galaxies. On top of that, there are two science areas that have been driving the key instrument requirements: circumstellar discs and extrasolar planets.

METIS will provide access to those regions of protoplanetary discs where the bulk of terrestrial planet formation takes place and will extend the existing studies of disc kinematics and (molecular) composition with the Atacama Large Millimeter/submillimeter Array (ALMA) toward the inner regions of the disc. Two key aspects will be the distribution of water and organic molecules in the innermost disc regions (for example, Pascucci et al., 2013; Banzatti et al., 2017) and the use of isotopologue abundances (of CO, for example) to investigate the mixing of material within a large number of discs (for example, Smith et al., 2009; Brown et al., 2013). Significantly, METIS will also be able to identify signatures of ongoing planet formation and even detect directly young forming planets embedded within discs from kinematical imprints (see, for example, Teague et al., 2018 and Pinte et al., 2018 for studies using ALMA). It is these applications that drive the requirements for the high-dispersion IFU mode in the *L* and *M* bands. For the first time, disc gaps and substructures, frequently detected with ALMA at (sub)millimetre wavelengths (for example, Andrews et al., 2018) and with the Spectro-Polarimetric High-contrast Exoplanet Research instrument (SPHERE) at near-infrared wavelengths in scattered light (for example, Avenhaus et al., 2018), can be revealed with comparable spatial resolution in the mid-infrared.

Truly new science is expected from the direct detection of extrasolar planets, for example, by constraining the luminosities of gas giant exoplanets that have an empirical mass estimate from radial velocity measurements (or, soon, from GAIA astrometry). The high-dispersion IFU mode in the *L* and *M* bands will allow the exoplanet community to expand significantly upon the pioneering work with CRIRES (and soon CRIRES+) to detect and characterise the atmospheric composition and dynamics of hot — and with METIS also warm — exoplanets (for

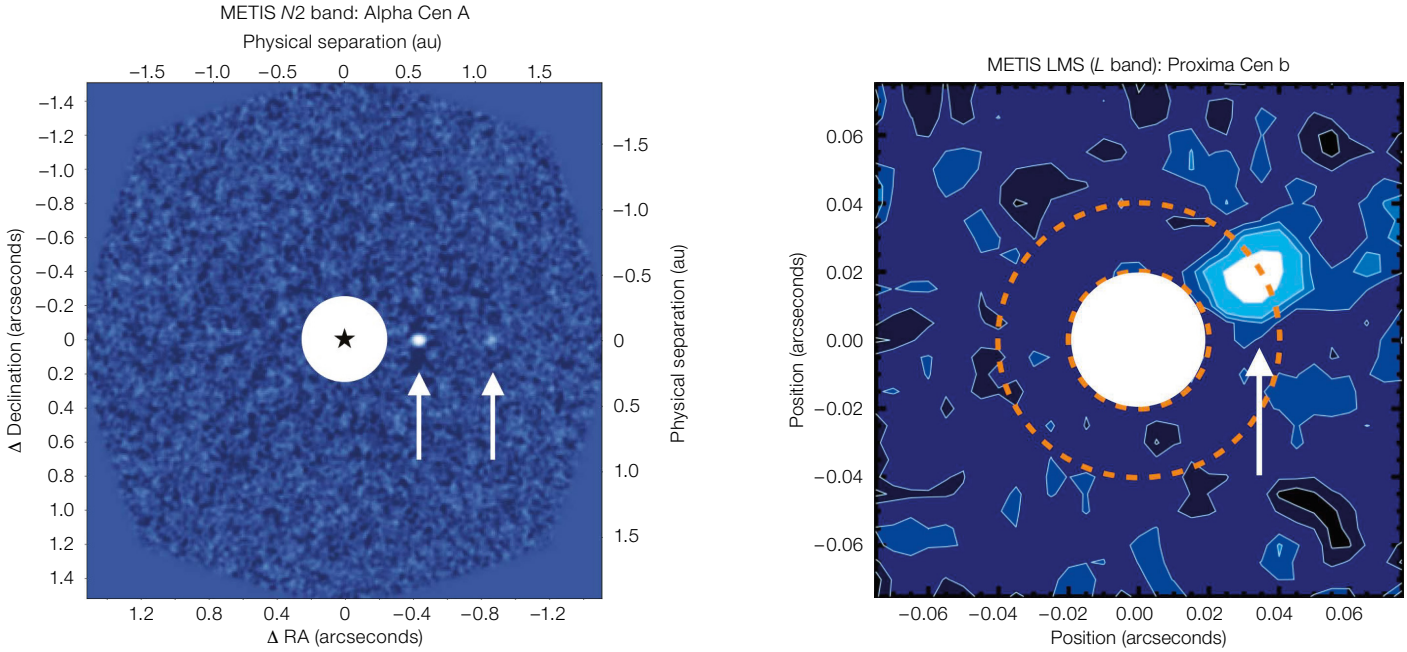

Figure 1. Left: Feasibility study to investigate if METIS can detect an Earth twin around Alpha Cen A at quadrature. These simulations are carried out with the METIS end-to-end high-contrast simulator and assume 5 hr of on-source time. In this case, two Earth-like (i.e., Earth radius and albedo) planets were inserted, one at 1.1 astronomical units (au) and one at 0.55 au (white arrows). Both planets are detected, with a signal-to-noise ratio of ~ 6 and ~ 10, respectively. Given the higher luminosity of the star, an Earth twin (i.e., same size and emission spectrum) would be located at ~ 1.1 au around Alpha Cen A. Right: Simulations of the METIS IFU performance on the Proxima system at 3.8 μm. Assuming a 1.1 $R_{\oplus}$ planet radius, a Bond albedo of 0.3, 50% illumination, an achieved coronagraph-aided contrast of 1:500 at 2 λ/D, and 10 hours of observing time, the planet is clearly detected in reflected light.

example, Brogi et al., 2016; Birkby et al., 2017). In addition, METIS will be able to investigate less massive, Saturn- and Neptune-like objects, and not only the Jupiter-class objects accessible today. Finally, it is expected that METIS will take the first steps towards the direct detection and characterisation of nearby temperate terrestrial exoplanets (see Figure 1). Following up on the New Earths in the Alpha Centauri Region (NEAR) experiment (Kasper at al., 2019) on the VLT, METIS will be able to test observationally whether our nearest neighbours harbour rocky worlds (cf. Quanz et al., 2015). The nearest star known to host a rocky, temperate planet is Proxima Centauri (Anglada-Escudé et al., 2016) and METIS will be able to detect the planet directly and — possibly — probe its atmospheric composition (see Figure 1).

A lot of effort is currently being devoted to expanding the capabilities of the METIS instrument simulator to assess the feasibility of (new) science cases and the required observational effort. The community is warmly invited to download, test and use SimMETIS[2], provide critical feedback and expand the suite of exciting science cases addressable with METIS.

Instrument concept

Main challenges

While any instrument on the ELT has to face numerous challenges, the two specific main challenges for METIS are the required high optical performance and the optimal control of the thermal background.

The METIS optical system is required to provide diffraction-limited performance in the *L*, *M* and *N* bands, corresponding to point spread functions ranging from 0.017 arcseconds FWHM at 3 μm to 0.070 arcseconds at 13 μm. METIS is equipped with a pyramid wavefront sensor inside the cryostat, operating in the *H* and *K* bands as part of the SCAO system which controls the ELT's adaptive mirrors M4 and M5. The AO guide star can be picked up anywhere within a circular field of view (FoV) with a diameter of 27 arcseconds, centred on the optical axis. In most cases the "guide star" will be the science target itself. To enhance the visibility of faint sources near bright stars, METIS uses various coronagraphic masks (see below), which require accurate and stable pupil alignment.

As with any ground-based thermal-infrared instrument, METIS needs to reduce the thermal emission from the atmosphere, the telescope mirrors and the telescope spiders to its fundamental limit. METIS is expected to operate in pupil-tracking mode to block the emission from the spiders effectively. Further background subtraction is accomplished via a combination of fast (~ 1 Hz) chopping offsets by a cold, fast, internal beam-chopping mirror, which enables more complex chopping patterns, and slow (~ 1 per min) nodding offsets by the telescope.

Conceptual design

The optical overview of METIS is shown in Figure 2. METIS consists of two

science modules: a diffraction-limited imager with two wavelength channels, one for the *LM* band and one for the *N* band; and an IFU-fed, diffraction-limited, high-resolution *LM*-band spectrograph.

These science modules are attached to the Common Fore-Optics (CFO), which consists of two re-imagers that prepare the beam such that it arrives stabilised at the science modules. For this purpose, the CFO includes an atmospheric dispersion corrector for two fixed zenith angles, a derotator to stabilise the field or the pupil orientation, a pupil stabilisation mirror, a beam chopper for background reference measurements, and several pupil- and focal-plane wheels which host coronagraphs, slits and field masks. After the first re-imager, the light is spectrally split by a dichroic to feed the cryogenic AO wavefront sensor. A pick-off element can be inserted to guide the light into the *LM*-spectrometer.

The imager includes a common collimator, after which a dichroic element splits the light into the two wavelength channels where a set of filters, pupil masks and grisms can be inserted into the beam. A three-mirror-anastigmat camera focuses the light onto the science detectors: a Teledyne HAWAII-2RG in the *L* and *M* bands, and a Teledyne GeoSnap in the *N* band. The *LM*-spectrometer optically rearranges the field by means of a mirror slicer, followed by the pre-dispersion prism. The user can select between the full IFU field or a subset of slits with an extended wavelength coverage. After the high-resolution immersed grating the light is focused onto a 2 × 2 mosaic of Teledyne HAWAII-2RG detectors.

All optics are cryogenically cooled to ~ 70 K with the exception of the imager, which is at ~ 40 K, and the detectors, which are at 30–40 K. A cryostat provides the cryo-vacuum environment using three 2-stage pulse-tube coolers and liquid nitrogen for its radiation shields. The cryostat is supported by a support structure (Figure 3). All 22 cryo-mechanisms, heaters and sensors and all elements of the warm calibration unit are controlled by the instrument control system. A warm calibration unit on top of the cryostat provides calibration and alignment tools for daytime calibration and for the instrument integration and test phase.

Observing modes

METIS offers five main observing modes, which are described in more detail below. These observing modes can be used in 24 different instrument configurations, not including the different science and neutral density filters. The online METIS app[3] offers a simple and interactive illustration of the METIS configuration for each observing mode.

Figure 2. Optical Layout of METIS.

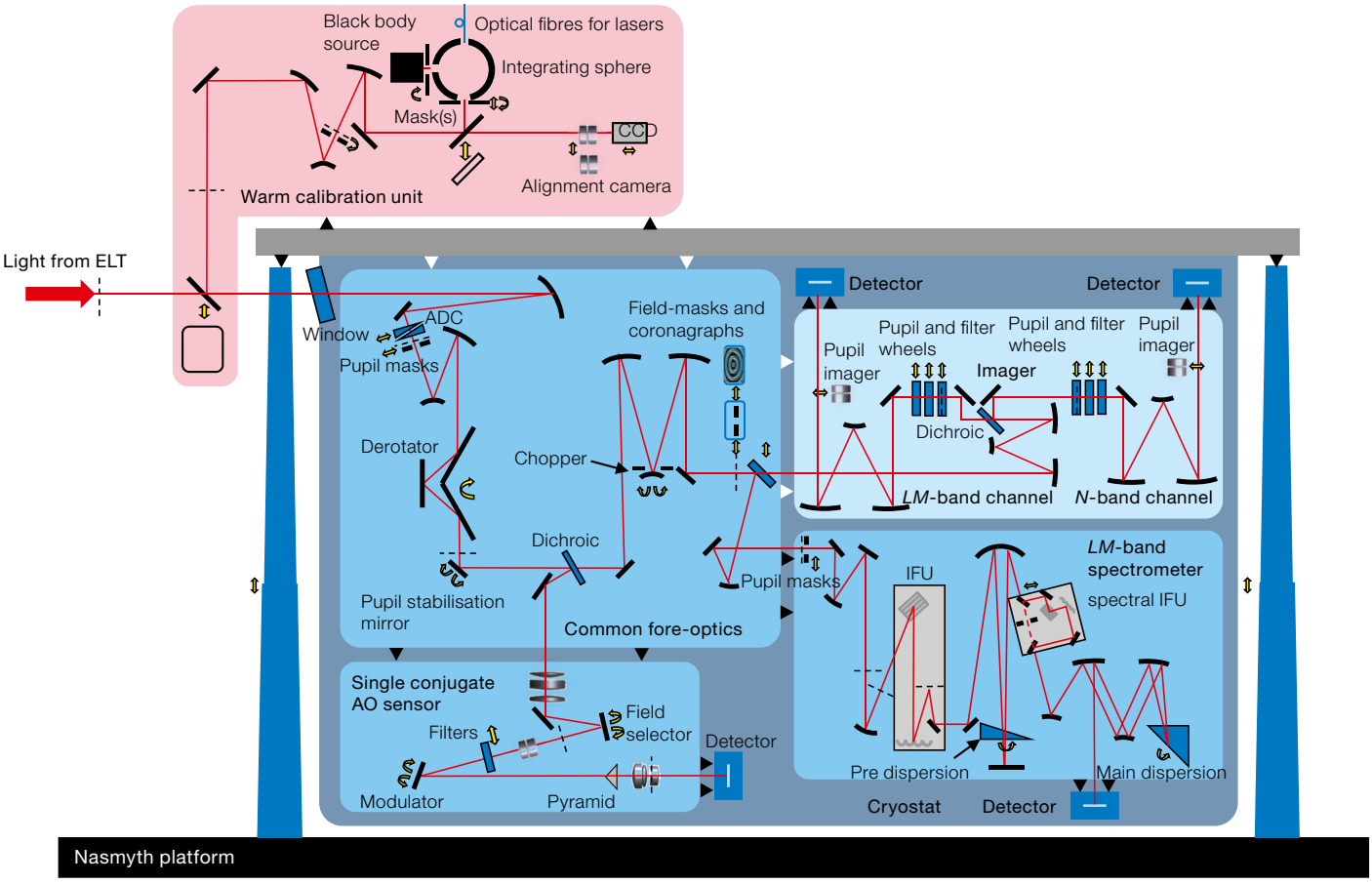

	Filter	λ_c	$\Delta\lambda$	Point source	Surface brightness
Units		µm	µm	µJy (5σ in 1 hr)	mJy arcsec^{-2} (5σ in 1 hr)
Continuum imaging	*L'*	3.79	0.63	0.48	1.0
	short-*L*	3.31	0.43	0.36	1.0
	HCI-*L* short	3.60	0.22	0.53	1.2
	HCI-*L* long	3.82	0.27	0.73	1.5
	M'	4.80	0.60	3.8	5.0
	N1	8.65	1.16	25	10
	N2	11.20	2.36	30	7.2
Spectral feature imaging	H_2O-ice	3.10	0.22	0.35	1.1
	PAH 3.3	3.30	0.07	1.3	3.5
	Br-alpha	4.05	0.03	4.4	8.0
	$CO_{(1-0)}$/ice	4.66	0.22	4.4	6.1
	PAH 8.6	8.60	0.45	39	16
	PAH 11.25	11.20	0.35	75	18
	[S IV]	12.82	0.23	89	24
	[Ne II]	10.50	0.19	170	31
Longslit spectroscopy	*L* (*R* ~1400)	3.53		5–9 × 10^{-18} erg s^{-1} cm^{-2}	
	M (*R* ~ 1900)	4.9		4 × 10^{-17} erg s^{-1} cm^{-2}	
	N (*R* ~ 400)	10.50		4 × 10^{-16} erg s^{-1} cm^{-2}	
IFU spectroscopy	*L* (*R* ~ 100 000)	3.8		7–20 × 10^{-19} erg s^{-1} cm^{-2}	
	M (*R* ~ 100 000)	4.8		8 × 10^{-18} erg s^{-1} cm^{-2}	

Table 1. METIS filter bands and achievable sensitivities. The listed sensitivities of 0.48 µJy (*L'*), 4.8 µJy (*M'*), and 30 µJy (*N2*) correspond to *L'* = 21.8 magnitudes, *M'* = 19.0 magnitudes, and *N2* = 15.1 magnitudes. The given ranges of spectroscopic sensitivities are caused by regions with high telluric line densities.

Direct imaging in the *L*, *M* and *N* bands

Imaging in the *L* and *M* bands is performed with the short-wavelength arm (the *LM*-arm) of the imager, which provides a square FoV of 10.5 arcseconds on a side, sampling the focal plane with 5.5-milliarcsecond pixels. The long-wavelength arm (the *N*-arm) of the imager provides *N*-band imaging with a 13.5 × 13.5 arcseconds FoV and 6.8-milliarcsecond pixels. Observations are usually performed in pupil-tracking mode for optimal background rejection, with image de-rotation and stacking of the short exposures in post-processing. The expected sensitivities to point sources and spatially extended emission, as well as the available filter bands, are listed in Table 1.

High-contrast imaging (HCI) in the *L*, *M* and *N* bands

METIS is equipped with several coronagraphs for HCI observations. The *LM*-arm of the imager contains an Apodised Phase Plate (APP), a coronagraph that is located in the pupil plane, works on all sources in the field, and is insensitive to pointing jitter. It delivers a dark region next to a bright source, where faint sources can be detected. The light from the bright source is not blocked. Both the *LM*-arm and the *N*-arm of the imager are equipped with several focal-plane-based coronagraphs. The Classical Vortex Coronagraph (CVC) efficiently blocks the light from a bright central source. It is only effective on-axis and requires the bright source to be precisely centred on the mask. Centring is achieved by applying the Quadrant Analysis of Coronagraph Images for Tip-Tilt Sensing (QACITS) algorithm on the science data at a closed loop control frequency of ~ 0.1 Hz. The vortex coronagraph can also be used in conjunction with an apodising pupil mask prior to the vortex phase mask, resulting in a Ring-Apodised Vortex Coronagraph (RAVC) for maximum contrast performance at the smallest angles from the central source.

Long-slit spectroscopy in the *L*, *M* and *N* bands

Each arm of the METIS imager is equipped with grisms and a set of five 10-arcsecond-long slits, ranging in width from 19 to 114 milliarcseconds. Their spectral resolutions are listed in Table 1. For maximum efficiency, chopping and nodding are usually done in two or more positions along the slit. Long-slit observations will be performed in field-tracking mode to maintain the position angle of the slit on the sky. The telluric calibration is expected to rely primarily on fitting the observations to synthetic transmission spectra using Molecfit for a given atmospheric water vapour and temperature profile, measured by an on-site radiometer in the direction of observation.

IFU spectroscopy in the *L* and *M* bands

The high-resolution (*R* ~ 100 000) spectrograph provides integral-field spectroscopy in the *L* and *M* bands. In its nominal mode the FoV of the IFU is 0.58 × 0.93 arcseconds, cut into 28 slices, each 0.021 arcseconds wide and 0.93 arcseconds long. All 28 slices of a selected spectral order are projected onto a 2 × 2 mosaic of detectors with a plate scale of 8.2 milliarcseconds per pixel. Since the point spread function is undersampled in the across-slice direction, a complete observation will consist of either a series of exposures with small dithers/offsets in the across-slice direction or a series of exposures where the field has been rotated by 90°, ensuring that both along- and across-slice directions are equally well sampled during part of that series. The telluric calibration is foreseen to be primarily model-based, analogues to the longslit modes.

The nominal simultaneous wavelength coverage (Table 1) can be increased in the so-called "extended wavelength coverage" mode, in which only three slices are projected on the focal plane, but with a larger $\Delta\lambda$ of the selected order than in the nominal mode. An instantaneous wavelength coverage of up to 300 nm can be achieved at the expense of spatial coverage.

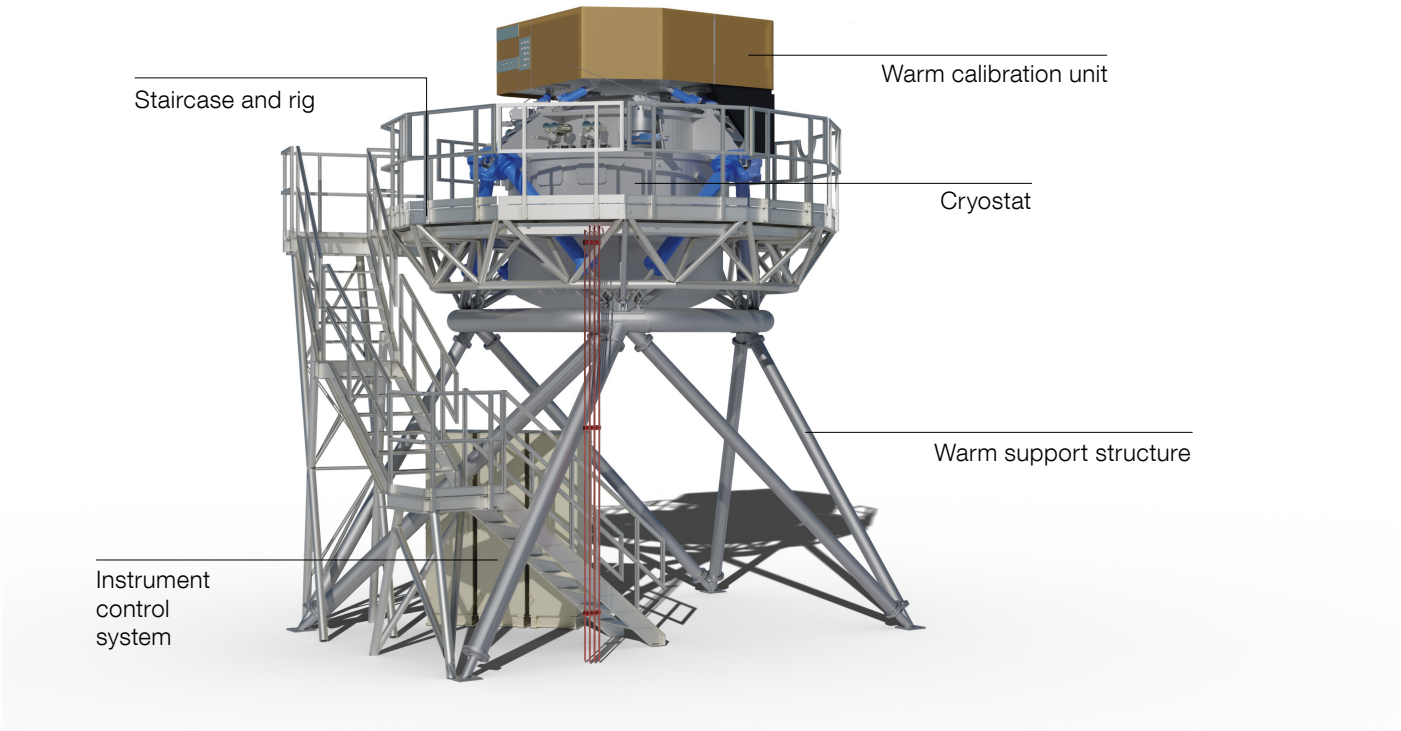

Figure 3. This engineering drawing of METIS shows its updated design following the Preliminary Design Review of the instrument.

IFU spectroscopy combined with coronagraphy

The *LM* high-resolution spectrograph can be used in combination with coronagraphy to suppress straylight from very bright sources. The observer can choose the APP coronagraph, which can be configured such that the point spread function dark region falls onto the image slicer while the bright source is directed toward a light trap. Alternatively, the observer can choose the Vortex Coronagraph, which rejects most of the starlight before encountering the IFU but allows a small fraction ($\lesssim$ 10%) to be sent to the imager, where frames are being recorded for the QACITS algorithm to keep the source positioned accurately.

Instrument performance

Image quality and contrast

METIS achieves fine-guiding accuracies below 0.02 λ/D root-mean-square (RMS) on-sky, which corresponds to 0.4 milliarcseconds RMS in the *L* band, and 1 milliarcsecond RMS in the *N* band. For bright ($K \lesssim 10$ mag) AO guide stars under median seeing conditions and moderate zenith angles (30 degrees), METIS will achieve a Strehl ratio of $\gtrsim$ 87% at 3.7 µm ($\gtrsim$ 95% at 10 µm), which drops to ~ 62% (~ 93%) for a $K \sim 12$ magnitude guide star. These numbers assume correction for non-common path aberrations and do not include degradation in the *N* band due to water vapour seeing in conditions of high precipitable water vapour.

The excellent optical performance enables efficient coronagraphy. For the RAVC the 5σ contrast for a bright ($L \leq 6$ magnitudes) star in the L band after post-processing is estimated to be $\sim 2 \times 10^{-4}$ at 2 λ/D and $\sim 2 \times 10^{-5}$ at 5 λ/D. The equivalent 5σ contrast for the APP is estimated to be $\sim 2 \times 10^{-3}$ at 2 λ/D and $\sim 2 \times 10^{-5}$ at 5 λ/D.

Sensitivity

Table 1 lists the sensitivities METIS will achieve in the specified wavebands for both imaging and spectroscopy.

References

Andrews, S. M. et al. 2018, ApJL, 869, L41
Anglada-Escudé, G. et al. 2016, Nature, 536, 437
Avenhaus, H. et al. 2018, ApJ, 863, 44
Banzatti, A. et al. 2017, ApJ, 834, 152
Birkby, J. L. et al. 2017, AJ, 153, 138
Brogi, M. et al. 2016, ApJ, 817, 106
Brown, J. M. et al. 2013, ApJ, 770, 94
Kasper, M. et al. 2019, The Messenger, 178, 5
Pascucci, I. et al. 2013, ApJ, 779, 178
Pinte, C. et al. 2018, ApJL, 860, L13
Quanz, S. P. et al. 2015, International Journal of Astrobiology, 14, 279
Smith, R. L. et al. 2009, ApJ, 701, 163
Teague, R. et al. 2018, ApJL, 860, L12

Links

[1] METIS website: https://metis.strw.leidenuniv.nl/
[2] SimMETIS can be found at https://metis.strw.leidenuniv.nl/simmetis/
[3] The METIS app can be found at http://metis-app.strw.leidenuniv.nl/

Notes

[a] The full list of METIS Consortium members can be found at https://metis.strw.leidenuniv.nl/about/

DOI: 10.18727/0722-6691/5219

HIRES, the High-resolution Spectrograph for the ELT

Alessandro Marconi[1, 2]
Manuel Abreu[3, 4]
Vardan Adibekyan[5, 6]
Matteo Aliverti[7]
Carlos Allende Prieto[8, 9]
Pedro Amado[10]
Manuel Amate[8]
Etienne Artigau[11]
Sergio Augusto[12]
Susana Barros[5, 6]
Santiago Becerril[10]
Björn Benneke[11]
Edwin Bergin[13]
Philippe Berio[14]
Naidu Bezawada[15]
Isabelle Boisse[16]
Xavier Bonfils[17]
François Bouchy[18, 16]
Christopher Broeg[19]
Alexandre Cabral[3, 4]
Rocio Calvo-Ortega[10]
Bruno Leonardo Canto Martins[20]
Bruno Chazelas[18]
Andrea Chiavassa[14]
Lise Christensen[21]
Roberto Cirami[22]
Igor Coretti[22]
Stefano Covino[7]
Giovanni Cresci[2]
Stefano Cristiani[22]
Vanderlei Cunha Parro[12]
Guido Cupani[22]
Izan de Castro Leão[20]
José Renan de Medeiros[20]
Marco Antonio Furlande Souza[12]
Paolo Di Marcantonio[22]
Igor Di Varano[23]
Valentina D'Odorico[22]
René Doyon[11]
Holger Drass[24, 25]
Pedro Figueira[15, 5]
Ana Belen Fragoso[8]
Johan Peter Uldall Fynbo[21]
Elena Gallo[13]
Matteo Genoni[7]
Jonay González Hernández[8, 9]
Martin Haehnelt[26]
Julie Hlavacek-Larrondo[27]
Ian Hughes[18]
Philipp Huke[28]
Andrew Humphrey[5]
Hans Kjeldsen[29]
Andreas Korn[30]
Driss Kouach[31]
Marco Landoni[7]
Jochen Liske[32]
Christophe Lovis[18]
David Lunney[33]
Roberto Maiolino[34]
Lison Malo[11]
Thomas Marquart[30]
Carlos Martins[5, 35]
Elena Mason[22]
Paolo Molaro[22]
John Monnier[13]
Manuel Monteiro[5]
Christoph Mordasini[19]
Tim Morris[36]
Alessio Mucciarelli[37]
Graham Murray[36]
Andrzej Niedzielski[38]
Nelson Nunes[3, 4]
Ernesto Oliva[2]
Livia Origlia[39]
Enric Pallé[8, 9]
Giorgio Pariani[7]
Phil Parr-Burman[33]
José Peñate[8]
Francesco Pepe[18]
Enrico Pinna[2]
Nikolai Piskunov[30]
José Luis Rasilla Piñeiro[8]
Rafael Rebolo[8, 9]
Phil Rees[33]
Ansgar Reiners[28]
Marco Riva[7]
Donatella Romano[39]
Sylvain Rousseau[14]
Nicoletta Sanna[2]
Nuno Santos[5, 6]
Mirsad Sarajlic[19]
Tzu-Chiang Shen[24]
Francesca Sortino[39]
Danuta Sosnowska[18]
Sérgio Sousa[5]
Eric Stempels[30]
Klaus Strassmeier[23]
Fabio Tenegi[8]
Andrea Tozzi[2]
Stéphane Udry[18]
Luca Valenziano[39]
Leonardo Vanzi[24]
Michael Weber[23]
Manfred Woche[23]
Marco Xompero[2]
Erik Zackrisson[30]
María Rosa Zapatero Osorio[40]

[1] Dipartimento di Fisica e Astronomia, Università di Firenze, Italy
[2] INAF – Osservatorio Astrofisico di Arcetri, Firenze, Italy
[3] Instituto de Astrofísica e Ciências do Espaço, Universidade de Lisboa, Portugal
[4] Departamento de Física, Faculdade de Ciências, Universidade de Lisboa, Portugal
[5] Instituto de Astrofísica e Ciências do Espaço, Universidade do Porto, Portugal
[6] Departamento de Física e Astronomia, Faculdade de Ciências, Universidade do Porto, Portugal
[7] INAF – Osservatorio Astronomico di Brera, Italy
[8] Instituto de Astrofisica de Canarias, La Laguna, Tenerife, Spain
[9] Departamento de Astrofisica, Universidad de La Laguna, Tenerife, Spain
[10] Instituto de Astrofisica de Andalucia-CSIC Glorieta de la Astronomia, Granada, Spain
[11] Institut de Recherche sur les Exoplanètes and Observatoire du Mont-Mégantic, Département de Physique, Université de Montréal, Canada
[12] Instituto Mauá de Tecnologia, São Caetano do Sul, Brazil
[13] Department of Astronomy, University of Michigan, USA
[14] Laboratoire Lagrange, Université Côte d'Azur, Observatoire de la Côte d'Azur, CNRS, France
[15] ESO
[16] Aix Marseille University, CNRS, CNES, LAM, France
[17] Université Grenoble Alpes, CNRS, IPAG, France
[18] Dèpartement d'Astronomie, Universitè de Geneve, Switzerland
[19] Physikalisches Institut, University of Bern, Switzerland
[20] Board of Observational Astronomy, Federal University of Rio Grande do Norte, Brazil
[21] Cosmic Dawn Center, Niels Bohr Institute, Copenhagen University, Denmark
[22] INAF – Osservatorio Astronomico di Trieste, Italy
[23] Leibniz Institute for Astrophysics Potsdam, Germany
[24] Centro de Astro Ingenieria, Pontificia Universidad Catolica de Chile, Santiago, Chile
[25] Millennium Institute of Astrophysics, Santiago, Chile
[26] Kavli Institute for Cosmology and Institute of Astronomy, Cambridge, UK
[27] Département de physique, Université de Montréal, Canada

[28] Institute for Astrophysics, Georg-August-Universität, Göttingen, Germany
[29] Department of Physics and Astronomy, Aarhus University, Denmark
[30] Division of Astronomy and Space Physics, Department of Physics and Astronomy, Uppsala University, Sweden
[31] CNRS, OMP, Université de Toulouse, France
[32] Hamburger Sternwarte, Universität Hamburg, Germany
[33] UK Astronomy Technology Centre, Edinburgh, UK
[34] Cavendish Laboratory, University of Cambridge, UK
[35] Centro de Astrofísica da Universidade do Porto, Portugal
[36] Centre for Advanced Instrumentation, Department of Physics, Durham University, UK
[37] Dipartimento di Fisica e Astronomia, Università di Bologna, Italy
[38] Institute of Astronomy, Nicolaus Copernicus University in Torun, Poland
[39] INAF – Osservatorio di Astrofisica e Scienze dello Spazio di Bologna, Italy
[40] Centro de Astrobiología (CSIC–INTA), Madrid, Spain

HIRES will be the high-resolution spectrograph at optical and near-infrared (NIR) wavelengths for ESO's Extremely Large Telescope (ELT). It will consist of three fibre-fed spectrographs providing a wavelength coverage of 0.4–1.8 µm (with a goal of 0.35–1.8 µm) at a spectral resolution of ~ 100 000. Fibre-feeding allows HIRES to have several interchangeable observing modes, including a single-conjugate adaptive optics (SCAO) module and a small diffraction-limited integral field unit in the NIR. It will therefore be able to operate in both seeing- and diffraction-limited modes. HIRES will address a wide range of science cases spanning nearly all areas of research in astrophysics and even fundamental physics. Some of the top science cases will be the detection of biosignatures from exoplanet atmospheres, finding the fingerprints of the first generation of stars (Pop III), tests on the stability of Nature's fundamental couplings, and the direct detection of the cosmic acceleration. The HIRES consortium is composed of more than 30 institutes from 14 countries, forming a team of more than 200 scientists and engineers.

Introduction

At first light, the ELT will be the largest ground-based telescope at visible and infrared wavelengths. The flagship science cases supporting the successful ELT construction proposal were the detection of life signatures from Earth-like exoplanets and the direct detection of the cosmic expansion re-acceleration, and it is no coincidence that both science cases require observations with a high-resolution spectrograph.

Over the past few decades high-resolution spectroscopy has been a truly interdisciplinary tool, which has enabled some of the most extraordinary discoveries spanning all fields of astrophysics, from planetary sciences to cosmology. Astronomical high-resolution spectrometers have allowed scientists to go beyond the classical domain of astrophysics and to address some of the fundamental questions of physics. In the wide-ranging field of research exploiting high-resolution spectroscopy, ESO has a long and successful tradition, thanks to the exquisite suite of medium- and high-resolution spectrographs offered to the community of Member States. The Ultraviolet and Visual Echelle Spectrograph (UVES), the Fibre Large Array Multi Element Spectrograph (FLAMES), the CRyogenic high-resolution InfraRed Echelle Spectrograph (CRIRES), the medium-resolution spectrograph X-shooter and the High Accuracy Radial velocity Planet Searcher (HARPS) have enabled European teams to lead in many areas of research. The Echelle SPectrograph for Rocky Exoplanet and Stable Spectroscopic Observations (ESPRESSO), which is now joining this suite of very successful high-resolution spectrographs, is fulfilling its promise by truly revolutionising some of these research areas. The scientific interest and high productivity of high-resolution spectroscopy are reflected in the fact that more than 30% of ESO publications can be attributed to its high-resolution spectrographs.

However, it is becoming increasingly clear that in most areas of research high-resolution spectroscopy has reached the "photon-starved" regime at 8–10-m-class telescopes. Despite major progress on the instrumentation front, further major advances in these fields desperately require a larger photon collecting area. Given its inherently "photon-starved" nature, amongst the various astronomical observing techniques high-resolution spectroscopy is most in need of the collecting area of Extremely Large Telescopes.

When defining the ELT instrumentation suite, ESO commissioned two Phase A studies for high-resolution spectrographs, one to work at visible wavelengths and known as CODEX (Pasquini et al., 2010), and SIMPLE (Origlia et al., 2010) to work in the NIR. Both studies were started in 2007 and completed in 2010. These studies demonstrated the importance of high-resolution optical and NIR spectroscopy at the ELT and ESO therefore decided to include a high-resolution spectrograph (HIRES) in the ELT instrumentation roadmap. Soon after conclusion of the respective Phase A studies the CODEX and SIMPLE consortia realised the great scientific importance of covering both the visible and NIR spectral ranges simultaneously. This marked the birth of the concept of an X-shooter-like spectrograph with higher resolution, capable of providing R ~ 100 000 over the full visible and NIR wavelength range. Following a community workshop in September 2012 the HIRES Initiative prepared a White Paper summarising a wide range of science cases proposed by the community (Maiolino et al., 2013) and also prepared a preliminary technical instrument concept.

With the start of construction of the ELT, the HIRES Initiative decided to organise itself as the HIRES Consortium and recruited additional institutes that had expressed an interest in HIRES. The Consortium, strongly motivated by the unprecedented scientific achievements that the combination of such an instrument with the ELT would enable, was commissioned by ESO to perform a Phase A study. The Phase A study started in March 2016 and concluded successfully in May 2018. Following the conclusion of the Phase A study, other institutes in the USA and Canada joined the HIRES Consortium.

The HIRES Consortium[a] is now composed of institutes from Brazil, Canada, Chile, Denmark, France, Germany, Italy, Poland, Portugal, Spain, Sweden, Switzerland, the United Kingdom and the USA. The Italian National Institute for Astrophysics (INAF) is the lead technical institute. See Marconi et al. (2018) for more details on the Consortium structure and organisation.

Science goals

During the Phase A study, the HIRES Science Advisory Team (SAT), chaired by the Project Scientist, defined the science priorities for HIRES and determined the corresponding top-level requirements. These science cases, briefly described below, were then prioritised in order to define the instrument baseline design. Many other science cases are possible with HIRES, but they will not be mentioned here, where we focus on a few representative science goals. A description of the prioritisation process can be found in, for example, Maiolino et al. (2013) and Marconi et al. (2018).

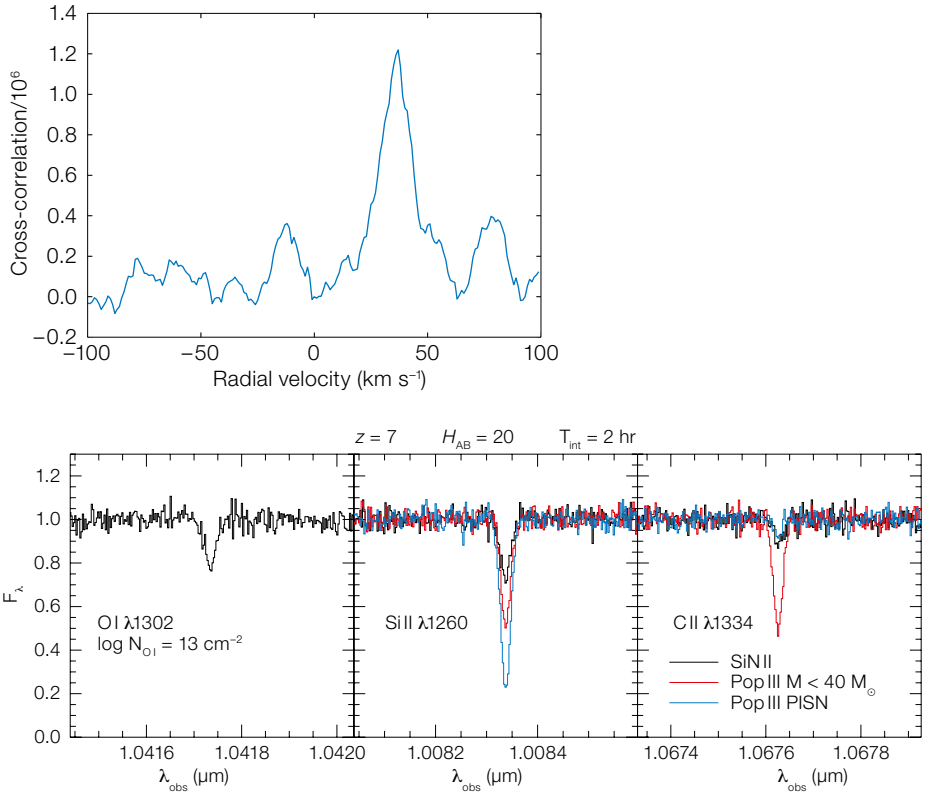

Figure 1. HIRES science highlights. Top: Cross-correlation signal indicating the clear detection of O_2 in a Proxima-b-like exoplanet in 70 hours of total integration (adapted from Figure 4 of Hawker & Parry, 2019). Bottom: Observations of a $z = 7$ quasar with $H_{AB} = 20$ and a total integration time of 2 hours showing HIRES's ability to distinguish IGM enrichment by normal SNII supernovae or by low mass and pair instability supernovae from Pop III stars (simulations by the HIRES Science Advisory Team).

Exoplanets and protoplanetary discs

The study of exoplanet atmospheres for a wide range of objects, from gas giants to rocky planets, and from hot to temperate planets, is a primary objective in the field for the next decade. In particular, the detection of components such as molecular oxygen, water and methane in Earth- or super-Earth-sized planets would be truly transformational, as they may be regarded as signatures of habitability or even signatures of life. Simulations of HIRES observations have been performed by Snellen et al. (2013, 2015) and Hawker & Parry (2019).

HIRES will be able to probe the atmosphere of an exoplanet in transmission during a transit in front of its host star. As an example, it will be possible to detect CO_2 absorption in Trappist-1b with a signal-to-noise ratio (S/N) of 6 in 4 transits of the planet, while O_2 absorption at 0.75 μm would be detected in only 25 transits of the planet, i.e., less than 30 hours of observation. HIRES will also be able to probe exoplanets directly, by spatially resolving them from their host star, focusing on their reflected starlight and taking advantage of the angular resolution of the ELT with AO-assisted observations. For example, it will be possible to detect the Proxima Centauri b planet in 4 nights of integration at a S/N of 8 with a relatively simple SCAO system similar to that used by other ELT first-light instruments. Figure 1, left, shows that HIRES will be able to detect O_2 from an exoplanet similar to Proxima b in 70 hours of integration.

Protoplanetary discs are a natural outcome of angular momentum conservation in star formation and are ubiquitous around young, forming stars. HIRES will be able to determine the properties of the gas in the inner star-disc region, where competing mechanisms of disc gas dispersal are at play. This will constrain, on the one hand, the mechanisms by which the forming star acquires mass and removes angular momentum, and, on the other hand, the initial conditions for planet formation.

Stars and stellar populations

The vast light-collecting power of the ELT will enable detailed high-resolution spectroscopy of individual stars, and in particular very faint red dwarfs and distant red giants in nearby galaxies, for which HIRES will be able to provide tight constraints on the atmospheric parameters. These constraints will be extremely important for characterising the stellar hosts of exoplanets.

HIRES will also expand our horizons by measuring the heavy-element abundances of the most primitive stars (with low mass and low metallicity) in our Galaxy and its satellites, helping us to understand what is the lowest metallicity

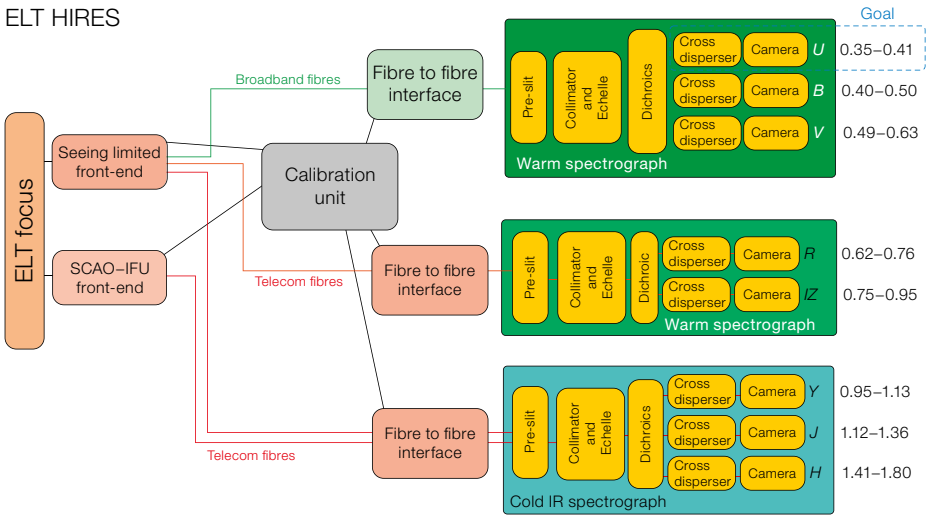

Figure 2. HIRES architectural design, outlining the instrument subsystems: Front-end (seeing-limited and AO assisted with SCAO unit), Fibre Link, Calibration Unit, VIS-Blue, VIS-Red and NIR (cold IR spectrograph).

at which gas can collapse to form low-mass stars, and what are the nature and yields of the very first generation of stars and their supernovae.

Last, but not least, the combination of very high spectral resolving power and diffraction-limited angular resolution makes the ELT a unique resource for deepening our understanding of the physics of stellar atmospheres and nucleosynthesis processes, by allowing us to spectroscopically resolve the effects of surface convection and to measure isotopic abundances of atomic species.

Galaxy formation and evolution, and the intergalactic medium

The detection of Population III stars and the observational characterisation of their properties are major objectives of extragalactic astrophysics. Protogalaxies hosting Pop III stars are expected to be too faint for direct detection, even with the JWST. However, the signature of Pop III stars can be detected through their nucleosynthetic yields, which can potentially be observed in the abundance patterns of very metal-poor absorption systems in the high-resolution, wide-range spectra of bright high-redshift sources provided by HIRES in the NIR (Figure 1, bottom).

The direct detection and characterisation of the beginning of the reionisation epoch is another very important goal in the study of galaxy formation. This process is believed to have been dominated by ultraviolet photons from the first generations of galaxies, most of which are too faint to be observed directly even with the JWST. By targeting bright quasars at high redshift as background continuum sources, HIRES will be able to study both transmission features in the Lyman-α forest and metal absorption lines associated with these reionisation-epoch sources, constraining the patchiness of the reionisation process, the properties of the ultraviolet background radiation and the chemical enrichment of the intergalactic medium (IGM) in this epoch.

Cosmology and fundamental physics

The observational evidence for the acceleration of the expansion of the Universe and the tensions that have been highlighted by different cosmological probes have shown that our canonical theories of cosmology or fundamental physics may be incomplete (and possibly incorrect) and that there might be unknown physics yet to be discovered. HIRES will allow us to search for, identify and ultimately characterise any new physics through several different but fundamentally inter-related observations which will enable a unique set of tests of the current cosmological paradigm.

HIRES will be able to constrain the variation of fundamental physical constants like the fine-structure constant α and the proton-electron mass ratio μ with the advantage, compared to laboratory measurements, of exploring variations over timescales of 12 Gyr and spatial scales of 15 Gpc. A detection of variation in the fundamental constants would be revolutionary: it would automatically prove that the Einstein Equivalence Principle is violated (i.e., gravity is not purely geometry), and that there is a fifth force.

HIRES will enable a test of the cosmic microwave background (CMB) temperature-redshift relation, $T(z) = T_0 (1 + z)$, which is a robust prediction of standard cosmology but one that must be directly verified by measurements. A departure from this relation can in turn reveal that the hypothesis of local position invariance (and thus the equivalence principle) is violated or that the number of photons is not conserved. HIRES measurements will greatly improve on the existing constraints on $T(z)$ compared to existing data.

The redshifts of cosmologically distant objects drift slowly with time — the so-called Sandage (or Sandage–Loeb) effect (see Liske et al., 2008). A redshift drift measurement is fundamentally different from all other cosmological observations; it can provide a direct detection of cosmic reacceleration, thus undoubtedly confirming cosmic acceleration and the existence of dark energy, and potentially providing evidence for new physics. HIRES will be capable of detecting the redshift drift in the Lyman-α forests of the brightest currently known QSOs (~ 6 cm s^{-1} decade^{-1} at $z = 4$ for a Planck-like standard cosmology). The ELT may thus become the first facility ever to watch the Universe change in “real time”.

Science priorities

These are just a few of the many science cases that can be addressed, a collection of which can be found in Maiolino et al. (2013). However, in order to define the instrument baseline design a prioritisation of the science cases was performed by

the HIRES Science Advisory Team following criteria of scientific impact (transformational versus incremental), feasibility and competitiveness.

Then, if the top level requirements (TLRs) of the top priority science cases were also enabling other science cases, the latter were not considered any further in the subsequent prioritisation, being considered as accomplished together with the top priority science cases. The top science priorities and associated requirements are:

1. Exoplanet atmospheres in transmission, requiring a spectral resolution of at least 100 000, a wavelength coverage of at least 0.50–1.80 μm and a wavelength calibration accuracy of 1 m s^{-1}. The implementation of the above TLRs would automatically enable the following science cases:
   – reionisation of the universe,
   – characterisation of cool stars,
   – detection and investigation of near pristine gas,
   – the study of extragalactic transients.

2. Variation of the fundamental constants of physics, requiring an extension to 0.37 μm in addition to the TLRs of priority 1. At wavelengths less than 0.40 μm the throughput of the ELT is expected to be low as a consequence of the planned coating. However, even in the range 0.37–0.40 μm the system is expected to outperform ESPRESSO at the VLT, and a new coating is under study which may be available a few years after first light. This extension towards the blue would also automatically enable investigation of:
   – the cosmic variation of the CMB temperature,
   – the determination of the deuterium abundance,
   – the investigation and characterisation of primitive stars.

3. Detection of exoplanet atmospheres in reflection, requiring, on top of the TLRs of priority 1, the addition of an SCAO system and an integral field unit. Reflected-light spectra allow atmospheric emission to be traced from lower altitudes on the day side of the exoplanet. These additional TLRs would automatically also enable the following science cases:
   – planet formation in protoplanetary discs,
   – characterisation of stellar atmospheres,
   – searching for low-mass black holes.

4. The Sandage test, for which the additional TLRs are a wavelength range of 0.40–0.67 μm and a stability of 2 cm s^{-1}, also enabling:
   – the mass determination of Earth-like exoplanets,
   – radial velocity searches and mass determinations for exoplanets around M-dwarf stars.

Instrument concept

Following Phase A and further studies before the start of construction, the HIRES baseline design is for a modular instrument consisting of three fibre-fed cross-dispersed echelle spectrographs — VIS-BLUE (*UBV*), VIS-RED (*RIZ*) and NIR (*YJH*) — providing a simultaneous spectral range of 0.4–1.8 μm (with a goal of 0.35–1.8 μm) at a resolution of 100 000. Fibre-feeding allows several, interchangeable, observing modes, ensuring maximisation of either accuracy, throughput or spatially resolved information. Together with the SCAO module, the proposed baseline design is capable of fulfilling the requirements of the 4 top science cases.

The baseline design is summarised below but several alternatives were also evaluated during the Phase A study. Also, several add-ons made possible by the modular nature of the instrument have been considered (for example, a polarimetric module at the intermediate focus, or a wavelength extension out to the *K* band (2.0–2.4 μm). The overall concept is summarised in Figure 2. In the front-end the light from the telescope is split, via dichroics, into 3 wavelength channels. Each wavelength channel interfaces with several fibre bundles that feed the corresponding spectrograph module. Each fibre bundle corresponds to an observing mode and together they constitute the Fibre Link. All three spectrographs, VIS-BLUE, VIS-RED and NIR, have a fixed configuration, i.e., there are no moving parts, thereby fulfilling the stability requirements. They include a series of parallel entrance slits consisting of linear micro-lens arrays each glued to the fibre bundles. The split in wavelengths between the spectrographs is influenced, along with other parameters, by the optical throughput of the different types of fibre available on the market; the different modules can therefore be positioned at

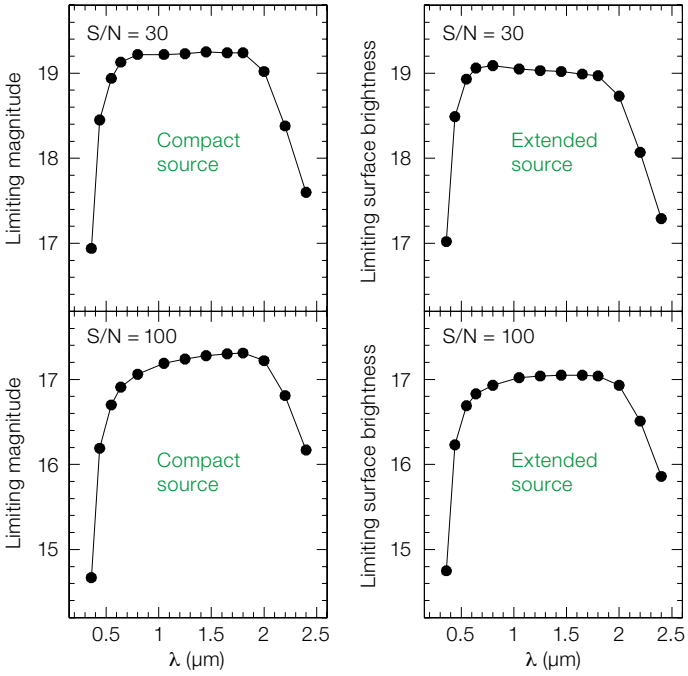

Figure 3. HIRES limiting magnitudes obtained from the Exposure Time Calculator for different S/N ratios (30 — top and 100 — bottom), and for compact and extended sources (left and right). Observations are in seeing-limited mode with R = 100 000 and a total exposure time of 1800 seconds.

different distances from the focal plane of the telescope.

The whole instrument should be placed on the Nasmyth platform, if enough volume and mass is available. If necessary, the fibre-feeding allows the VIS-RED and NIR modules to be placed in the Coudé Room, which can also host the Calibration Unit.

Performance

The Exposure Time Calculator (ETC), regularly updated to take into account modifications to the design, is maintained by INAF-Arcetri and can be run online[2]. The ETC can compute the limiting magnitude achievable at a given wavelength in a given exposure time and at a given S/N, or it can compute the S/N achievable at a given wavelength in a given exposure time and at a given magnitude. HIRES expected performances, computed with the ETC, are summarised in Figure 3.

Conclusions

The HIRES baseline design is for three ultra-stable and modular fibre-fed cross-dispersed echelle spectrographs providing a simultaneous spectral coverage of 0.4–1.8 μm (with a goal of 0.35–1.8 μm) at a resolution of 100 000 with several, interchangeable, observing modes ensuring maximisation of either accuracy, throughput or spatially resolved information. Overall, the studies conducted so far have shown that the HIRES baseline design can address the 4 top priority science cases, being able to provide ground-breaking science results with no obvious technical showstoppers.

The construction of HIRES involves the majority of the institutes in ESO Member States with expertise in high-resolution spectroscopy and will require an estimated 30 million euros for hardware (excluding contingencies) and about 500 full time equivalent personnel. Contingencies are expected to be low (5–10%) because the proposed baseline design is based on proven technical solutions and can benefit from heritage from HARPS and ESPRESSO and other earlier high-resolution spectrographs, for example the Potsdam Echelle Polarimetric and Spectroscopic Instrument (PEPSI) at the 11.8-m Large Binocular Telescope, the SPectropolarimètre InfraRouge (SPIRou) at the 3.6-m Canada France Hawaii Telescope and the Calar Alto high-Resolution search for M dwarfs with Exoearths with Near-infrared and optical Échelle Spectrographs (CARMENES) instrument at the 3.5-m telescope of Calar Alto Observatory. Construction will take about 8–10 years, so with Phase B starting in 2021, HIRES could be at the telescope as early as 2030.

Overall, HIRES is an instrument capable of addressing ground-breaking science cases whilst being almost (telescope) pupil independent, as it can operate in both seeing- and diffraction-limited modes; the modularity ensures flexibility during construction and the possibility to adapt quickly to new developments in both the technical and the science landscapes.

Acknowledgements

The Italian effort for HIRES is supported by the Italian National Institute for Astrophysics (INAF). HIRES work in the UK is supported by the Science and Technology Facilities Council (STFC) at the UK Astronomy Technology Centre, the University of Cambridge (grants ST/S001387/1 and ST/N002873/1) and Heriot Watt University (grant ST/S001328/1), as part of the UK ELT Programme. We acknowledge financial support from the Spanish Ministry of Science and Innovation (MICINN) under projects AYA2017-86389-P, RYC-2013-14875, PGC2018-098153-B-C31, and PID2019-109522GB-C51/52. The German efforts for HIRES are funded by the Federal Ministry for Education and Research (BMBF). Klaus Strassmeier thanks the BMBF-Verbundforschung for support through grants 05A17BAB and 05A2020. This work was supported by FCT – Fundação para a Ciência e a Tecnologia through national funds and by FEDER through COMPETE2020 – Programa Operacional Competitividade e Internacionalização under these grants: UID/FIS/04434/2019; UIDB/04434/2020; UIDP/04434/2020; PTDC/FIS-AST/32113/2017 & POCI-01-0145-FEDER-032113; PTDC/FIS-AST/28953/2017 & POCI-01-0145-FEDER-028953; PTDC/FIS-AST/28987/2017 & POCI-01-0145-FEDER-028987. Research activities of the observational astronomy board at the Federal University of Rio Grande do Norte are supported by continuous grants from the Brazilian funding agencies CNPq, FAPERN, and INCT-INEspaço. This study was financed in part by the Coordenação de Aperfeiçoamento de Pessoal de Nível Superior, Brazil (CAPES), Finance Code 001.

References

Hawker, G. A. & Parry, I. R. 2019, MNRAS, 484, 4855
Liske, J. et al. 2008, MNRAS, 386, 1192
Maiolino, R. et al. 2013, arXiv:1310.3163
Marconi, A. et al. 2018, Proc. SPIE, 10702, 107021Y
Origlia, L. et al. 2010, Proc. SPIE, 7735, 77352B
Pasquini, L. et al. 2010, Proc. SPIE, 7735, 77352F
Snellen, I. et al. 2013, ApJ, 764, 182
Snellen, I. et al. 2015, A&A, 576, A59

Links

[1] Instrument Web Page http://hires.inaf.it
[2] Exposure time calculator http://hires.inaf.it/etc.html

Notes

[a] Partners of the HIRES Consortium (CI = Coordinating Institute within a country) Brazil: Núcleo de Astronomia Observacional, Universidade Federal do Rio Grande do Norte (CI); Instituto Mauá de Tecnologia. Canada: Institut de Recherche sur les Exoplanètes and Observatoire du Mont-Mégantic, département de physique, Université de Montréal. Chile: Pontificia Universidad Catolica de Chile (CI); Centre of Astro Engineering, Universidad de Chile; Department of Astronomy, Universidad de Concepcion; Center of Astronomical Instrumentation, Universidad de Antofagasta. Denmark: Niels Bohr Institute, University of Copenhagen (CI); Department of Physics and Astronomy, Aarhus University. France: Laboratoire d'Astrophysique de Marseille, CNRS, CNES, AMU (CI); Institut de Planétologie et d'Astrophysique de Grenoble, Université Grenoble Alpes; Laboratoire Lagrange, Observatoire de la Côte d'Azur; Observatoire de Haute Provence, CNRS, AMU, Institut Pythéas, Institut de Recherche en Astrophysique et Planétologie, Observatoire Midi-Pyrénées; Laboratoire Univers et Particules, Université de Montpellier. Germany: Leibniz-Institut für Astrophysik Potsdam (CI); Institut für Astrophysik, Universität Göttingen; Zentrum für Astronomie Heidelberg, Landessternwarte; Thüringer Landesternwarte Tautenburg; Hamburger Sternwarte, Universität Hamburg. Italy: INAF – Istituto Nazionale di Astrofisica (Lead Technical Institute). Poland: Faculty of Physics, Astronomy and Applied Informatics, Nicolaus Copernicus University in Torun. Portugal: Instituto de Astrofísica e Ciências do Espaço at Centro de Investigaço em Astronomia/Astrofísica da Universidade do Porto (CI), Instituto de Astrofísica e Ciências do Espaço at Faculdade de Ciências da Universidade de Lisboa. Spain: Instituto de Astrofísica de Canarias (CI); Instituto de Astrofísica de Andalucía-CSIC; Centro de Astrobiología Sweden: Dept. of Physics and Astronomy, Uppsala University. Switzerland: Département d'Astronomie, Observatoire de Sauverny, Université de Genève (CI); Universität Bern, Physikalische Institut. United Kingdom: Science and Technology Facilities Council (CI); Cavendish Laboratory & Institute of Astronomy, University of Cambridge; UK Astronomy Technology Centre; Institute of Photonics and Quantum Sciences, Heriot-Watt University. USA: Department of Astronomy, University of Michigan.

DOI: 10.18727/0722-6691/5220

MOSAIC on the ELT: High-multiplex Spectroscopy to Unravel the Physics of Stars and Galaxies from the Dark Ages to the Present Day

François Hammer[1]
Simon Morris[2]
Jean-Gabriel Cuby[3]
Lex Kaper[4,18]
Matthias Steinmetz[5]
José Afonso[6]
Beatriz Barbuy[7]
Edwin Bergin[8]
Alexis Finogenov[9]
Jesus Gallego[10]
Susan Kassin[11]
Chris Miller[8]
Goran Östlin[12]
Laura Pentericci[13]
Daniel Schaerer[14]
Bodo Ziegler[15]
Fanny Chemla[1]
Gavin Dalton[16]
Fatima De Frondat[1]
Chris Evans[17]
David Le Mignant[3]
Mathieu Puech[1]
Myriam Rodrigues[1]
Ruben Sanchez-Janssen[17]
Sylvestre Taburet[1]
Lidia Tasca[3]
Yanbin Yang[1]
Sandrine Zanchetta[1]
Kjetil Dohlen[3]
Marc Dubbeldam[2]
Kacem El Hadi[3]
Annemieke Janssen[18]
Andreas Kelz[5]
Marie Larrieu[19]
Ian Lewis[20]
Mike MacIntosh[17]
Tim Morris[2]
Ramon Navarro[18]
Walter Seifert[21]

[1] Paris Observatory, Paris Science et Lettres, CNRS, France
[2] Durham University, UK
[3] LAM, Université Aix-Marseille, CNRS, France
[4] University of Amsterdam, the Netherlands
[5] Leibniz-Institut für Astrophysik Potsdam, Germany
[6] IACE, Universidade de Lisboa, Portugal
[7] IAG, São Paulo, Brazil
[8] University of Michigan, USA
[9] University of Helsinki, Finland
[10] Universidad Complutense de Madrid, Spain
[11] Space Telescope Science Institute, Baltimore, USA
[12] Stockholm University, Sweden
[13] INAF – Osservatorio Astronomico di Roma, Italy
[14] University of Geneva, Switzerland
[15] Vienna University, Austria
[16] STFC-RALSPACE & University of Oxford, UK
[17] UK Astronomy Technology Centre, STFC, Edinburgh, UK
[18] NOVA, the Netherlands
[19] IRAP, Université de Toulouse, CNRS, France
[20] University of Oxford, UK
[21] Landessternwarte Königstuhl, Universität Heidelberg, Germany Heidelberg, Germany

The powerful combination of the cutting-edge multi-object spectrograph named MOSAIC with the world largest visible/near-infrared telescope, ESO's Extremely Large Telescope (ELT), will allow us to probe deeper into the Universe than ever before. MOSAIC is an extremely efficient instrument for obtaining spectra of the numerous faint sources in the Universe, including the very first galaxies and sources of cosmic reionisation. MOSAIC has a high multiplex in the near-infrared (NIR) and in the visible, and also has multi-integral field units (Multi-IFUs) in the NIR. It is therefore perfectly suited to carrying out an inventory of dark matter (from rotation curves) and baryons in the cool–warm gas phases in galactic haloes at z = 3–4. MOSAIC will enable detailed maps of the intergalactic medium at z = 3, the evolutionary history of dwarf galaxies during a Hubble time, and the chemistry as directly measured from stars up to several Mpc. It will also measure faint features in cluster gravitational lenses or in streams surrounding nearby galactic haloes. The preliminary design of MOSAIC is expected to begin next year and its level of readiness is already high, given the instrumental studies already carried out by the team.

Science cases for MOSAIC

The science case for a multi-object spectrograph on the ELT covers all areas of astronomy for which the collection of light from tens to hundreds of scientific targets is required. This includes targets which are too faint to be accessible spectroscopically to 10-m telescopes, particularly stars, star clusters, and all types of galaxies across cosmic history. As a major workhorse for the ELT, MOSAIC will provide access to the visible and NIR wavelength ranges.

Access to visible wavelengths is an important priority for the large community of scientists interested in collecting numerous stellar spectra in the Milky Way and nearby galaxies (see, for example, Evans et al., 2013, 2015). In cosmology, this enables maps of the intergalactic medium (IGM) and also the determination of galactic halo abundances at z = 3–4 from absorption lines in the spectra of the numerous Lyman break galaxies (Japelj et al., 2019; Rahmani et al., in preparation). In the NIR, MOSAIC will constrain the physics of early star formation by determining the metallicity distribution functions of stellar populations in the local Universe, and it will excel at deep spectroscopic studies of faint Galactic satellites — from the chemodynamics of ultra-faint dwarf galaxies to detailed chemical abundances of old globular clusters in the inner Galaxy via high-resolution spectroscopy. Furthermore, MOSAIC's unique system of multi-IFUs will enable measurements of the rotation curves of distant galaxies. With such observations MOSAIC will lead the efforts to characterise and understand baryonic and dark matter structure at an epoch when the Universe was only 1.5 billion years old. Looking into the even more distant Universe, MOSAIC's multi-IFUs will study the physical properties of the stars, interstellar medium (ISM), radiation field, and ionising power of the overall population of faint very high-z galaxies. This will enable a precise characterisation of the ionisation state of the IGM during the first billion years after the Big Bang. MOSAIC will allow astronomers to reconstruct the timeline and topology of reionisation, and to observe the formation and growth of the first galaxies in much more detail than any other instrument.

The MOSAIC Science Team has collected science cases that should revolutionise astrophysics and cosmology in the 2030s. It has also defined a number of large surveys that could be carried out with MOSAIC (Evans et al., 2018; Puech

et al., 2018) to illustrate the survey speed of the instrument. Although subject to revision during the construction phase, these exciting science cases span a range of redshift from our "backyard" to the dark ages:

- First-light galaxies and reionisation (with multi-IFUs in the NIR, and the high-multiplex mode in the NIR for Lyman-α emitters).
- An inventory of the matter distribution at large scales, including tomography of the IGM and its metal content (with the high-multiplex mode in the visible) and dark matter distributions from rotation curves of distant galaxies (with multi-IFUs in the NIR).
- Mass assembly and evolution of dwarf galaxies (with the high-multiplex mode in the visible and NIR).
- Extragalactic stellar populations (with the high-multiplex mode in the visible and multi-IFUs in the NIR).

Instrument concept

The MOSAIC instrument was conceived as a multi-purpose multi-object spectrograph for the ELT (Hammer et al., 2016; Morris et al., 2018). It has three main operating modes, including two high-multiplex mono-aperture modes (in the visible and NIR) and the multi-IFU mode, as shown in Figure 1. The requirement to achieve a multiplex of ~ 200 in the high-multiplex mode with a multi-IFU mode essentially predetermines that MOSAIC shall be a fibre-fed instrument. Furthermore, the design is considerably simplified by allowing the spectrograph hardware to be shared between the different modes. The spectral range of the instrument is from 0.45 to 1.8 µm, with a break between a system optimised for visible and a system optimised for the NIR at 0.8–0.9 µm. Six bands provide R = 5000 coverage over the full bandwidth, with selected smaller bands available at R ~ 20 000 in the visible and in the NIR. The instrument is designed to use as much of the adaptive-optics-corrected field of view of the ELT as possible (> 7 arcminutes in diameter). It is the only currently planned instrument that takes advantage of the wide ELT field of view with high optical quality enabled by its 5-mirror telescope design.

The design shown in Figure 2 has been adopted to achieve an acceptable resistance to gravity-induced deformations on the platform. MOSAIC will include two spectrographs in the visible and four in the NIR. Owing to the large plate scale offered by the ELT (> 3 mm arcsecond^{-1}) and the non-telecentricity of the telescope optical design, a number of compromises are required in order to realise a practical and affordable multi-object spectrograph instrument design. In particular, it has been necessary to subdivide individual pick-offs into multiple fibre-spaxels in order to produce an optical design that is feasible. A wider simultaneous spectral coverage is appealing, but it has to be balanced against the need to keep the spaxel size sufficiently small. This is to ensure the leading role of MOSAIC in measuring the complex kinematics of high-z galaxies (for example, Hammer et al., 2009; Kassin et al., 2012) and detecting spectral features in the faintest sources, including the first galaxies.

Performance

Studies in the visible wavelength range

The ELT's light-gathering power will exceed that of all sixteen currently existing 8–10-m-class telescopes put together. In the visible, MOSAIC will provide world-leading science by producing ≥ 200 spectra simultaneously for Galactic and nearby Universe science. Studies of the Local Group have shown that precise chemical abundances and stellar kinematics can break the age-metallicity degeneracy. MOSAIC will bring a wealth of new and exciting target galaxies within our grasp for the first time, spanning a much broader range of galaxy morphologies, star formation histories and metallicities than those available to us at present and enabling us to test theoretical models of galaxy assembly and evolution in systems out to distances of several or even tens of Mpc. Another key objective in this area is also to investigate the existence of the "Spite Plateau" (Spite & Spite, 1982) in the Li abundances of metal-poor stars in extragalactic systems. Because the observed Li is likely primordial, the Spite Plateau provides an estimate of the baryonic density of the Universe. This case requires high-resolution spectroscopy (R > 20 000).

For cosmology, the visible mode will enable a detailed mapping of the IGM

High multiplex mono-fibres	Visible	Near IR	Multiple integral field units	Near IR
	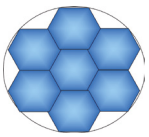			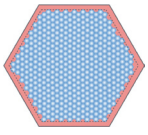
Number of apertures	220	160 (80 sci + 80 sky)	Number of apertures	10
Patrol area	52.1 arcmin^2	47.3 arcmin^2	Patrol area	44.2 arcmin^2
Operating bandwidth	0.45-0.88 µm	0.8-1.8 µm	Operating bandwidth	0.8-1.8 µm
Diameter of the aperture on sky	690 mas	500 mas	Outer diameter of on-sky subfield	2.5 arcsec (hexagonal)
Spectral resolution	5000 & 20000	5000 & 20000	Sampling	120 mas
AO performance	GLAO (~seeing limited)	GLAO	Spectral resolution	5000 & 20000
			AO performance	25% encircled energy in 150 mas

Figure 1. The three observing modes of MOSAIC. Left: the two high-multiplex modes (HMMs); right: the 10 multi-IFUs.

at z = 3–4. Figure 3 shows simulations indicating that MOSAIC will be able to measure Lyman-α forest tomography, even with relatively faint background Lyman break galaxies at z ~ 4, as shown by Japelj et al. (2019). By measuring the optical depths of redshifted ultraviolet metallic absorption lines, one may also characterise the metal content in the haloes of z = 3–4 galaxies (Rahmani et al., in preparation). That will yield a comprehensive inventory of baryons in the distant haloes, which can be compared to what is presently done in nearby haloes by the HST-COS Halo collaboration (see, for example, Werk et al., 2014).

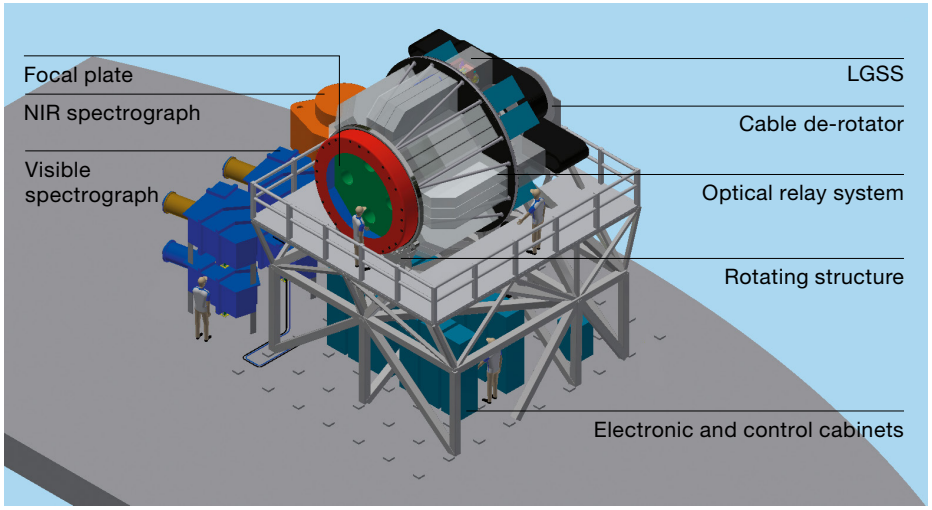

Figure 2. Schematic of MOSAIC as it will be on the ELT Nasmyth platform.

First galaxies and cosmic reionisation in the NIR wavelength range

The ELT's light-gathering power will allow us to study the physical properties of the faintest sources ever reached by medium- or high-resolution spectroscopy, including the very first sources in the Universe, which are barely detected today. These objects are challenging because they fall into the category of ultra-low surface brightness sources (ULSBs, $\mu_{AB} \geq 25$ mag arcsecond^{-2}) as a result of cosmological dimming. Whereas the James Webb Space Telescope (JWST) will excel at very deep NIR and mid-IR imaging, and will measure for the first time the strong rest-frame optical emission lines for large numbers of high-z galaxies, it will not be able to perform moderate-resolution ($R \geq 5000$) spectroscopy, which is essential for measuring the absorption and faint emission lines of these distant sources. Combining the ELT's large collecting area with multi-IFUs to optimise sky subtraction (cf. below), MOSAIC will allow NIR spectroscopy significantly beyond the reach of the JWST (cf. Vanzella et al., 2014).

As regards studying the sources of cosmic reionisation, the JWST is in practice limited by the fact that so far no method has been found to measure the Lyman continuum escape fraction of galaxies from their rest-frame optical emission lines (for example, Plat et al., 2019; Wang et al., 2019; Ramambason et al., 2020), whereas the rest-frame ultraviolet spectra admit several methods to determine this fundamental quantity (Izotov et al., 2018; Chisholm et al., 2018, 2020). Observing the ultraviolet rest-frame continuum and faint emission lines of a large sample of $z > 6$ galaxies, which is uniquely feasible with the ELT, is crucial for understanding cosmic reionisation and the first sources of light, for several reasons:

- Low-ionisation absorption lines (for example, Si II, C II) provide a unique tool from which to derive the Lyman continuum escape fraction and to determine the neutral gas coverage in these sources (Steidel et al., 2018; Chisholm et al., 2018; Gazagnes et al., 2018). This is essential in order to establish the contribution of galaxies to cosmic reionisation, and to determine which galaxy types dominate.
- Measurements of Lyman-α emission (which is generally fairly weak at $z > 6.5$), the detailed line profiles, and statistics (for example, the fraction of galaxies showing Lyman-α emission) provide critical information about the ionisation state of the IGM, the timeline of cosmic reionisation, and its topology (for example, Castellano et al., 2016; Mason et al., 2018; Mesinger et al., 2015).
- Other emission lines (such as C III], O III], C IV, He II etc.) provide important insight into the ISM, stellar metallicity and massive star populations, and the radiation field of these galaxies. In particular, MOSAIC will enable the search for primordial, metal-free star-formation for an unprecedented sample of galaxies through the He II emission line (for example, Raiter, Schaerer & Fosbury, 2010). The rest-frame ultraviolet emission lines are weak and therefore require ultra-deep spectroscopy (Stark, 2016).

High multiplex with mono-aperture fibres in the NIR will be very useful for investigating bright Lyman-α line sources at high redshift. However, for the numerous very distant and intrinsically faint galaxies that have no strong emission, MOSAIC will be unique in its ability to measure continuum, absorption lines and very faint emission lines. The effective depth provided by the ELT's light-gathering power is affected by the strong and variable sky signal, and even for spectroscopic studies operating between the bright OH sky lines, the NIR sky continuum μ_{AB} = 18.5–19.5 mag arcsecond^{-2} (see Sullivan & Simcoe, 2012) is far brighter than the typical surface brightness associated with the continuum of very distant galaxies at $\mu_{AB} \geq 25$ mag arcsecond^{-2}. Achieving the best sky subtraction is therefore a major driver for the design of a multi-object spectrograph on the ELT. Weilbacher et al. (2020) have recently presented detailed results from the Multi Unit Spectroscopic Explorer (MUSE) IFU, demonstrating that it is capable of reaching a dark sky removal down to 0.3% between 0.82 and 0.9 µm. Figure 4 compares the mono-aperture fibre performance to that of IFUs (see also Disseau et al., 2014). To recover signals well below the sky, we estimate that an IFU could be 2 to 3 times more efficient than mono-aperture fibres, after taking account of the sky spatial variations near and far from the target (see, for example, Yang et al., 2012), the sky

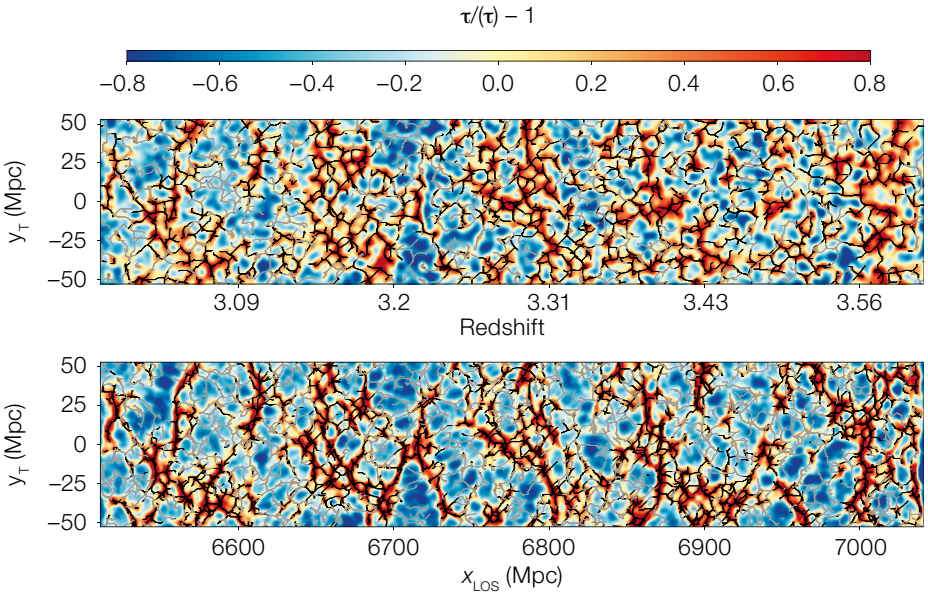

Figure 3. Simulations of MOSAIC performance when observing simultaneously the ISM absorption lines in the spectra of numerous $R_{AB} \leq 25.5$ Lyman break galaxies enabling a vast area (100 Mpc in diameter) of the sky plane to be sampled. This allows the study of 10-Mpc-thick longitudinal slices lying from redshift 3 to 3.6, of the simulated (top, signal-to-noise ratio = 4) and original (bottom) optical depth contrast field ($\tau/\langle\tau\rangle - 1$), where $\tau = -\log F$ and F is transmitted flux (τ is taken as a proxy for the HI density). The y-axis is the projected transverse dimension (y_T). Filaments extracted are over-plotted in grey and black. The black lines correspond to the 50% densest filaments. As noise in the spectra increases, the reconstruction shows lower contrast, and filaments are more randomly located (from Japelj et al., 2019).

temporal variations, and the expected aperture losses. Multi-IFUs are essential for recovering spectra of most $z \sim 8$ galaxies, as illustrated in the right-hand panel of Figure 4.

Comparison with other instruments and telescopes

Puech et al. (2018) carried out a systematic comparison between the efficiency of MOSAIC and that of other facilities implemented on the ELT and 8–10-m-class telescopes. Expressed in a survey speed metric — for example, how fast a given instrument can observe a given number of sources to equivalent signal-to-noise ratio levels — it demonstrates that only MOSAIC on the ELT will be able to construct large statistical samples in reasonable time and to address the science cases described in the first section of this article. Interestingly, the JWST will serve to identify many ultra-faint targets that MOSAIC will follow up to derive their physical, chemical, and kinematical properties. MOSAIC also nicely complements the High Angular Resolution Monolithic Optical and Near-infrared Integral field spectrograph (HARMONI), whose largest spaxel scale is 3 times smaller than that of MOSAIC. HARMONI will excel at studying compact sources or targets with high-contrast small-scale clumps while MOSAIC will be optimised to study the large number of $z > 6$ galaxies, which have relatively small sizes but are extended (Bowler et al., 2017) and are in the range of ultra-low-surface-brightness sources.

Conclusions

In addition to the four scientific topics listed in the first section of this article, as a workhorse instrument MOSAIC will be able to address a huge number of science cases. The Science Team is presently developing many new science cases, including, for example, kinematics and stellar populations of faint stellar streams surrounding nearby galaxies (Martínez-Delgado, 2018), velocity dispersion measurements of dwarf spheroidals surrounding galactic haloes situated up to 50 Mpc from us (as done by MUSE on Crater I, see Voggel et al., 2016), and many others. The large MOSAIC science community will continue to prepare innovative and cutting-edge observational programmes for studying stars and galaxies in many environments and across cosmic history.

The construction phase of MOSAIC could begin in 2021. This has been folded into the planning by the MOSAIC team to ensure we deliver an instrument that will have no equal when it comes to exploring the deep Universe towards the epoch of reionisation. MOSAIC will be a unique instrument with which to investigate how the gas, stars, and dark matter were distributed more than 10 billion years ago, to determine the properties of the faintest building blocks of galaxies, and to provide a gigantic step towards understanding the local Universe well beyond the Local Group. In short, it is the ideal instrument with which to investigate the physical properties of statistical samples of the vast majority of extragalactic sources because they are extended and have very low surface brightness. The MOSAIC team remains very keen to work with the ELT community to deliver a world-class instrument serving as many scientific interests as possible.

Acknowledgements

The MOSAIC Consortium is very grateful to the MOSAIC Science Team[1] for their considerable help in envisioning the future multi-object spectrograph for the ELT. We are indebted to the whole MOSAIC technical team whose efforts are invaluable for preparing and conceiving MOSAIC and making it a reality. Special thanks go to Thierry Botti (LAM) and Frederique Auffret (Paris Observatory) for their help within the communication team, and to Clotilde Laigle and Jure Japelj for sending us Figure 3 in original form.

This article is dedicated to the memory of Olivier Le Fèvre, who contributed so brilliantly to the science discussed here. The MOSAIC Consortium is very grateful for his crucial support over the years.

References

Bouwens, R. J. et al. 2015, ApJ, 803, 34
Bowler, R. A. A. et al. 2017, MNRAS, 466, 3612
Castellano, M. et al. 2016, ApJL, 818, L3
Chisholm, J. et al. 2018, A&A, 616, A30
Chisholm, J. et al. 2020, MNRAS, 498, 2554
Disseau, K. et al. 2014, Proc. SPIE, 9147, 914791
Evans, C. et al. 2013, arXiv:1303.0029
Evans, C. et al. 2015, arXiv:1501.04726
Evans, C. et al. 2018, The Messenger, 171, 47
Gazagnes, S. et al. 2018, A&A, 616, A29

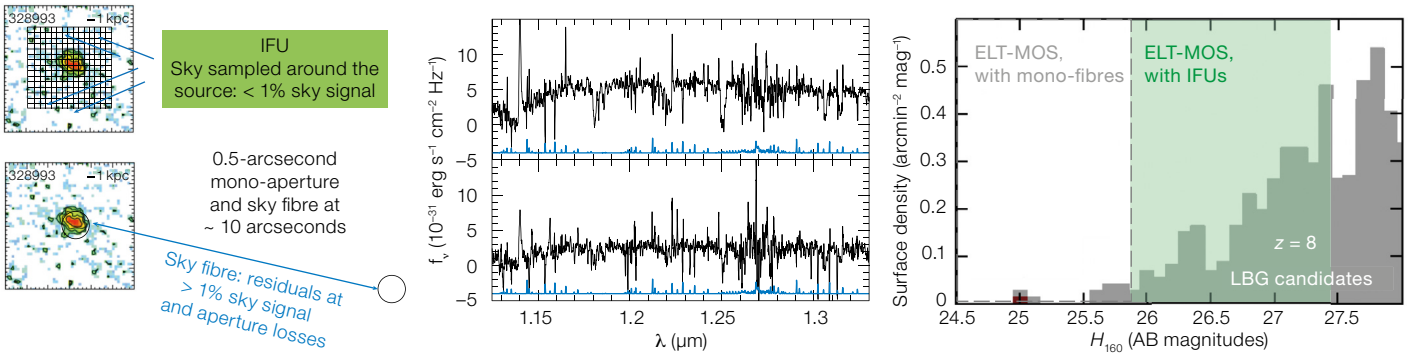

Hammer, F. et al. 2009, A&A, 507, 1313
Hammer, F. et al. 2016, Proc. SPIE, 9908, 990824
Izotov, Y. et al. 2018, MNRAS, 478, 4851
Japelj, J. et al. 2019, A&A, 632, A94
Kassin, S. et al. 2012, ApJ, 758, 106
Martínez-Delgado, D. 2018, Proc. XIII Scientific Meeting of the Spanish Astronomical Society, 146
Mason, C. et al. 2018, ApJ, 856, 2
Mesinger, A. et al. 2015, MNRAS, 446, 566
Morris, S. M. et al. 2018, Proc. SPIE, 10702, 107021W
Oesch, P. A. et al. 2015, ApJL, 804, L30
Plat, A. et al. 2019, MNRAS, 490, 978
Puech, M. et al. 2016, Proc. SPIE, 9908, 99089P
Puech, M. et al. 2018, Proc. SPIE, 10702, 107028R
Raiter, A., Schaerer, D. & Fosbury, R. A. E. 2010, A&A, 523, A64
Ramambason, L. et al. 2020, A&A, 644, A21
Rigby, J. et al. 2018, AJ, 155, 104
Spite, M. & Spite, F. 1982, Nature, 297, 483
Stark, D. P. 2016, ARAA, 54, 761
Steidel, C. C. et al. 2018, ApJ, 869, 123
Sullivan, P. W. & Simcoe, R. A. 2012, PASP, 124, 1336
Vanzella, E. et al. 2014, A&A, 569, A78
Voggel, K. et al. 2016, MNRAS, 460, 3384
Wang, B. et al. 2019, ApJ, 885, 57
Weilbacher, P. et al. 2020, A&A, 641, A28
Werk, J. K. et al. 2014, ApJ, 792, 8
Yang, Y. B. et al. 2012, Proc. SPIE, 8446, 84467Q

Links

[1] Science Team list: http://www.mosaic-elt.eu/index.php/science/46-science-team

Figure 4. Comparison between IFU and mono-aperture performance, illustrating the necessity of MOSAIC's multiple observing modes. Left: Sky subtraction schemes for the two modes. Middle: Spectra of SGASJ122651.3+215220 (see Rigby et al., 2018) redshifted to z = 8.38 and AB = 27. The top spectrum has been extracted using WEBSIM (Puech et al., 2016) assuming an IFU on the ELT (30 hrs exposure), providing a signal-to-noise ratio of ~ 30 for the absorption lines. The bottom spectrum extraction is the same but made with a 0.5-arcsecond fibre aperture and a sky correction uncertainty of 1%, showing that it does not allow absorption line measurements. A similar result would be obtained by using 0.5% and 1.2% sky residuals for an IFU and mono-aperture fibre, respectively. Right: Adapted from Figure 4 of Oesch et al. (2015), this shows the surface density of the full sample of z ~ 8 galaxies in the deep fields studied by Bouwens et al. (2015) (grey histogram). The green area shows the magnitude range of Lyman break galaxy (LBG) candidates that can be targeted with the multi-IFUs of MOSAIC, thanks to their better throughput when observing low-surface-brightness sources.

P. Horálek/ESO

The arrival of daylight at ESO's La Silla Observatory reveals the splendour of the Universe beyond our little planet in dazzling detail. The Milky Way stretches overhead as a streaming banner of dust backlit by the light of billions of stars. Clouds of interstellar dust grow thickest towards the constellation of Sagittarius (The Archer), which marks the centre of the galaxy — the core around which the spectacular spiral arms rotate.

DOI: 10.18727/0722-6691/5221

PCS — A Roadmap for Exoearth Imaging with the ELT

Markus Kasper[1]
Nelly Cerpa Urra[1]
Prashant Pathak[1]
Markus Bonse[2]
Jalo Nousiainen[3]
Byron Engler[1]
Cédric Taïssir Heritier[1]
Jens Kammerer[1]
Serban Leveratto[1]
Chang Rajani[4]
Paul Bristow[1]
Miska Le Louarn[1]
Pierre-Yves Madec[1]
Stefan Ströbele[1]
Christophe Verinaud[1]
Adrian Glauser[2]
Sascha P. Quanz[2]
Tapio Helin[3]
Christoph Keller[5]
Frans Snik[5]
Anthony Boccaletti[6]
Gaël Chauvin[7]
David Mouillet[7]
Caroline Kulcsár[8]
Henri-François Raynaud[8]

[1] ESO
[2] Institute for Particle Physics and Astrophysics, ETH Zürich, Switzerland
[3] Lappeenranta-Lahti University of Technology, Finland
[4] Department of Computer Science, University of Helsinki, Finland
[5] Leiden University, the Netherlands
[6] LESIA, Observatoire de Paris-Meudon, France
[7] Université Grenoble Alpes, CNRS, IPAG, France
[8] Institut d'Optique, Université Paris-Saclay, France

The Planetary Camera and Spectrograph (PCS) for the Extremely Large Telescope (ELT) will be dedicated to detecting and characterising nearby exoplanets with sizes from sub-Neptune to Earth-size in the neighbourhood of the Sun. This goal is achieved by a combination of eXtreme Adaptive Optics (XAO), coronagraphy and spectroscopy. PCS will allow us not only to take images, but also to look for biosignatures such as molecular oxygen in the exoplanets' atmospheres. This article describes the PCS primary science goals, the instrument concept and the research and development activities that will be carried out over the coming years.

Science Case — nearby exoplanets down to Earth-size

One of the most rapidly developing fields of modern astrophysics is the study of extrasolar planets (exoplanets) and exoplanetary systems. The key goals of the field include understanding the architectures of exoplanetary systems, the formation and evolution of planetary systems, and the composition and structure of exoplanet atmospheres. With over 3000[1] confirmed exoplanets (identified mostly by indirect methods by NASA's Kepler mission), we have developed a basic statistical understanding of the inner regions of planetary systems, i.e., planets with periods less than a few years and orbital separations smaller than a few astronomical units (au), and have thereby made considerable progress towards the first goal. However, the architectures of the outer planetary systems remain essentially unexplored. Given that we do not yet have a complete picture of planetary system architectures, progress towards understanding their formation has been limited. Furthermore, since over 99% of the planets discovered so far have been found indirectly, we have only limited data with which to study and understand the properties of exoplanet atmospheres.

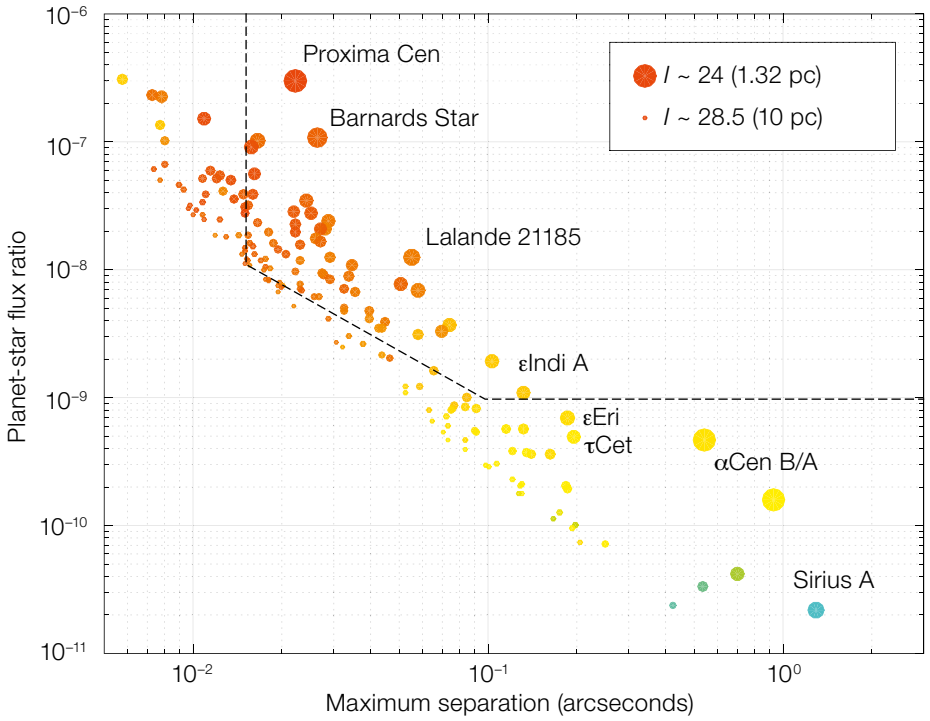

Figure 1. Angular separation and *I*-band flux ratio between hypothetical exoearths (Earth size and insolation, one per star) and parent stars within 10 pc (from the Hipparcos catalogue) observable from Cerro Armazones. The symbol size indicates the planet's apparent brightness, and the colours indicate stellar spectral type (red: M-stars, yellow: solar-type stars). The dotted lines indicate the approximate contrast boundaries for PCS.

The main reason behind the small number of directly imaged exoplanets is that such observations are extremely challenging. The intensity contrast between the stellar light reflected by an exoplanet and the star itself is less than one part in a million at angular separations of a few tens of milliarcseconds in the case of nearby giant planets discovered by the radial velocity (RV) method, and it becomes even smaller for larger separations between planet and star. Potentially habitable planets with sizes, masses and temperatures like those of Earth are even harder to observe.

Figure 1 shows the approximate *I*-band contrast and angular separation estimated for hypothetical exoearths (planets with Earth-like size and insolation) around the nearest stars.

Therefore in order to directly image and characterise a sizeable number of exoplanets, the combination of telescope and instrument must provide an extremely high contrast and very good sensitivity. Contrast levels around 10^{-8} at 15 milliarcseconds and 10^{-9} at 100 milliarcseconds are needed for the observation of nearby planetary systems with a limiting exoplanet magnitude of *I* ~ 27. This would allow us to image giant planets in orbits of a few au already discovered by the RV method, and even to observe potentially habitable planets around very nearby M-stars, as shown in Figure 1. The low-mass M-stars are particularly interesting because around 80% of all stars belong to this group and a considerable number of them are within 20 light-years (~ 6 pc) of the Sun. Temperate small planets have already been found around Proxima Cen (at a distance of 1.3 pc; Anglada-Escudé et al., 2016), Barnard's star (at 1.8 pc; Ribas et al., 2018), Lalande 21185 (at 2.5 pc; Díaz et al., 2019), and Teegarden's star (at 3.8 pc; Zechmeister et al., 2019), and many more are expected to be identified by ongoing and future RV missions (for example, Quirrenbach et al., 2018; Wildi et al., 2017). It is therefore of the utmost scientific importance to understand whether such planets might provide habitable conditions or even show atmospheric fingerprints of biological activity.

The most prominent of these biosignatures is molecular oxygen (O_2), which was originally identified as a promising way to find extraterrestrial life in exoplanet atmospheres by Lovelock (1965). It is currently the most easily detectable signal of life in Earth's atmosphere (20% by volume), created as a product of photosynthesis. Most prominent for optical to near-infrared (NIR) observations is the O_2 A-band around 765 nm, which consists of a forest of narrow lines. A spectral resolution of several hundred thousand would resolve the unsaturated lines (see López-Morales et al., 2019), and even a spectral resolution of around one hundred thousand would be sufficient to resolve the saturated lines expected to be present in the spectrum of a directly imaged exoearth. In addition, such a high-dispersion spectrum also presents an opportunity to spectrally isolate the planet signal and differentiate it from residual stellar light, thus improving the achievable contrast and sensitivity. Contrast improvements of at least 1:10 000 have been realised with high-dispersion spectroscopy (HDS), which would in principle multiply with the contrast achievable by other methods to supress stellar light at the position of a planet (Snellen et al., 2015).

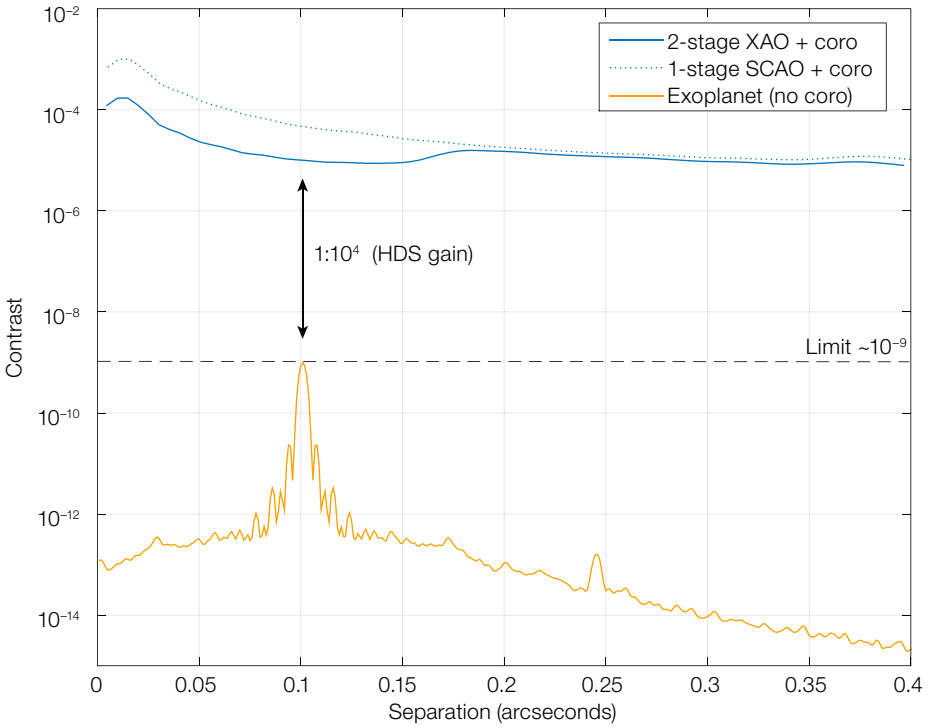

Figure 2. Toy model illustrating how the combination of high-contrast imaging with the ELT and high-dispersion spectroscopy can achieve a contrast of 10^{-9} at small angular separations.

Besides the observation of exoearths and the search for biosignatures, a remarkable finding in exoplanetary science in the past decade has been that sub-Neptune planets of around three Earth radii are among the most abundant planets in the solar neighbourhood, despite the absence of any such planet in the Solar System. This planet category sits at the most important transition in the process of planetary formation, namely the onset of runaway accretion of a large gaseous envelope by a rocky core of a critical mass (Pollack et al., 1996). Those planets are so far barely constrained by observations, apart from some H_2O detections in sub-Neptune atmospheres by transit spectroscopy (Tsiaras et al., 2019; Benneke et al., 2019). PCS will detect them in large numbers, allowing us to study their global demographics and explore their role in the conditions of formation of smaller exoearths. PCS will also characterise them and search for molecular features, for example H_2O, CO_2 and CH_4, with medium-resolution spectroscopy in the NIR.

PCS concept and challenges

To achieve its scientific goals, PCS must provide an imaging contrast of ~ 10^{-8} at 15 milliarcseconds angular separation from the star and 10^{-9} at 100 milliarcseconds and beyond. In addition, it must provide the spectroscopic capability to observe individual spectral lines due to molecules at optical and NIR wavelengths. The most promising approach for reaching these capabilities is a combination of XAO, coronagraphy and HDS, which must each individually be pushed to the limit.

Figure 2 illustrates this approach. Assuming an HDS contrast of better than 10^{-4}, the remaining gap to reach the contrast requirements must be provided by the high-contrast imaging (HCI) system consisting of XAO and a coronagraph.

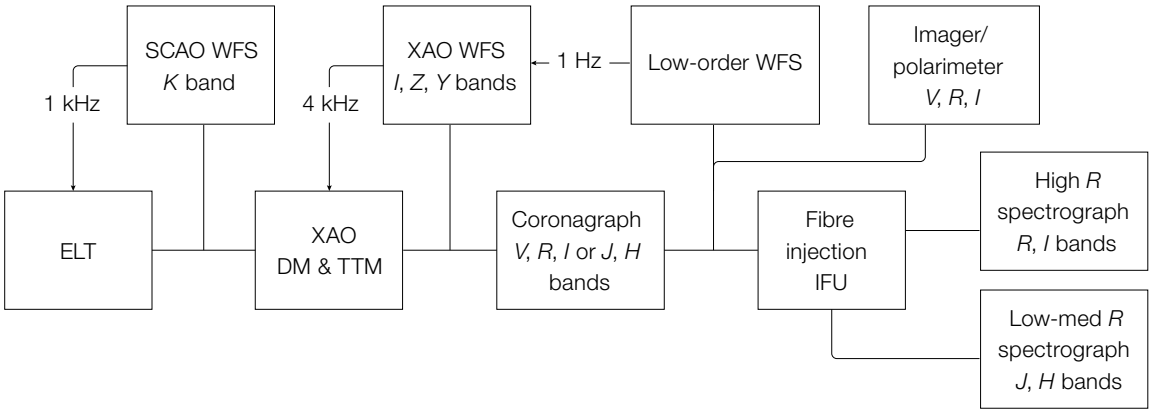

Figure 3. Concept diagram of PCS showing the main building blocks.

The block concept for PCS is shown in Figure 3. The stellar light is suppressed by the HCI as employed by several instruments in operation such as the Spectro-Polarimetric High-contrast Exoplanet REsearch instrument (SPHERE) at ESO's Very Large Telescope (VLT) (Beuzit et al., 2019). The incoming turbulent wavefront will be pre-flattened by a first-stage AO correction with the ELT's M4 mirror (Vernet et al., 2019). The leftover turbulence will be further reduced by a high-speed second stage XAO system working at a wavelength as close as possible to the science wavelength to minimise chromatic residuals. The coronagraph will then strongly attenuate the telescope's diffraction pattern and leave a high-contrast image, as illustrated in Figure 4. The high-contrast raw image is finally fed by an array of single-mode fibres to one of the possible science instruments, for example, a high-dispersion spectrograph working in the red optical *R* and *I* bands where the O_2 A band is located.

Extreme adaptive optics

XAO is a key technology still requiring significant research and development (R&D). It is critically important to minimise the photon noise introduced by stellar light scattered to the position of the nearby planet, which is the main noise source for ground-based exoplanet detection. For example, an XAO-residual halo with contrast on the order of 5 x 10^{-5} at the smallest angular separations forces us to collect 5 x 10^3 exoplanet photons for a 1σ detection of a 10^{-8} exoplanet. Correspondingly, a 5σ detection of this exoplanet would require 25 times more — about 10^5 — photons. In order to collect that many photons in 10 hours with the ELT (assuming *J* band, 50-nm bandwidth, 10% throughput), the exoplanet must have an apparent magnitude of at most *J* = 26. This is the typical brightness of an exoearth around an M-star at 5 pc. This simple reasoning shows that the required exposure times are inversely proportional to the raw point spread function (PSF) contrast and illustrates how important it is to push XAO performance to its limits.

Figure 4 shows the simulated XAO residual PSF in the *I* band for a VLT-like system. The error budget of the conventional SPHERE-like system shown on the left is dominated by the temporal delay error (see, for example, Guyon, 2005), which shows up as the slightly elongated bright area of increased residuals near the centre. The temporal delay in the system is introduced by wavefront sensor detector integration, detector readout, computation of the correction signal and its application to the deformable mirror (DM). It amounts to at least two update steps of the AO system, during which time the atmospheric turbulence has evolved and no longer perfectly matches the DM correction.

A straightforward approach to reducing the temporal delay is to run the AO system faster. In practice, this is most easily achievable by installing a second small AO system (called the second stage), which corrects a smaller area of the PSF at a much higher update rate, for example 4 kHz instead of the ~ 1 kHz of the first stage. The effect is a greatly improved raw PSF contrast near the star, where most exoplanets are located, as shown in the right panel of Figure 4. This approach is, for example, proposed for the upgrade of SPHERE (called SPHERE+; Boccaletti et al., 2020) and for the potential VLT visitor instrument the high-Resolution Integral-field Spectrograph for the Tomography of Resolved Exoplanets Through Timely Observations (RISTRETTO), aimed at the spectral characterisation of Proxima b (outlined in Lovis et al., 2017).

An even greater performance improvement is expected from predictive control, i.e., by using past measurements to predict the wavefront at the time of the correction. This approach would not only reduce the temporal delay error but could also mitigate the impact of photon noise, thus making the AO system operate better on faint stars (for example, Males & Guyon, 2018). Another important gain could come from controlling the contrast instead of flattening the wavefront, which would require nonlinear control.

A very promising field of research aimed at realising these gains is the application of machine learning techniques. In particular, reinforcement learning (RL) is an active branch of machine learning that provides an automated environment for control. It promises to cope with some of the limitations of current AO systems. Unlike classical control methods, RL methods aim to learn a successful closed-loop control strategy by interacting with the system. Hence, they do not require accurate models of the control loop components and can adapt to a changing environment.

Fibre-fed spectroscopy

Another field of active R&D for exoplanet detection is the optimised adaptation of high-dispersion integral field spectrographs (IFS) to the HCI case. As HDS also helps to improve the imaging contrast, integral field capability is needed to precisely locate the exoplanets before being able to characterise them. While a fair number of small, nearby exoplanets have already been discovered by the RV method (see above), and many more discoveries are expected for the coming decade, the orbit inclinations and therefore the precise locations of these planets are not accessible by RV.

Fibre-based integral field units may offer some advantages over image slicers or lenslet-array-based solutions. Optical fibres provide a relatively simple means of rearranging the two-dimensional field of view along a single dimension perpendicular to the spectral dispersion direction. In addition, the modal filtering capability of single-mode fibres can be used to create coronagraphs with smaller inner-working angles or higher throughput (Por & Haffert, 2020), and it can also reject random speckles from the XAO system to increase contrast by a factor of a few (Mawet et al. 2017). Single-mode fibres are also well adapted to diffraction-limited imaging, allow light to be efficiently manipulated in photonic integrated circuits, and allow for high-dispersion spectrographs the size of a shoe box. The true potential of such innovative solutions for HCI and HDS, however, remains to be evaluated by laboratory experiments and on-sky observations.

Integral field spectroscopy will be a crucial PCS capability both for improving the contrast performance and for characterising exoplanets and their environments. Current HCI IFS have spectral resolutions of less than 100. To assess and correct instrument aberrations undergoing (chromatic) Fresnel propagation and to detect broad spectral lines and narrow spectral bands, an IFS with a medium spectral resolution (a few thousand) is required for PCS. Since an IFS is always limited by the number of available detector pixels, the medium-dispersion IFS will be able to cover a much larger field and/or a broader spectral range than the high-dispersion IFS. This will be particularly beneficial for detecting and locating exoplanets. The first on-sky testing with a pathfinder has already been carried out by a team led by Leiden University (Haffert et al., 2020). To reach the required technological readiness level for PCS, a visitor instrument could be to be developed and tested with SPHERE at the VLT or the XAO system MagAO-X at the Magellan Clay Telescope (Males et al., 2018).

PCS planet yield

The scientific capabilities of PCS are best illustrated by the number of small ($R < 4$ Earth radii) exoplanets that PCS would be able to observe as predicted by the Python package P-pop (Kammerer & Quanz, 2018). Assuming planet occurrence rates from NASA's Kepler mission (as in Dressing & Charbonneau, 2015 for M-stars and Kopparapu et al., 2018 for AFGK-stars), circular and randomly oriented orbits, geometric albedos distributed uniformly between 0 and 0.6, and Bond albedos distributed uniformly between 0 and 0.8, we simulated synthetic exoplanets around a sample of 1272 nearby stars within 20 pc of Earth and observable from Cerro Armazones. Then, for each simulated planet, we determined whether it is bright enough to pass the PCS sensitivity limit with an assumed value of 27.5 magnitudes in a 50-hr *I*-band observation, and whether it exceeds the anticipated contrast curve of PCS (dotted lines in Figure 1). Repeating this procedure many times enabled us to statistically assess the number of planets that PCS could detect, as summarised in Figure 5. Of course, PCS will not look at more than a thousand stars for 50 hours each. Our assumption is rather that many of the targets will be identified by ongoing and future RV missions (for example, Quirrenbach et al., 2018; Wildi et al., 2017) and added to the list of already known nearby small exoplanets.

Besides the large number of relatively nearby giant planets already detected by RV observations, PCS has the potential to detect and characterise more than 40 nearby exosuperearths and exoearths. Sub-Neptunes (2–4 Earth radii) are even more likely to be observed, because they are both brighter (since they reflect more light from the host star) and more numerous. Moreover, most detectable planets have equilibrium temperatures of ~ 200–300 K. Colder small planets receive less light from their parent stars and are therefore faint in reflected light, while hotter planets are often too close to their host star to be spatially resolved even by the ELT. Most of the detectable Earth-sized planets orbit M-stars, while a larger number of sub-Neptunes can be observed around AFGK stars.

PCS's high sensitivity to small planets around late-type stars makes it very complementary to thermal-infrared HCI as deployed, for example, in the Mid-infrared

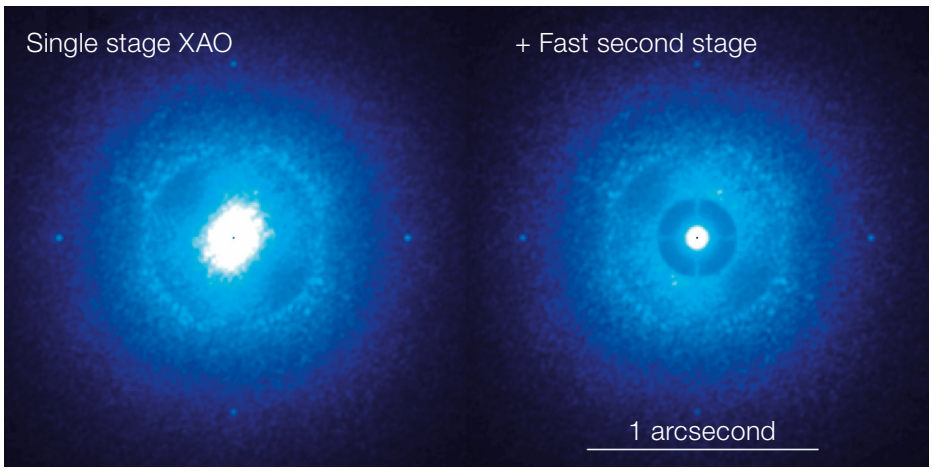

Figure 4. Simulated coronagraphic *I*-band PSFs for an 8-m telescope with a conventional XAO (for example, SPHERE-SAXO) in the left panel, and with an additional fast 4-kHz second stage AO shown in the right panel.

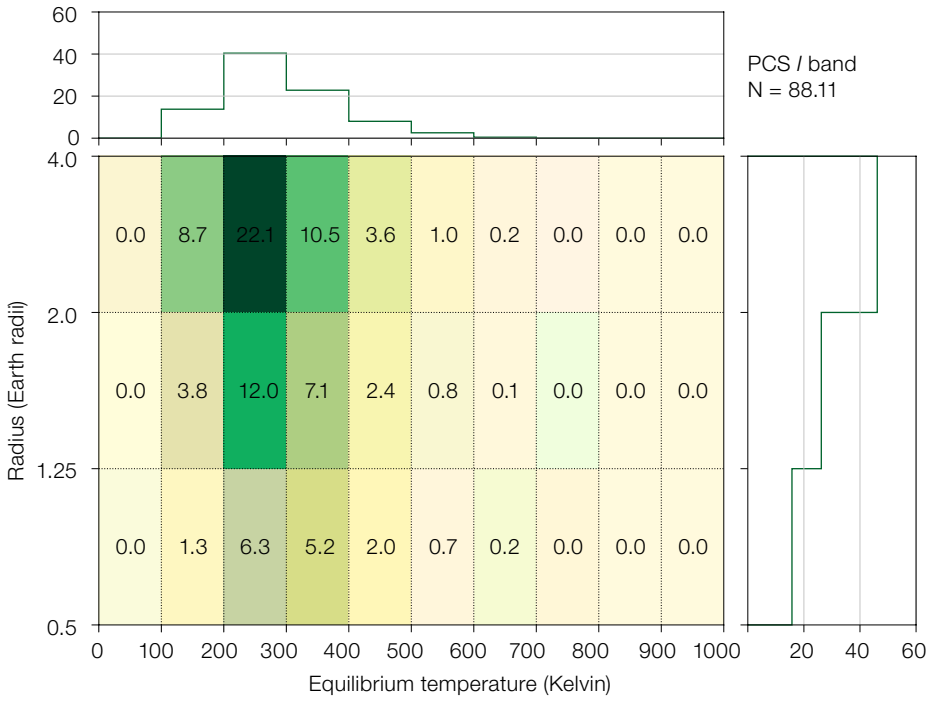

Figure 5. Number of small planet detections in the planet equilibrium temperature vs planet radius plane predicted for PCS observing in the *I* band at quadrature. The marginal histograms show the number of detectable planets as functions of temperature (top) and radius (right).

ELT Imager and Spectrograph (METIS) (Brandl et al., 2018), which is most sensitive to small planets around the handful of very nearby solar-type stars. The visible and NIR also contain many relevant spectral lines and molecular bands, which are crucial for Earth-like exoplanet characterisation and complement the spectral features observable in the thermal-infrared.

Roadmap towards project start

Prior to the start of the PCS instrument project in a few years, ESO's Technology Development Program is carrying out dedicated R&D activities concentrating on the XAO problem in HCI. In particular, the development of a fast DM with well above 10 000 actuators, excellent positioning resolution (down to 0.06 nm surface deformation) and a small settling time (down to 0.1 ms) is being pursued with European industry. ESO initiated such a development in 2016, and two contracts have been awarded, to ALPAO (France) and to a German consortium comprising Fraunhofer IOF and Physik Instrumente. The goal was to deliver an XAO DM conceptual design backed up by a strong prototyping activity. These two contracts were completed by the end of 2019 and both contractors managed to deliver conceptual designs, based on completely different technologies and compliant with most of the XAO requirements. While the ALPAO design is based on their well-known voice coil approach, Fraunhofer IOF and Physik Instrumente derived a concept based on exchangeable piezoelectric stacked actuators. In each case some limitations have been identified, some of which are being addressed in a second development phase to improve the design and to build a prototype. Other aspects, such as increasing the number of actuators and the corresponding drive electronics, are not yet part of the Technology Development Programme but are projected to be in the roadmap for the next phase of development.

The second major activity, running until 2023, is the development of predictive control methods using classical (see, for example, Kulcsár et al., 2006) and machine learning techniques. Here, the goal is to improve the XAO raw PSF contrast over conventional control methods by factors of 3 to 10 and accordingly reduce the required observing time to obtain a given signal-to-noise ratio by the same factor. Special attention will be given to the feasibility of implementing these methods into the hardware envisaged. We need fast algorithms which have the potential to run in real time at the ELT in about one decade.

The predictive control R&D follows the classical approach. After analysing the problem, promising methods will first be tested in computer models with simulated turbulence and with turbulence measured on-sky by real XAO systems such as, for example, VLT-SPHERE or the Subaru Coronagraphic Extreme Adaptive Optics (SCExAO; Lozi et al., 2018) at the Subaru telescope. This work is being done in collaboration with the ETH Zürich, the Institut d'Optique of the Université Paris-Saclay, the Lappeenranta-Lahti University of Technology, Leiden Observatory and the research organisation TNO in the Netherlands. Furthermore, ESO and the Microsoft Research Laboratory are working to establish a collaboration on Machine Learning-based Predictive Control, which could be of great benefit for PCS R&D.

The best-performing methods will then be implemented and tested in the laboratory. For this, the ETH Zürich and ESO are currently developing an XAO test setup called the GPU-based High-order adaptive OpticS Testbench (GHOST), which will be located in ESO's AO laboratory and will be available in early 2021. GHOST (see Figure 6 for the opto-mechanical setup) will feature a spatial light modulator (SLM) to inject programmable turbulence, measured on-sky by existing XAO instruments. Its XAO system will consist of a Pyramid Wavefront Sensor using a GPU-based real-time computer (RTC) and the freely available CACAO[2] software to control a Boston Micromachines 492-actuator DM. The RTC will be similar to the SCExAO RTC built around the CACAO framework and data format. This concept was also adopted for MagAO-X at the Magellan Clay Telescope and the Keck Planet Imager and Characterizer (KPIC) at the

Keck II Telescope (Mawet et al., 2018). Consequently a user community already exists and it will be relatively easy to share code and experience. Interfaces to cameras and DMs frequently used in AO are readily available.

Finally, if a predictive control method shows a significant potential during the GHOST testing period between mid-2021 and the end of 2022, we plan to implement and test it on-sky in 2023. The tests are expected to use the existing SCExAO instrument at the Subaru telescope and possibly a fast second stage AO system added to SPHERE. SCExAO already uses a software architecture similar to that foreseen for GHOST, which should greatly facilitate the porting of algorithms.

In parallel with the R&D on XAO mentioned above, complementary activities are being carried out in the community. The High-Resolution Imaging and Spectroscopy of Exoplanets instrument (HiRISE; Vigan et al., 2018) is a VLT visitor instrument that will use single-mode fibres to feed the high-contrast PSF delivered by SPHERE to the upgraded CRyogenic high-resolution InfraRed Echelle Spectrograph (CRIRES+; Dorn et al., 2016) thereby implementing and validating the general PCS concept. Similar ideas are also being pursued by RISTRETTO, KPIC, MagAO-X and SPHERE+.

After the conclusion of these R&D activities at ESO and within the community, all major ingredients of PCS should be validated and lifted to a high enough level of technology readiness to enable the project to start. PCS will then prepare for the observation of nearby rocky planets and maybe the discovery of an exoplanet that's truly habitable — or even already inhabited — in the 2030s.

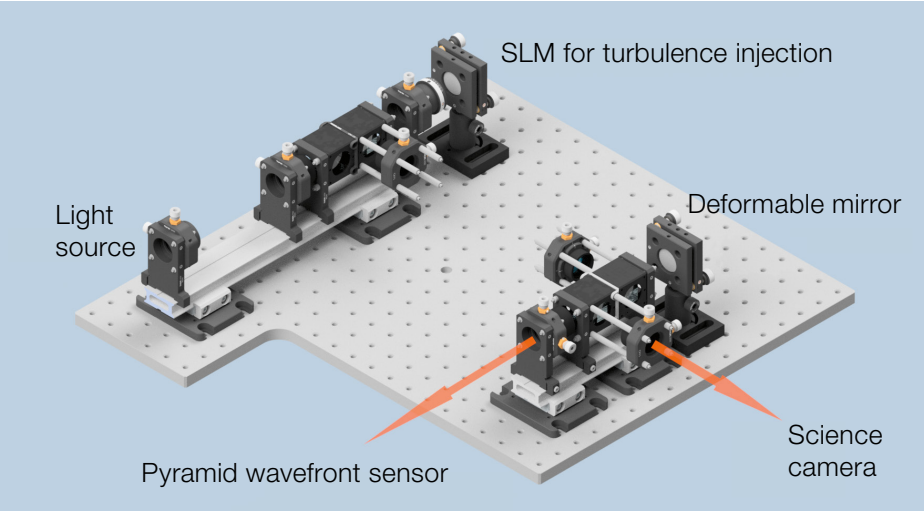

Figure 6. Optomechanical setup of GHOST.

References

Anglada-Escudé, G. et al. 2016, Nature, 536, 437
Beuzit, J.-L. et al. 2019, A&A, 631, A155
Benneke, B. et al. 2019, ApJL, 887, L14
Boccaletti, A. et al. 2020, arXiv:2003.05714
Brandl, B. et al. 2018, Proc. SPIE, 10702, 107021U
Dressing, C. D. & Charbonneau, D. 2015, ApJ, 807, 45
Díaz, R. F. et al. 2019, A&A, 625, A17
Dorn, R. J. et al. 2016, Proc. SPIE, 9908, 99080I
Guyon, O. 2005, ApJ, 629, 592
Haffert, S. Y. et al. 2020, arXiv:2009.03529v1
Kammerer, J. & Quanz, S. P. 2018, A&A, 609, A4
Kopparapu, R. K. et al. 2018, ApJ, 856, 122
Kulcsár, C. et al. 2006, Opt. Express, 14, 7464
López-Morales, M. et al. 2019, AJ, 158, 24
Lovelock, J. E. 1965, Nature, 207, 568
Lovis, C. et al. 2017, A&A, 599, A16
Lozi, J. et al. 2018, Proc. SPIE, 10703, 1070359
Males, J. R. & Guyon, O. 2018, JATIS, 4, 019001
Males, J. R. et al. 2018, Proc. SPIE, 10703, 1070309
Mawet, D. et al. 2017, ApJ, 838, 92
Mawet, D. et al. 2018, Proc. SPIE, 10703, 1070306
Pollack, J. B. et al. 1996, Icarus, 124, 62
Por, E. H. & Haffert, S. Y. 2020, A&A, 635, A55
Quirrenbach, A. et al. 2018, Proc. SPIE, 10702, 107020W
Ribas, I. et al. 2018, Nature, 563, 365
Snellen, I. et al. 2015, A&A, 576, A59
Tsiaras, A. et al. 2019, Nature Astronomy, 3, 1086
Vernet, E. et al. 2019, The Messenger, 178, 3
Vigan, A. et al. 2018, Proc. SPIE, 10702, 1070236
Wildi, F. et al. 2017, Proc. SPIE, 10400, 1040018
Zechmeister, M. et al. 2019, A&A, 627, A49

Links

[1] Exoplanet Orbit Database: http://exoplanets.org/
[2] CACAO software: https://github.com/cacao-org/cacao

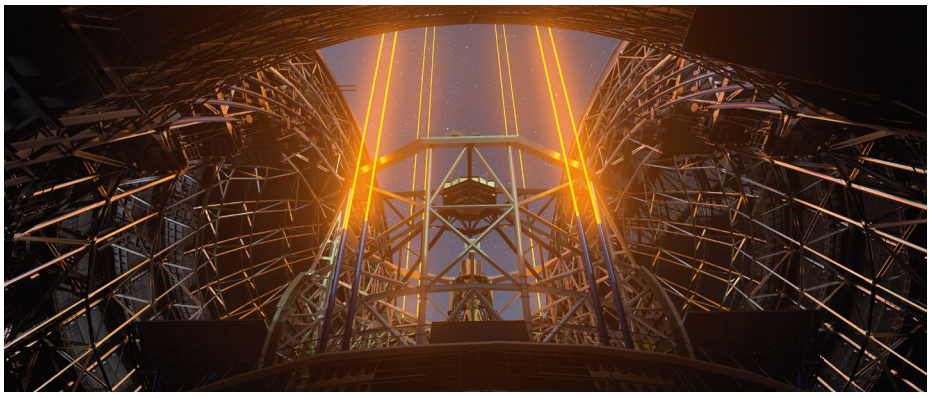

This artistic illustration depicts the laser guide stars of the future Extremely Large Telescope (ELT). Like many other systems on the ELT, the multiple laser guide stars are vital to its operation, helping it adapt to the ever-changing atmospheric conditions above the telescope. This information is sent to the ELT's M4 mirror which will adjust its shape to compensate for the distortion caused by atmospheric turbulence, allowing astronomers to observe finer details of much fainter astronomical objects than would otherwise be possible from the ground.

Astronomical Science

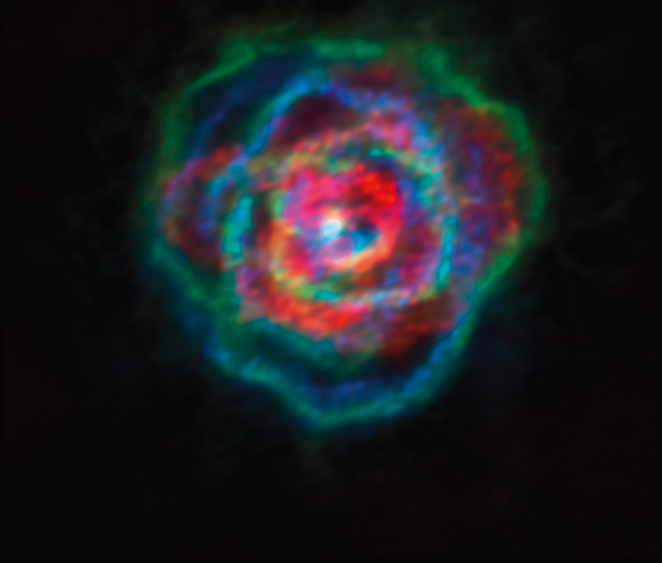

ALMA (ESO/NAOJ/NRAO), Decin et al.

The ATOMIUM project is set out to map the stellar winds blowing out from a dozen red giant stars, an ambitious goal made possible thanks to ALMA's spectacular resolution. The team has found out that in all cases the stellar winds were not spherical, but had different shapes, just like seen in the image above of the winds around the star R Aquilae. The patterns seen in the stellar winds have a striking resemblance to those of planetary nebulae.

DOI: 10.18727/0722-6691/5222

SUPER — AGN Feedback at Cosmic Noon: a Multi-phase and Multi-scale Challenge

Vincenzo Mainieri[1]
Chiara Circosta[2]
Darshan Kakkad[1]
Michele Perna[3]
Giustina Vietri[4]
Angela Bongiorno[5]
Marcella Brusa[6,7]
Stefano Carniani[8]
Claudia Cicone[9]
Francesca Civano[10]
Andrea Comastri[7]
Giovanni Cresci[11]
Chiara Feruglio[12]
Fabrizio Fiore[12]
Antonis Georgakakis[13]
Chris Harrison[14]
Bernd Husemann[15]
Alessandra Lamastra[5]
Isabella Lamperti[2,1]
Giorgio Lanzuisi[7]
Filippo Mannucci[11]
Alessandro Marconi[16,11]
Nicola Menci[5]
Andrea Merloni[17]
Hagai Netzer[18]
Paolo Padovani[1]
Enrico Piconcelli[5]
Annagrazia Puglisi[19]
Mara Salvato[17]
Jan Scholtz[20]
Malte Schramm[21]
John Silverman[22,23]
Christian Vignali[6,7]
Gianni Zamorani[7]
Luca Zappacosta[5]

[1] ESO
[2] Department of Physics & Astronomy, University College London, UK
[3] Departamento de Astrofísica, Centro de Astrobiología (CSIC–INTA), Madrid, Spain
[4] INAF IASF – Milano, Italy
[5] INAF – Osservatorio Astronomico di Roma, Italy
[6] Dipartimento di Fisica e Astronomia dell'Universitá degli Studi di Bologna, Italy
[7] INAF – Osservatorio di Astrofisica e Scienza dello Spazio di Bologna, Italy
[8] Scuola Normale Superiore, Pisa, Italy
[9] Institute of Theoretical Astrophysics, University of Oslo, Norway
[10] Center for Astrophysics | Harvard & Smithsonian, Cambridge, MA, USA
[11] INAF – Osservatorio Astrofisico di Arcetri, Firenze, Italy
[12] INAF – Osservatorio Astronomico di Trieste, Italy
[13] Institute for Astronomy & Astrophysics, National Observatory of Athens, Greece
[14] School of Mathematics, Statistics and Physics, Newcastle University, UK
[15] Max Planck Institute for Astronomy, Heidelberg, Germany
[16] Dipartimento di Fisica e Astronomia, Università di Firenze, Italy
[17] Max Planck Institute for Extraterrestrial Physics, Garching, Germany
[18] School of Physics and Astronomy, Tel-Aviv University, Israel
[19] Centre for Extragalactic Astronomy, Department of Physics, Durham University, UK
[20] Onsala Space Observatory, Chalmers University of Technology, Sweden
[21] National Astronomical Observatory of Japan, Tokyo, Japan
[22] Kavli Institute for the Physics and Mathematics of the Universe, The University of Tokyo, Japan
[23] Department of Astronomy, School of Science, The University of Tokyo, Japan

Theoretical models of galaxy evolution suggest that galaxy-wide outflows driven by active galactic nuclei (AGN), one of the so-called AGN-feedback mechanisms, are a fundamental process affecting the bulk of the baryons in the Universe. While the presence of such outflows out to kpc scales is now undisputed, their impact on the star formation, gas content and kinematics of the host galaxy is hotly debated. Here we report on the results from our Large Programme SUPER, which used the Spectrograph for INtegral Field Observations in the Near INfrared (SINFONI) on the Very Large Telescope (VLT) to carry out the first statistically sound high-spatial-resolution investigation of AGN outflows at $z \sim 2$, covering four orders of magnitude in AGN bolometric luminosity.

The role of AGN in galaxy evolution

The cosmic evolution of galaxies has been one of the key research topics in

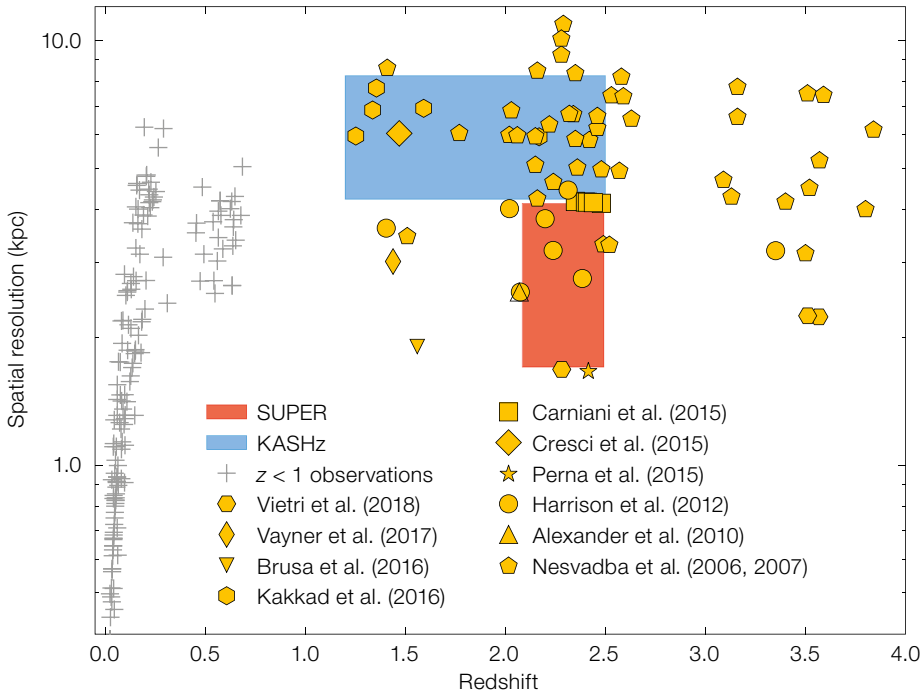

Figure 1. Summary of integral field spectroscopic observations from the literature characterising ionised outflows through the [O III] 5007 Å emission line in AGN host galaxies (adapted from Circosta et al., 2018). SUPER observations have an unprecedented spatial resolution (~ 1.7–4 kpc) for a sizeable sample of 39 AGN.

astrophysics during the last half century and is fundamental to understanding how the Universe evolved into its current form. Theoretical arguments (for example, Silk & Rees, 1998) suggest that the energy released by the black hole at the centre of most galaxies may shape the properties of the interstellar medium (ISM), itself the fuel of star formation, and consequently the growth of galaxies. AGN-feedback may therefore be a physical phenomenon that is key to regulating the evolution of galaxies. One promising mechanism to link the growth of the AGN and the evolution of its host galaxy involves fast winds launched from the accretion disc surrounding the supermassive black hole (SMBH) (for example, King & Pounds, 2003; Begelman, 2003; Menci et al., 2008; Zubovas & King, 2012; Faucher-Giguère & Quataert, 2012). These winds shock against the surrounding gas and drive outflows which propagate out to large distances from the AGN, heat the ISM and potentially eject large amount of gas out of the system (for example, Zubovas & King, 2012). Observationally, outflows have been detected in AGN at both low and high redshift. Very fast outflows have been revealed by X-ray and ultraviolet emission and absorption line studies on pc scales (with velocities up to 30% the speed of light) and via high-resolution infrared and millimetre spectroscopic observations at kpc scales (with velocities up to a few thousand km s^{-1}). But past observational studies of AGN-driven outflows were plagued by two major limitations. First, to maximise the chances of detection, observational campaigns have been conducted on AGN preselected to feature an outflow by the use of selection criteria such as broad [O III] lines or colour selection techniques. Second, most previous studies were not able to link the properties of such outflows with those of the central SMBH for a statistically significant sample, mostly owing to the lack of the necessary multiwavelength data or sufficient spatial resolution. The SUPER project was conceived to overcome these two main limitations.

The SUPER project

The SINFONI Survey for Unveiling the Physics and the Effect of Radiative feedback (SUPER[1]), is an ESO Large Programme (196.A-0377) which was awarded 280 hours of SINFONI time and which is aimed at providing the first unbiased investigation of the ionised gas in AGN at $z \sim 2$. The survey strategy, presented in Circosta et al. (2018), was to conduct a blind search of AGN-driven outflows, without preselecting the targets in a way that would maximise the chances of detecting an outflow. Our targets have been selected from deep and wide-area X-ray surveys (CDFS, COSMOS-Legacy, XMM XXL, Stripe 82X); each target has a secure spectroscopic redshift in the range $z = 2.0–2.5$, which ensures sampling of the Hβ and [O III] lines in the *H* band and the Hα and [S II] lines in the *K* band. It is crucial to study AGN outflows at those redshifts, since their impact depends critically on the ambient conditions and, because of the high gas content, the ISM conditions in star-forming galaxies at $z \sim 2$ are different from what is observed in local analogues (for example, Kewley et al., 2013; Steidel et al., 2014; Coil et al., 2015). Furthermore, since $z \sim 2–3$ is the peak of star-formation and AGN activity we may expect that if AGN-feedback has a substantial role in galaxy evolution this is the right cosmic time to verify it.

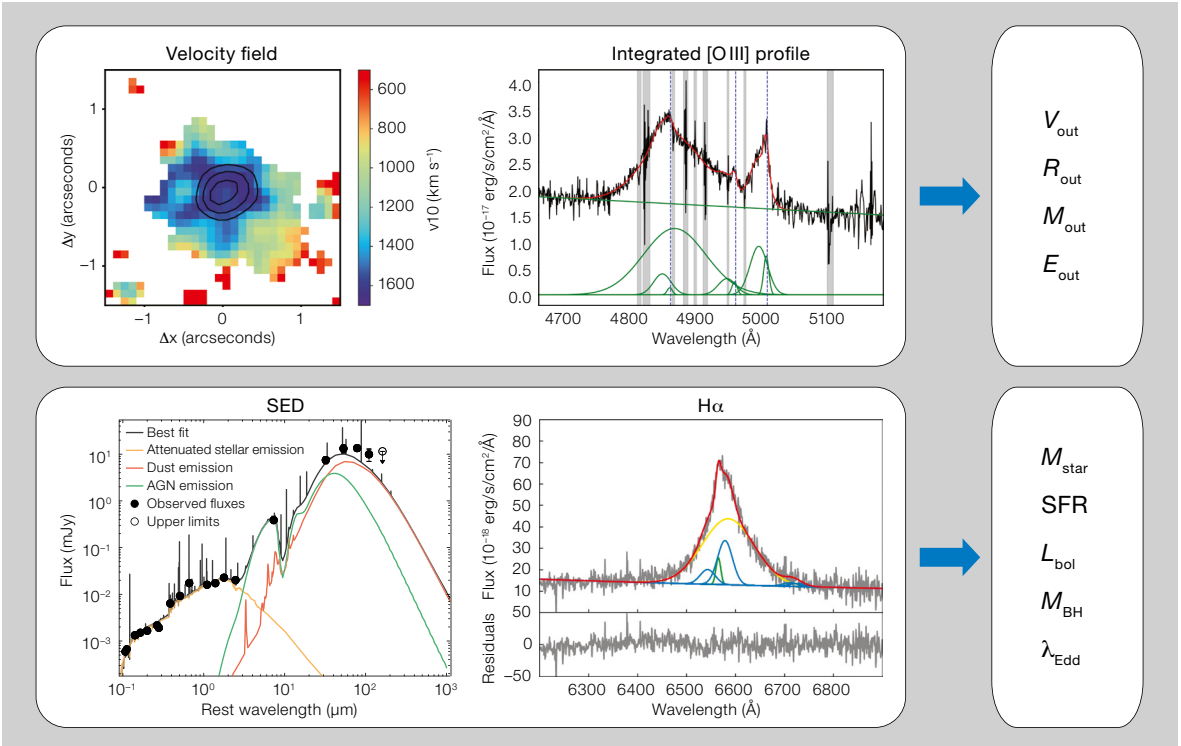

Figure 2. Upper panel: example of the [O III] velocity field reconstructed from the SINFONI observations and the extracted 1D spectra which we use to determine the velocity V_{out}, extension R_{out}, mass outflow rate M_{out} and kinetic energy E_{out} of the ionised gas outflows. Lower panel left: multi-component SED fitting from the ultraviolet to the far-infrared to characterise the properties of the host galaxy (stellar mass M_{star} and star formation rate, SFR) and the bolometric luminosity L_{bol} of the AGN. Lower panel right: line fitting of the Hα line to determine the black hole mass.

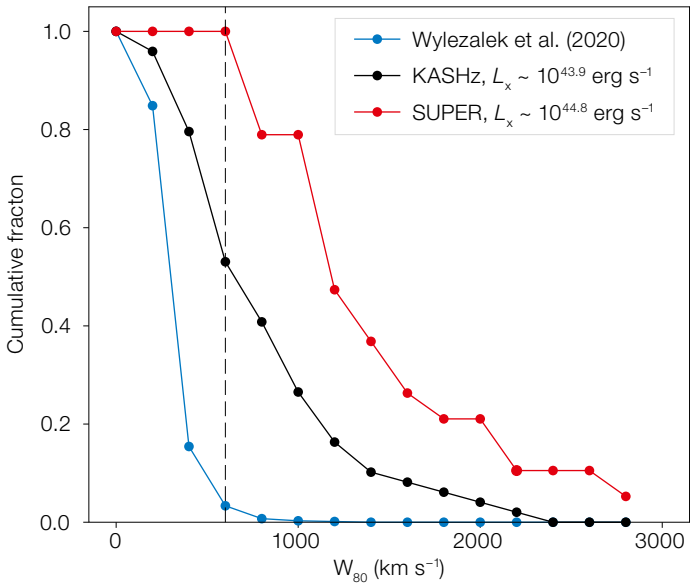

Figure 3. The inverse cumulative W80 distribution for the Type-1 AGN in the SUPER survey (red; Kakkad et al., 2020), the KASHz survey matched in redshift (black; Harrison et al., 2016), a mass-matched low-redshift star-forming sample (blue; Wylezalek et al., 2020). The dashed black-line at 600 km s^{-1} corresponds to the W80 value used to define that a target hosts an AGN-driven outflow (well justified from the fact that almost all star-forming galaxies have W80 values below this cut). Based on the above W80 criteria, all the Type-1 targets in SUPER show the presence of outflows, and ~ 52% of the redshift matched targets in the KASHz survey show outflows. The difference between the W80 distributions for SUPER and KASHz surveys is due to the different luminosity range of the AGN sampled by these surveys.

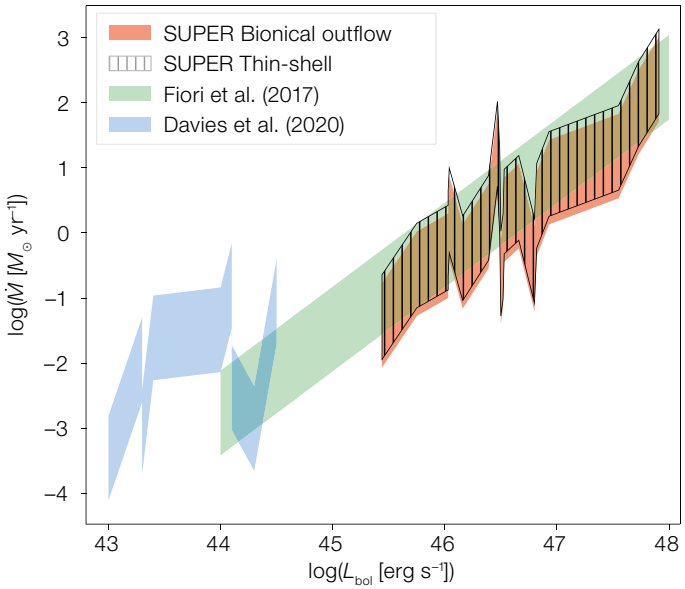

Figure 4. Ionised gas [O III] mass outflow rate vs. the bolometric luminosity of the AGN in the SUPER Type-1 sample (from Kakkad et al., 2020). The red shaded area and the black hatched area show the mass outflow rates for the SUPER targets assuming a bi-conical outflow model and a thin shell model, respectively. The green shaded area shows the outflow rates for ionised gas from literature data compiled in Fiore et al. (2017) and the blue shaded region shows the outflow rates for a low redshift X-ray AGN sample from Davies et al. (2020). The shaded regions all correspond to mass outflow rates assuming an electron density of 500–10 000 cm^{-3}.

The final sample consists of 39 AGN (Circosta et al., 2018) for which we have superb multi-wavelength ancillary data that allow us to properly characterise the central SMBH and its host galaxy: stellar masses ($4 \times 10^9 - 2 \times 10^{11}$ $M_\odot$), star formation rates (25–680 $M_\odot$ yr^{-1}) and AGN bolometric luminosities ($2 \times 10^{44} - 8 \times 10^{47}$ erg s^{-1}). Of the 39 targets, 22 are classified as Type-1 (56%) and the remaining 17 as Type-2 (44%), based on the presence or absence of broad emission lines such as Mg II or C IV in the rest-frame ultraviolet spectra.

The SINFONI adaptive optics (AO) observations were performed in Laser Guide Star Seeing Enhancer (LGS-SE) mode, which has demonstrated the capability to achieve a point spread function (PSF) full width half maximum (FWHM) of 0.2–0.3 arcseconds. This allows us to spatially resolve any outflows with sizes larger than ~ 2 kpc. This is a key feature of the survey that allows us to resolve the kinematics of the ionised gas at a finer spatial scale than seeing-limited observations (see Figure 1), and consequently decreases significantly the uncertainties in the derived physical properties of the detected outflows. We set our observational strategy to be able to properly trace the PSF using directly the light distribution of the broad Hβ components for Type-1 AGN and dedicated observations of PSF reference stars that we performed close to the science observations of Type-2 AGN. Curve-of-growth analysis and more sophisticated methodologies have been used to take into account any beam-smearing effect in the data cubes and thereby to retrieve the best estimates of the outflowing gas properties (for example, extension and velocity; Kakkad et al., 2020).

AGN outflow demography and scaling relations

One of the main goals of SUPER is to perform a demographic study of the incidence of AGN-driven outflows at z ~ 2.

In Kakkad et al. (2020) we present the results obtained for the Type-1 AGN in the SUPER sample and find that all of them feature a galaxy-wide outflow (Figure 3). The parameter adopted to identify outflows is the velocity width of the [O III] line containing 80% of the flux (i.e., W80). A value of W80 larger than 600 km s^{-1} is considered a clear signature of an AGN-driven outflow, based on the W80 distributions of large galaxy samples at z ~ 2 (see Kakkad et al., 2020). We therefore show that AGN-driven outflows are common in a blind-selected sample of AGN at z ~ 2, which obviously further supports the hypothesis that AGN-feedback plays an important role in galaxy evolution. A detailed comparison of the PSF and the [O III] radial profile shows that the [O III] emission is spatially resolved for ~ 35% of the Type-1 sample and the outflows show an extension up to ~ 6 kpc.

Another main goal of SUPER was to link the properties of the observed outflows with the properties of the central SMBH (for example, its bolometric luminosity).

Theoretical models of AGN outflows predict that fast winds originating from the accretion disc impact on the ISM, resulting in a forward shock that expands within the host galaxy. This would naturally predict positive correlations between outflow properties (for example, velocity and mass outflow rate) and AGN properties (see, for example, King & Pounds, 2015). In Kakkad et al. (2020), we explore a range of plausible assumptions about the physical properties of the outflow (its geometry, velocity and radius) and of the outflowing gas (its electron density) and report the range of derived mass outflow rates for each target. The mass outflow rates for the Type-1 sample are in the range ~ 0.01–1000 $M_{\odot}$ yr^{-1}. After factoring in the systematic uncertainties in the outflow models, these outflow rates seem to correlate with the bolometric luminosity of the AGN (see Figure 4), as expected on the basis of the above theoretical arguments.

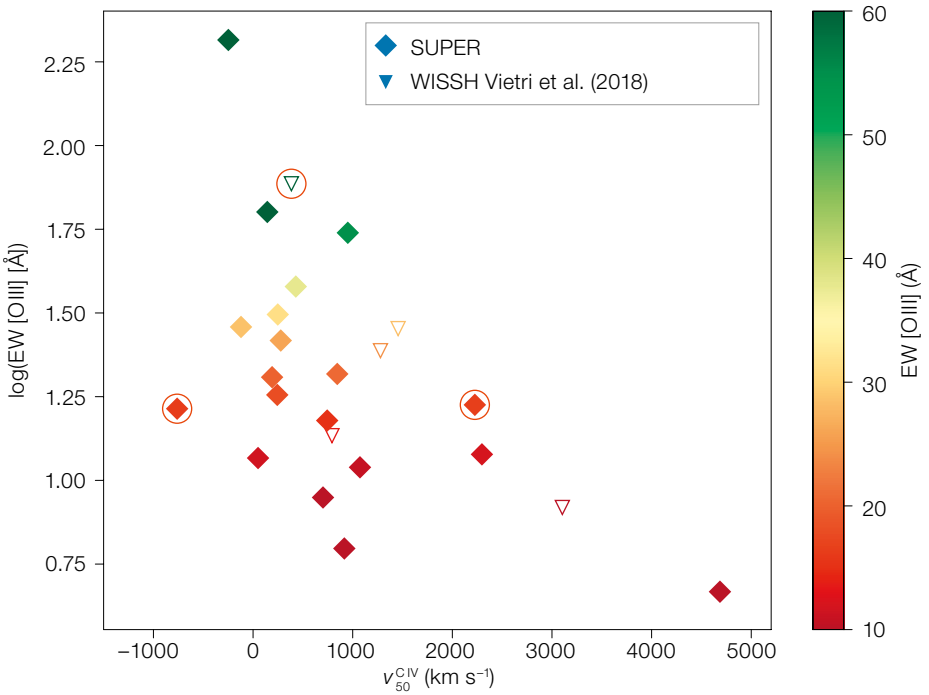

Figure 5. [O III] equivalent width as a function of the velocity shift of the C IV emission line for the SUPER sample (diamonds), colour-coded according to the [O III] equivalent width. Additionally, the WISE/SDSS Selected Hyperluminous quasars (WISSH; Bischetti et al., 2017) sample with reliable [O III] measurements are also reported (empty triangles). A clear anti-correlation is present, which supports the idea that the BLR winds traced by the C IV are connected with the winds on kpc scales detected in the NLR using the [O III] line (Vietri et al., 2020).

Tracing AGN winds from pc to kpc scales

Several theoretical models have been proposed to describe how the energy released by the central SMBH couples to the surrounding medium and generates the outflows observed on galaxy scales. With SUPER we have the remarkable opportunity to constrain the different models, since we are able to trace the winds from scales smaller than 1 pc out to several kpc. In Vietri et al. (2020), we use ancillary data to study the high-ionisation C IV 1549 Å line originating from the broad line region (BLR) surrounding the central SMBH. We confirm the well-known fact that the C IV line width does not correlate with the Balmer lines and the peak of the line profile is blueshifted with respect to the [O III]-based systemic redshift. These findings support the idea that the C IV line is tracing outflowing gas in the BLR, for which we estimated velocities up to ~ 4700 km s^{-1}. We inferred BLR mass outflow rates in the range 0.005–3 $M_{\odot}$ yr^{-1}, showing a correlation with the bolometric luminosity consistent with that observed for ionised winds in the narrow line region (NLR) and X-ray winds detected in local AGN. Finally, we found an anti-correlation between the equivalent width of the [O III] line and the C IV velocity shift (see Figure 5), and a positive correlation with the [O III] outflow velocity. These findings, for the first time in an unbiased sample of AGN at z ~ 2, support a scenario in which BLR winds are connected to galaxy-scale detected outflows and are therefore actually capable of affecting the gas in the NLR located at kpc scales (Vietri et al., 2020).

Ongoing work, data releases and outlook

At the time of writing all the data for the Large Programme have been acquired, and a first set of results has been already published. The SUPER first data release is accessible via the ESO Science Archive Facility (SAF)[2] and consists of flux-calibrated data cubes for half of the sample. Next year we plan to have a second and final data release for the whole SUPER sample.

The team is working on a series of additional studies, combining the SINFONI data with follow-up data obtained in recent years. These include:

– A systematic study of the molecular gas reservoir, as traced by ALMA CO(3-2) observations, in the SUPER AGN host galaxies, to assess the impact that the AGN may have on them (Circosta et al., 2021).
– The dust properties of our targets, as traced by ALMA Band-7 continuum observations at high resolution, compared with the spatial location of the outflow and of the unobscured star formation as traced by the SINFONI Hα emission (Lamperti et al., in preparation).
– The outflow properties of the full SUPER sample, and the dependence on the host galaxy properties, for example stellar mass and star formation rate (Perna et al., in preparation).

SUPER has already fulfilled its ambition and represents a major advancement in the systematic studies of AGN-driven outflows at a crucial cosmic epoch corresponding to the peak of volume-averaged star formation and supermassive black hole accretion in the Universe. It further

represents the ideal sample for follow-up studies with current and future facilities. The hot ionised gas kinematics need to be complemented with a significant investment of ALMA time to trace the cold molecular phase of the outflows (for example, Cicone et al., 2018). The launch of the JWST will enable the study of the H_2 rotational emission lines in the mid-infrared which could be used as an alternative means to trace the molecular phase of these outflows. Finally, the next generation of integral field units at the forthcoming extremely large telescopes (for example, the High Angular Resolution Monolithic Optical and Near-infrared Integral field spectrograph [HARMONI] at ESO's Extremely Large Telescope) will have the necessary sensitivity and spatial resolution to trace the dependency of the mass outflow rate as a function of radius inside the galaxy, which is very much needed to provide strong constraints on the different theoretical models. Finally, these observational efforts should be complemented by the investment of substantial resources in the modelling of the multi-phase outflows, in particular with detailed simulations able to trace the cold molecular gas.

Acknowledgements

We are extremely grateful to the numerous ESO staff in Paranal Observatory for their dedication in carrying out the SINFONI observations, and to Elena Valenti of ESO's User Support Department for excellent support during the execution of the Large Programme.

References

Alexander, D. M. et al. 2010, MNRAS, 402, 2211
Begelman, M. C. 2003, Science, 300, 1898
Bischetti, M. et al. 2017, A&A, 598, A122
Brusa, M. et al. 2016, A&A, 588, A58
Carniani, S. et al. 2015, A&A, 580, A102
Cicone, C. et al. 2018, Nature Astronomy, 2, 176
Circosta, C. et al. 2018, A&A, 620, 82
Circosta, C. et al. 2021, A&A, in press, arXiv:2012.07965
Coil, A. L. et al. 2015, ApJ, 801, 35
Cresci, G. et al. 2015, ApJ, 799, 82
Davies, R. et al. 2020, MNRAS, 498, 4150
Faucher-Giguère, C.-A. & Quataert, E. 2012, MNRAS, 425, 605
Fiore, F. et al. 2017, A&A, 601, A143
Harrison, C. M. et al. 2012, MNRAS, 426, 1073
Harrison, C. M. et al. 2016, MNRAS, 456, 1195
Kakkad, D. et al. 2016, A&A, 592, A148
Kakkad, D. et al. 2020, A&A, 642, 147
Kewley, L. J. et al. 2013, ApJ, 774, 100
King, A. R. & Pounds, K. 2003, MNRAS, 345, 657
King, A. R. & Pounds, K. 2015, ARA&A, 53, 115
Menci, N. et al. 2008, ApJ, 686, 219
Nesvadba, N. P. H. et al. 2006, ApJ, 650, 693
Nesvadba, N. P. H. et al. 2007, A&A, 475, 145
Perna, M. et al. 2015, A&A, 583, A72
Silk, J. & Rees, M. J. 1998, A&A, 331, L1
Steidel, C. C. et al. 2014, ApJ, 795, 165
Vayner, A. et al. 2017, ApJ, 851, 126
Vietri, G. et al. 2018, A&A, 617, A81
Vietri, G. et al. 2020, A&A, 644, 175
Wylezalek, D. et al. 2020, MNRAS, 492, 4680
Zubovas, K. & King, A. 2012, ApJ, 745, L34

Links

[1] SUPER website: www.super-survey.org
[2] SUPER first data release access via the ESO SAF: https://archive.eso.org/scienceportal/home?data_collection=SUPER&publ_date=2020-09-29

ESO/P. Horálek

As the Sun sets, ESO's Very Large Telescope (VLT) springs into action to begin its nightly mission. Consisting of four 8.2-metre Unit Telescopes (UTs) — named Antu, Kueyen, Melipal, and Yepun — and four smaller 1.8-metre Auxiliary Telescopes (ATs), the VLT is one of the most advanced telescope facilities in the world. All eight telescopes can be seen in this image, the smaller and rounder ATs scattered amongst the larger and more angular UTs.

DOI: 10.18727/0722-6691/5223

Mapping the Youngest and Most Massive Stars in the Tarantula Nebula with MUSE-NFM

Norberto Castro[1]
Martin M. Roth[1]
Peter M. Weilbacher[1]
Genoveva Micheva[1]
Ana Monreal-Ibero[2,3]
Andreas Kelz[1]
Sebastian Kamann[4]
Michael V. Maseda[5]
Martin Wendt[6]
and the MUSE collaboration

[1] Leibniz-Institut für Astrophysik Potsdam, Germany
[2] Instituto de Astrofísica de Canarias, La Laguna, Tenerife, Spain
[3] Departamento de Astrofísica, Universidad de La Laguna, Tenerife, Spain
[4] Astrophysics Research Institute, Liverpool John Moores University, UK
[5] Leiden Observatory, Leiden University, the Netherlands
[6] Institut für Physik und Astronomie, Universität Potsdam, Germany

The evolution of the most massive stars is a puzzle with many missing pieces. Statistical analyses are key to providing anchors to calibrate theory, but performing these studies is an arduous job. The state-of-the-art integral field spectrograph Multi Unit Spectroscopic Explorer (MUSE) has stirred up stellar astrophysicists, who are excited about its ability to take spectra of up to a thousand stars in a single exposure. The excitement was even greater with the commissioning of the MUSE narrow-field mode (MUSE-NFM) that has demonstrated angular resolution akin to that of the Hubble Space Telescope (HST). We present the first mapping of the dense stellar core R136 in the Tarantula nebula based on a MUSE-NFM mosaic. We aim to deliver the first homogeneous analysis of the most massive stars in the local Universe and to explore the impact of these peculiar objects on the interstellar medium (ISM).

Resolving the heart of NGC 2070 with MUSE-NFM

The evolution of the Universe is tied to massive stars. They live fast, only a few Myrs, but in very dramatic ways. The energy released during their short lives, and their deaths in supernova explosions, shape the chemistry and dynamics of their host galaxies. Ever since the reionisation of the Universe, massive stars have been significant sources of ionisation. Nonetheless, the evolution of massive O- and B-type stars is far from being well understood, a lack of knowledge that is even worse for the most massive stars (Langer, 2012). These missing pieces in our understanding of the formation and evolution of massive stars propagate to other fields in astrophysics. Supernova rates, ionisation radiation, and chemical yields will depend on the evolutionary paths of massive stars. Ultimately, understanding the evolution of star-forming galaxies depends first and foremost on our ability to constrain the evolution of massive stars.

Stellar evolution is mainly governed by the initial mass. Nevertheless, other factors can play a significant role. Metallicity, rotational velocity, duplicity or strong stellar winds affect their lifetimes (Maeder & Meynet, 2000; Langer, 2012). Large systematic surveys are fundamental if we are to unveil the nature of the most massive stars, to constrain the role of these parameters in their evolution, and to provide homogeneous results and landmarks for the theory. Spectroscopic surveys have transformed the field in this direction, yielding large samples for detailed quantitative studies in the Milky Way (for example, Simón-Díaz et al., 2017) and in the nearby Magellanic Clouds (for example, Evans et al., 2011). However, massive stars are rarer than smaller stars, and very massive stars (> 70 $M_{\odot}$) are even rarer. The empirical distribution of stars on the upper part of the Hertzsprung-Russell (HR) diagram remains questionable and more data are essential.

The heart of the Tarantula nebula (NGC 2070) in the Large Magellanic Cloud (LMC) is intrinsically the brightest

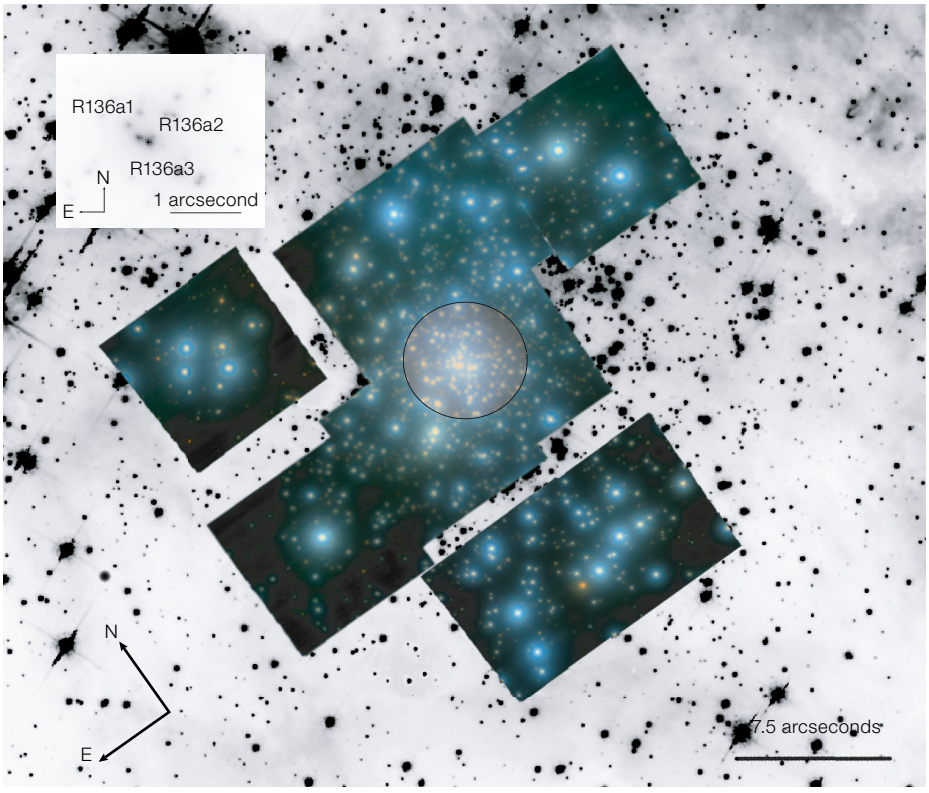

Figure 1. Colour-composite mosaic (RGB: *I*, *R* and *V* filters) of nine of the fields observed with MUSE-NFM in the core of NGC 2070. Image quality ranges between 50 and 80 milliarcseconds, akin to the spatial resolution of the HST. The HST image in the F555W band (Sabbi et al., 2013) is displayed in the background. The inset image is a zoom into the core of R136 (marked by a circle in the mosaic) resolving R136a1, 2 and 3 WR stars.

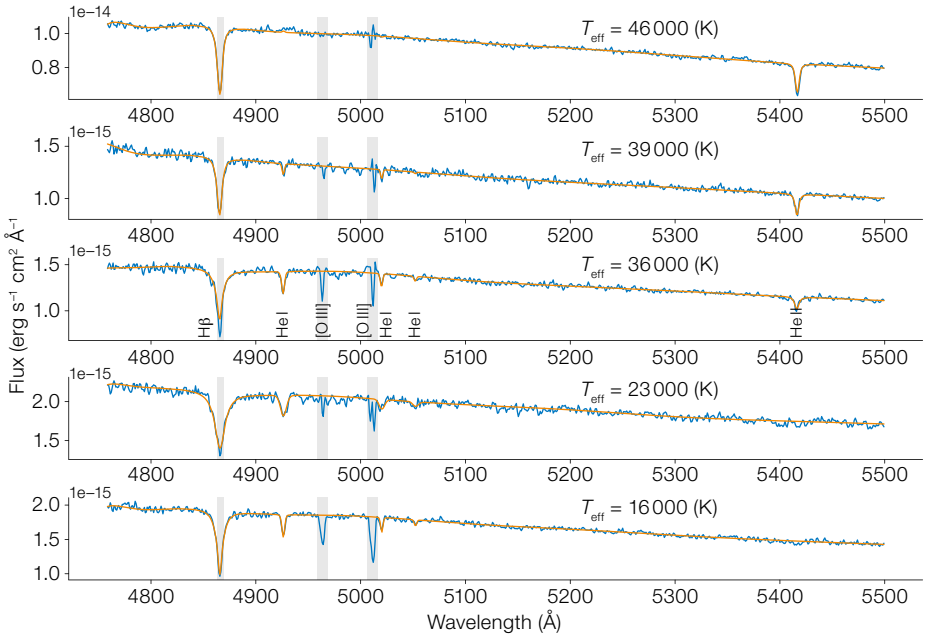

Figure 2. Representative OB stars extracted from the central field of the R136 cluster (blue). The stars were modelled (orange) with a dedicated FASTWIND grid (Puls et al., 2005). The effective temperature and key diagnostic lines are also indicated. The areas that could be affected by the sky subtraction are highlighted (grey shading).

star-forming region in the Local Group. Its proximity makes it a perfect laboratory in which to resolve the stellar population and test evolutionary theories. NGC 2070 hosts the most massive stars reported in the literature (Crowther et al., 2010), enclosing the massive cluster R136 at its core. Understandably, NGC 2070 has been of great interest to stellar astrophysicists, and it is considered the Rosetta Stone of the field (Schneider et al., 2018). However, in light of the severe stellar crowding in the core of NGC 2070, the R136 cluster has largely been omitted from many optical surveys (Evans et al., 2011).

The integral field spectrograph (IFS) MUSE (Bacon et al., 2014) on the VLT is capable of resolving crowded stellar fields and taking high-quality spectra of thousands of stars in the dense cores of globular clusters (Kamann et al., 2016). In fact, this capability has even been exploited out to nearby galaxies (Roth, Weilbacher & Castro, 2019). The large field of view and sensitivity of MUSE have allowed us to systematically analyse large stellar populations in unprecedented detail, and to study the ISM (for example, Weilbacher et al., 2018; Roth et al., 2018). Castro et al. (2018a) presented MUSE wide-field-mode (MUSE-WFM) observations of the central part of NGC 2070. This work provided a homogeneous spectroscopic census of the massive stars in the vicinity of R136. However, the R136 cluster is impossible to resolve with MUSE-WFM.

MUSE-NFM, commissioned in 2018 (Leibundgut et al., 2019), has opened a window for optical stellar spectroscopy that until now was only available to the HST. The field of view of 7.5 × 7.5 arcseconds and an expected spatial resolution close to that of the HST offer unique capabilities for mapping R136. These capabilities have been successfully tested during ESO programme 0104.D-0084. We observed ten fields in NGC 2070 with MUSE-NFM and mosaicked the R136 cluster from a total of nine pointings. The tenth one was centred on the Wolf-Rayet (WR) system R140. The outstanding performance of MUSE-NFM and its associated Ground Atmospheric Layer Adaptive optiCs for Spectroscopic Imaging (GALACSI) module in combination with the Adaptive Optics Facility of the VLT provides a spatial resolution that is similar to that of the HST (~ 0.07 arcseconds), but with spectroscopic information for each single pixel (see Figure 1). A peak in the centre of the cluster reveals how the spatial resolution is sufficient to resolve the WR stars R136a1, 2, and 3 (see the inset in Figure 1).

R136 cluster: dissecting and modelling

MUSE-NFM has unveiled a treasure-trove of OB stars to advance our understanding of the stellar evolution of very massive stars. Based on the integrated light of the MUSE-NFM data cubes, we created a new catalogue of the stellar content of the cluster. The MUSE-NFM catalogue lists approximately 1900 sources in ten fields, with a cutoff in the *V* band at ~ 22 magnitudes. A first crossmatch with the Hubble Tarantula Treasury Project

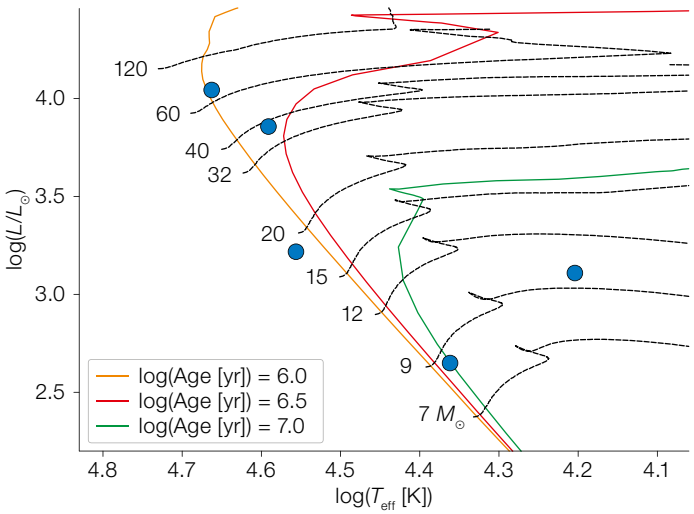

Figure 3. Distribution of the representative OB stars (see Figure 2) in the spectroscopic HR diagram (Langer & Kudritzki, 2014). The positions of the O-type and early B-type stars (blue dots) mainly match the expected young age of NGC 2070, approximately 2 Myr (for example, Schneider et al., 2018). Rotating evolutionary tracks from Ekström et al. (2012) are included in the plot (dotted black lines). The isochrones were calculated using the SYCLIST[1] online tool.

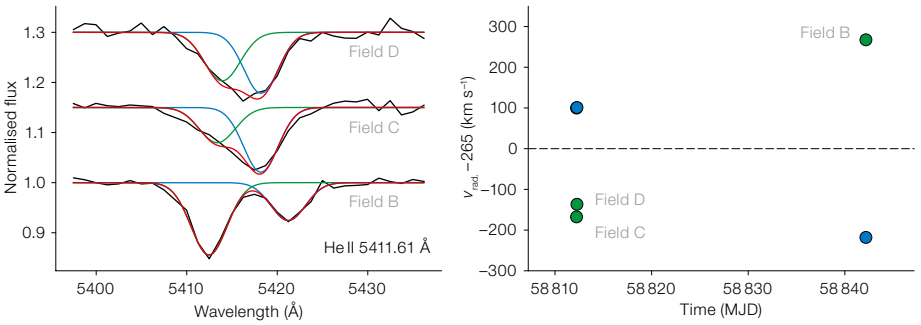

Figure 4. O+O spectroscopic binary resolved with MUSE-NFM. On the left, the kinematic evolution of He II 5411 Å (black line) at different epochs in overlapping fields. We perform a preliminary characterisation of the binary using Gaussian models (coloured lines). On the right, the velocity of each component is displayed. Note that the blue components of fields D and C overlap. The systemic velocity of R136, 265 km s^{-1}, has been subtracted.

catalogue (HTTP; Sabbi et al., 2013) showed additional detections and better accuracy for some of the fainter sources close to the brightest stars that are saturated in some of the HST images. The data will allow us to extract the spectra of ~ 200 stars with good signal-to-noise ratio (S/N), a sufficient number and distribution to obtain a clear snapshot of the evolution of OB stars at the age of R136, to approximately 10 $M_{\odot}$ in the HR diagram.

The MUSE-NFM wavelength range of 4700–9300 Å does not cover the classic transitions used for spectral classification and stellar atmosphere analysis (Castro et al., 2018a). These canonical features are located at bluer wavelengths than the MUSE cutoff. Nevertheless, MUSE-NFM data offer alternative diagnostics. For O-type and early B-type stars, several He I (4713, 4921, 5876, 6678 Å) and He II (5411, 6683 Å) transitions are included. Hα and Hβ lines and the bluest part of the hydrogen Paschen series are also visible, offering additional constraints on the effective temperature and gravity.

Previous work (for example, Crowther et al., 2017) shows that stellar analyses with MUSE datasets are possible. Figure 2 displays the analysis of five representative OB stars extracted from one of the central fields in R136. The analysis was performed by comparing the observed spectra with a grid of FASTWIND (Puls et al., 2005) synthetic models (see Castro et al., 2018b). The five examples in Figure 2 show a good match for the key diagnostic lines marked in the plot, i.e., Hβ, He I 4921 Å and He II 5411 Å. The residuals observed in the [O III] 4959, 5007 Å nebular lines are indicative of the difficulty of performing an impeccable sky subtraction, despite the outstanding spatial resolution.

Stellar atmosphere characterisation is indeed possible. As shown in Figure 3, the stars shown in Figure 2 match well the expected young age of NGC 2070, approximately 2.5 Myr. The full analysis of the 200 stars with S/N > 50 will populate the diagram, creating the building blocks of a better understanding of the formation and evolution of R136. Only the coolest star of these five departs from the expected young age, beyond the theoretical main-sequence proposed by Ekström et al. (2012) (see Castro et al., 2018b).

Binary fraction and stellar evolution

Binary stellar evolutionary models have shown that drastic effects on each member result from their evolving together. Interactions, mass transfer and eventual mergers shape each star's path in the HR diagram and the time it spends in different regions (for example, Wang et al., 2020). If 70% of OB stars were indeed tied to a companion (Sana et al., 2012), the evolution of massive stars in isolation would be rare. The spectral resolution of MUSE, around 50 km s^{-1}, may be considered a limitation before attempting a study of the OB star binary fraction. But we expect massive close-contact spectroscopic binaries to have strong radial velocity variations over short timescales, that can be monitored even with MUSE's moderate spectral resolution.

Our programme was designed to probe the capabilities of MUSE-NFM in a single epoch. Nevertheless, the observations were spread out in time for technical reasons, so for some of the stars we obtained data from multiple epochs (see Figure 1). These overlapping regions are priceless for carrying out a preliminary test of OB stellar variability. Several resolved spectroscopic binaries were detected in the extracted spectra. Figure 4 shows an example of an O+O binary system, where both He II 5411 Å components are resolved. A Gaussian modelling of both components shows a maximum peak-to-peak variability of ~ 500 km s^{-1}. Close binaries can indeed be characterised at MUSE's spectral resolution.

An ISM shaped by the most massive stars

MUSE-WFM provided new insights into the ISM around the most massive, newly born stars (Castro et al., 2018a). The gas intensity and kinematics were mapped, showing a bimodal blueshifted and redshifted motion with respect to the R136 systemic velocity, thereby sketching out the ISM in unprecedented detail. A peak in the core revealed redshifted, possibly infalling, material surrounding the strongest X-ray sources (see Figure 11 of Castro et al., 2018a). However, the kinematics in the inner part of the cluster could not be explored at the spatial resolution of MUSE-WFM.

MUSE-NFM can pierce and dissect the ISM kinematics in the highly dense R136 cluster, where MUSE-WFM capabilities could not probe. Figure 5 shows a coloured image of the central fields using some of the strongest emission lines in the MUSE wavelength range: [S II] 6717 Å, Hα and [O III] 5007 Å. The strong emission in Hα and the extended stellar wings of the WR population are clearly visible in Figure 5, as is the effect of the radiation carving out the ISM at HST-like spatial resolution. We have discovered several new Hα emitters in this first emission map, probably linked to Oe/Be stars and/or pre-main-sequence objects. The

latter are expected in an ongoing star-forming region such as NGC 2070. New insight into the formation of massive stars and feedback between the ISM with strong stellar winds and the radiative pressure of the most massive stars will be delivered by MUSE-NFM observations.

Future prospects

We are aiming to get a complete snapshot of the stellar evolution of the cluster R136 and to explore the role of different parameters (for example, binarity) in that evolution. However, the image quality reached in Period 104 and the time allocated over the forthcoming semesters lead us to dream of further possible outcomes. Exploring individual targets of interest in R136 can help us to address open questions, for instance about the physics driving stellar winds in O-type stars. The rich WR population in R136 will be examined, paying special attention to their strong and extended stellar winds. The data will include the strongest X-rays sources in the field (see Castro et al., 2018a), undoubtedly linked to the most massive WRs: Mk34, R136abc and R140ab (Crowther et al., 2010).

We will explore proper motions in combination with HST data over a baseline of almost ten years since the first HST program (PI: Lennon GO-12499, GO-13359). Mapping the runaway population and its possible links with the cluster will bring insights into the different mechanisms — dynamical ejection and/or a binary supernova scenario — that have been suggested to remove the stars from the cluster (for example, Dorigo Jones et al., 2020).

The MUSE-NFM observations have revealed a detailed spectroscopic picture of the massive stellar cluster R136. The combined MUSE IFS capabilities (i.e., field of view, spatial resolution and spectral coverage) outperform the HST, the only installation capable of resolving the stellar content of R136 at optical wavelengths. This is an outstanding technological achievement, emphasising the growing role of IFS for stellar astrophysics, whose future is very promising. Blue-MUSE (Richard et al., 2019) for the VLT, will open the much desired blue wavelength range so that detailed chemical composition analyses will be possible. ESO's Extremely Large Telescope (ELT) and the next generation of instruments, such as the High Angular Resolution Monolithic Optical and Near-infrared Integral field spectrograph (HARMONI) and the multi-object spectrograph MOSAIC, will allow us to leave the Local Group and explore clusters similar to R136 in other galaxies and in even stronger starburst environments.

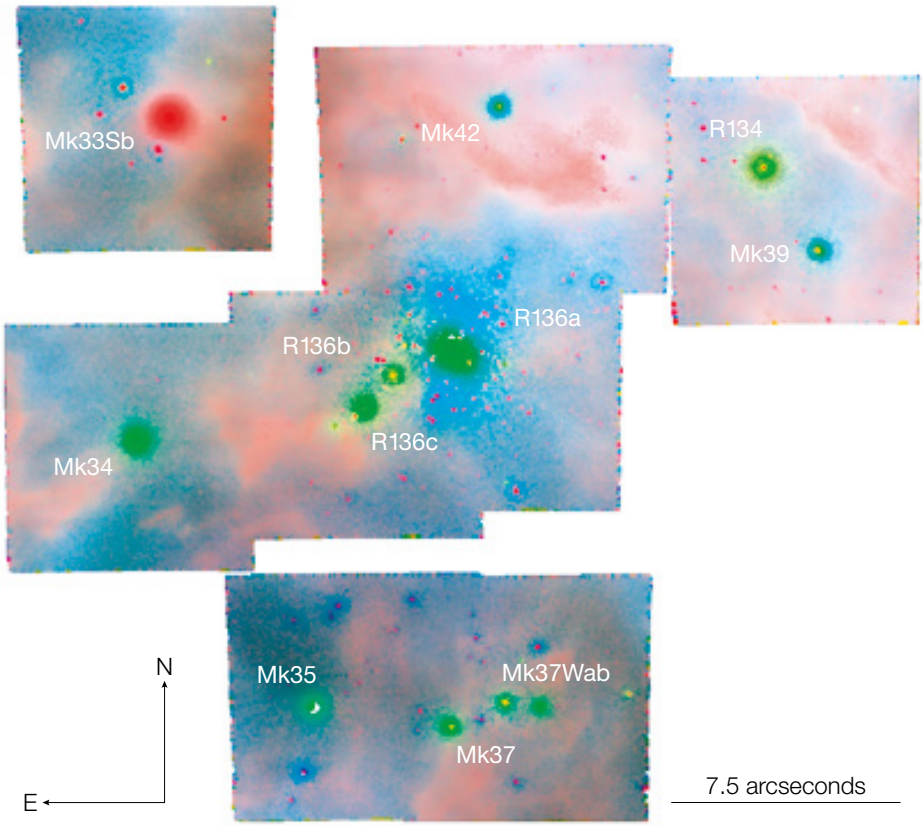

Figure 5. MUSE-NFM colour-composite mosaic of the nine fields in the core of NGC 2070 sampling narrow filters around the emission lines [S II] 6717 Å (red), Hα (green), and [O III] 5007 Å (blue). The WRs in the field are labelled (for example, Crowther et al., 2010).

Acknowledgements

This project has been funded by the Deutsche Forschungsgemeinschaft (DFG) – CA 2551/1-1. Norberto Castro and Genoveva Micheva gratefuly acknowledge funding from BMBF 05A17BA1, and Peter Weilbacher and Andreas Kelz from BMBF 05A17BAA for the MUSE-NFM project.

References

Bacon, R. et al. 2014, The Messenger, 157, 13
Castro, N. et al. 2018a, A&A, 614, A147
Castro, N. et al. 2018b, ApJ, 868, 57
Crowther, P. A. et al. 2010, MNRAS, 408, 731
Crowther, P. A. et al. 2017, The Messenger, 170, 40
Dorigo Jones, J. et al. 2020, 903, 43
Ekström, S. et al. 2012, A&A, 537, A146
Evans, C. J. et al. 2011, A&A, 530, A108
Kamann, S. et al. 2016, The Messenger, 164, 18
Langer, N. 2012, ARA&A, 50, 107
Langer, N. & Kudritzki, R. P. 2014, A&A, 564, A52
Leibundgut, B. et al. 2019, The Messenger, 176, 16
Maeder, A. & Meynet, G. 2000, ARA&A, 38, 143
Richard, J. et al. 2019, arXiv:1906.01657
Roth, M. M. et al. 2018, A&A, 618, A3
Roth, M. M., Weilbacher, P. M. & Castro, N. 2019, AN, 340, 989
Sabbi, E. et al. 2013, AJ, 146, 53
Sana, H. et al. 2012, Science, 337, 444
Schneider, F. R. N. et al. 2018, Science, 361, 7032
Simón-Díaz, S. et al. 2017, A&A, 597, A22
Puls, J. et al. 2005, A&A, 435, 669
Weilbacher, P. M. et al. 2018, A&A, 611, A95
Wang, C. et al. 2020, ApJL, 888, L12

Links

[1] SYCLIST: https://www.unige.ch/sciences/astro/evolution/en/database/syclist/

ESO/G. Hüdepohl

Among the largest nebulae in the southern night sky, the Carina Nebula is a perfect viewing target for ESO's Very Large Telescope (VLT). In this image, the nebula appears as a pink cloud in the clear sky above ESO's Paranal Observatory in Chile, home of the VLT. The cutting-edge Adaptive Optics Facility installed on UT4 of the VLT is in full operation here, propagating the orange laser beams into the atmosphere where they excite sodium atoms, causing them to glow and serve as reference stars to correct for the blurring effect of Earth's atmosphere.

DOI: 10.18727/0722-6691/5224

Fellows at ESO

Trystyn A. M. Berg

Just as the moon waxes and wanes, my childhood was full of a constant flux of interests. While my maths and science skills came easier to me than those in writing and social sciences, nothing in school really grabbed me. Growing up in "northern" Canada (near Edmonton, Alberta), I had access to beautiful skies, and often looked up and wondered about what was beyond Earth. It wasn't until my teenage years that I started to follow up these thoughts about the Universe. During my first physics class, I was struck by the elegance of applying maths to describe the Universe. Fortuitously, this occurred at the same time I was reading about the moons of Jupiter and the potential of Europa's harbouring life.

At that point I became determined to study planetary science and focused my studies on physics, maths, and geology when I started as an undergraduate at the University of Victoria in Canada. My interest in astronomy slowly migrated out of the Solar System as a result of the strong cooperative education programme that provided me with research-related work experience even as an undergraduate. Through the programme, I was fortunate to spend time on diverse projects at four research institutes. At the Joint Astronomy Centre in Hawai'i, I reduced spectroscopic data from the UK InfraRed Telescope (UKIRT) to study massive star formation. In Lethbridge, Canada, I spent time developing visualisation software for a Fourier transform spectrometer instrumentation lab responsible for building spectrometers for the Space Infrared telescope for Cosmology and Astrophysics (SPICA), the Herschel Space Observatory, and the James Clerk Maxwell Telescope. I compared the mass-size relation of bulges with ellipticals in the "local" Universe at the Herzberg Institute for Astrophysics in Victoria. And, finally, I searched for boron in quasar absorption line systems 3 Gyr after the Big Bang at the University of Victoria. This progression to higher redshifts led to my continuing my research in Victoria. I completed both my MSc and my PhD with Dr Sara Ellison, with whom I studied the use of intervening absorption lines imprinted on quasar spectra to reveal various facets of galaxy evolution. My research made heavy use of ESO's Ultraviolet and Visual Echelle Spectrograph (UVES) and the X-shooter spectrograph, as well as Hubble's Cosmic Origins Spectrograph.

In light of my experience with various instrumentation groups and ESO spectrographs, I recognised that being an ESO Fellow in Chile would be the prime postdoctoral experience for me — providing first-hand experience supporting telescopes I used heavily in my graduate studies, as well as nights of observing (an increasingly rare opportunity for young astronomers). I was very fortunate to be selected for one of the fellowship positions and joined ESO in October 2018. This was just in time to get involved as the Instrument Fellow for the Echelle Spectrograph for Rocky Exoplanet and Stable Spectroscopic Observations (ESPRESSO) on the Very Large Telescope (VLT), where I support the instrument operations team to make ESPRESSO observations easier. Currently, my duties for ESPRESSO lean towards developing software for quality control analysis, as well as preparing to test an upcoming mode of ESPRESSO meant for observing faint targets (like quasars) with a single Unit Telescope (UT). During the night, I am a support astronomer for UT2 (Kueyen), which primarily has been observing with UVES, X-shooter (now replaced by the VLT Imager and Spectrometer for mid-InfraRed, VISIR), and the Fibre Large Array Multi Element Spectrograph (FLAMES). Every time I see the night sky from Paranal, I am still in awe at how much detail one can see with the naked eye! On top of all these duties, I am also one of the developers of SCUBA, a software common to all instruments at Paranal for inspecting and assessing the quality of fresh data. While it is often a challenge balancing science and duties, it is refreshing to always have something on the go, as well as being exposed to excellent instrumentation and scientific research beyond my field.

My research to date focuses on the gas within the interstellar, circumgalactic and intergalactic media as probed by absorption seen along quasar sightlines. My recent work has made use of the XQ-100 legacy survey (a set of 100 $z \sim 4$ quasars observed with X-shooter) to study the contribution of damped and sub-damped Lyman-α absorbers to the neutral gas and metal budgets of the Universe, and to look at how we can use these systems as tracers of galaxy evolution. I am keenly interested in chemically peculiar systems, searching for interesting absorbers associated with the products of either the first generation of stars (such as carbon and oxygen), or the most chemically enriched systems (such as boron, manganese, and zinc) to understand the underlying stellar populations and galactic processes that can reproduce these effects. My PhD work also focused on studying the effects of active galactic nuclei on the gaseous reservoirs surrounding a galaxy. While we expected to see hotter or less dense gas, owing to feedback from the supermassive black hole, we instead found the opposite (at least for neutral gas). This puzzle still intrigues me and am currently seeking further evidence on the underlying processes to explain this apparent contradiction.

Beyond the night sky, I take every opportunity I get to relax at the curling club, on the golf course, or lost in nature while kayaking or hiking — typical hobbies for a western Canadian. The hiking in Chile is amazing, from hiking up to glaciers to ascending active volcanoes. Unfortunately, curling does not exist in Chile, so the large hole in my spare time has now been filled with playing tabletop games and exploring an eclectic mix of new hobbies: sculpting miniatures, learning bass guitar, and reading philosophy.

Álvaro Ribas

Like many others, I was fascinated by the night sky as a child. I remember filling up notebooks with space-related facts that I would read in books and coming up with my own (at the time, very reasonable) explanations for some of those incredible things that existed out there. However, astronomy was not the only thing that captured my attention, and I would also spend a lot of time reading about dinosaurs, or ants, or collecting rocks and minerals. I probably matched the stereotype of the kid who is always asking questions, and I am truly grateful to my parents for always fostering that curiosity.

I grew up in Salamanca, a beautiful city near Madrid with one of the oldest universities in Europe. My list of interests also grew and by the time high school was over I was quite unsure about what I wanted to study, the options extending from philosophy or literature to computer science or physics. I finally decided to go with the last of those, and I studied the first three years of the degree in physics at Universidad de Salamanca before moving to Madrid to continue with a specialisation in astrophysics at Universidad Complutense de Madrid.

My first encounter with real research came during the last year of my degree, when I had the opportunity to do a European Space Agency (ESA) traineeship at the European Space Astronomy Centre (ESAC) in Madrid. There I worked on processing and analysing far-infrared observations of protoplanetary discs from the Herschel Space Observatory. Not only did this experience get me quickly interested in planet formation, but I also immediately fell in love with scientific research and its collaborative, international environment. Getting to hear about cutting-edge science daily was a dream come true. Luckily, I was able to continue working at ESAC (testing the software used to process Herschel observations) during my master's degree, which also allowed me to continue my research projects there.

I did my PhD at ESAC with Bruno Merín and Hervé Bouy, aiming to improve our understanding of protoplanetary disc evolution. The evolution of these sources plays a key role in planet formation, but it occurs over some millions of years so it needs to be studied indirectly. During my thesis, I gathered ancillary photometry (from the ultraviolet to the mid-infrared) for a large sample of young stars in different star-forming regions and determined how many of them showed an infrared excess (produced by dust in the discs) at different ages. This information can be used to measure the typical lifetime of protoplanetary discs, which limits how much time gas-giant planets have to form. The sample was large enough that I could also break it into smaller pieces to study the impact of stellar mass on disc evolution. I also used Herschel data to characterise the outer regions of some discs with gaps, maybe carved by newborn planets. Those were some intense years, but I absolutely enjoyed them.

I defended my PhD in 2015 and continued my research as a postdoc working with Catherine Espaillat at Boston University. There I completed the spectral energy distributions of discs in the Taurus, Ophiuchus, and Chamaeleon I regions down to (sub)millimetre wavelengths, with the idea of combining them with disc models and statistics to learn more about the conditions in which planet formation takes place. However, protoplanetary discs are complex and so are their models, and computing them takes way too long for such an analysis to be feasible. This problem led me to start what has been my most challenging research project to date: using artificial neural networks to speed up and apply disc models to large samples of discs. It was also in Boston that I started working with interferometric observations while using data from the Karl G. Jansky Very Large Array (VLA) to study a circumbinary disc that has somehow survived for several million years in a quadruple system. Being used to unresolved photometry, working with data that could resolve scales of a few astronomical units in discs completely blew my mind and led me to learn more about this technique.

As an ESO/ALMA Fellow in Chile, I have the opportunity to work on my own research as well as to perform functional duties at the observatory, which has been a very unique and enriching experience for me. During my research time, I continue trying to better understand disc evolution and planet formation by combining Atacama Large Millimeter/submillimeter Array (ALMA) observations and statistics. The scientific environment in Santiago is really vibrant, not only because of the interactions at ESO, ALMA, and the many Chilean universities, but also because of the continuous flow of visitors from all over the world. On the other hand, thanks to the duties at the observatory I get to learn a lot more about interferometry and observatory operations, and even make some small contributions to those operations. Pointing the antennas to gather some precious photons feels like getting one step closer to a fascinating answer. But then, leaving the control room at night, the incredible night sky of the Atacama Desert above leaves me in absolute awe and wonder — an immediate reminder that, no matter how much we learn, there will always be many more questions to ask.

DOI: 10.18727/0722-6691/5225

In memoriam Nichi D'Amico

Filippo Maria Zerbi[1]
Adriano Fontana[2]

[1] INAF, Rome, Italy
[2] INAF – Osservatorio Astronomico di Roma, Italy

INAF

Figure 1. Nichi D'Amico during the second SKA Intergovernmental Organisation Negotiations meeting in January 2016 at the Accademia dei Lincei in Rome, Italy.

Nicolò (Nichi) D'Amico, President of the Italian National Institute for Astrophysics, passed away on 14 September 2020 at his home in Sardinia. Appointed as president of INAF in 2015, he was confirmed for a second term on December 2019, the first president to be reconfirmed in the history of this prestigious Italian institution.

Nichi was a radio-astronomer with a passion, more than an interest, for pulsars. Following a career as INAF staff, he was appointed full Professor of Astrophysics at the University of Cagliari. He directed the construction and the early operation of the Sardinia Radio Telescope (SRT), one of the largest single-dish radio telescopes in the world. He received the CSIRO Medal certificate in 1993 and the European Cartesio Prize in 2005 for the first discovery of a "double pulsar".

In his role as INAF President he boosted research in astrophysics in Italy, paying special attention to international collaborations and common research infrastructures. He represented Italy on the ESO Council during a key phase in its history, providing decisive national support to the construction of ESO's Extremely Large Telescope (ELT) and its instrumentation.

He was the head of the Italian delegation in the negotiations that led to the Square Kilometre Array (SKA) becoming an Intergovernmental Organisation and his fundamental interest in the Cherenkov Telescope Array brought the Headquarters of CTA to the INAF premises in Bologna.

CTAO

A rendering of several telescopes of the Cherenkov Telescope Array, at the southern site at ESO's Paranal Observatory in Chile. With its large collecting area and wide sky coverage, the CTA will be the largest and most sensitive array of gamma-ray telescopes in the world.

DOI: 10.18727/0722-6691/5226

Message from the Editor

Mariya Lyubenova[1]

[1] ESO

My first encounter with The Messenger was in my student years when I was given a research assignment on extremely large telescopes. To this date I vividly remember my fascination with OWL, the OverWhelmingly Large telescope that I read about in The Messenger No. 100. It is a great honour for me to be the new editor of this journal, especially now that ESO is well under way to building its Extremely Large Telescope (ELT). I take this opportunity to thank you for your patience with the delay in publishing the current volume during this transition period. I hope that this special issue — dedicated to ELT's instrumentation — will be as inspiring, in particular to our junior readers, as The Messenger No. 100 was for me.

I am looking forward to continuing the traditions of this communications channel to reach out to ESO's astronomical user community with high-quality articles, as well as to feature new content that will spark the curiosity of a broader range of professionals whose interests cross paths with ESO and astronomy. Do not hesitate to submit[1] your ideas for topical contributions showcasing the usage of ESO's various programmes and facilities.

I am indebted to my predecessor Gaitee Hussain for her guidance into the intricacies of The Messenger, as well as for steering the journal over the past three years. Gaitee has been a true role model for me and for many colleagues at ESO and beyond. As per the journal's tradition, a composite of all the cover images of The Messenger under her direction is shown on p. 59. I am wishing her all the best in her new professional endeavour at the European Space Agency.

Links

[1] Guidelines for articles in The Messenger: https://www.eso.org/sci/publications/messenger/mes-guide.html


with Ultra-Precise Photometry
spectives & A View from VMC, Gaia and Beyond
bservatory Comes of Age
pectrograph for the VLT
the Largest Main Belt Asteroids


The Messenger
No. 182 – Quarter 3 | 2020
ESPRESSO Science Verification
The VST-FLAMES Tarantula Survey
NGTS – Uncovering New Worlds with Ultra-Precise Photometry
Magellanic Clouds – Historical Perspectives & A View from VMC, Gaia and Beyond


The Messenger
No. 180 – Quarter 2 | 2020
The Chilean Telescope Array Observatory Comes of Age
HOROS – A New Multi-Object Spectrograph for the VLT
The ALPINE–ALMA [CII] Survey

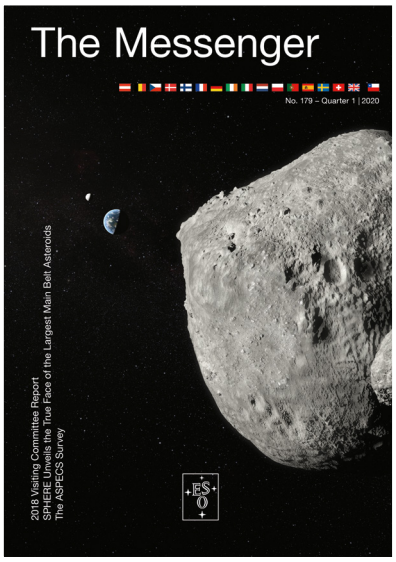
The Messenger
No. 179 – Quarter 1 | 2020
2018 Visiting Committee Report
SPHERE Unveils the True Face of the Largest Main Belt Asteroids
The ASPECS Survey


The Messenger
No. 178 – Quarter 4 | 2019
ELT M4 – The Largest Adaptive Mirror Ever Built
ALMA Observations of Galaxy Clusters
The ESO Summer Research Programme 2019

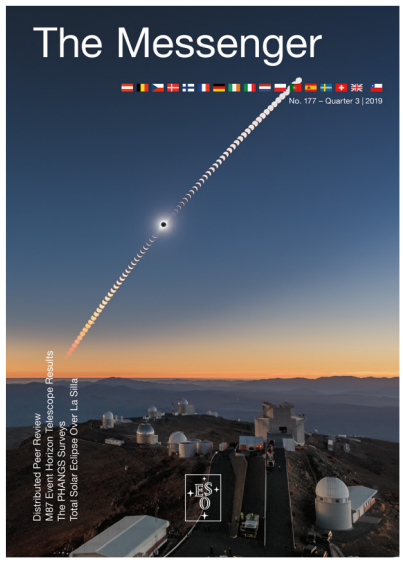
The Messenger
No. 177 – Quarter 3 | 2019
Distributed Peer Review
M87 Event Horizon Telescope Results
The PHANGS Surveys
Total Solar Eclipse Over La Silla


The Messenger
No. 176 – Quarter 2 | 2019
Astronomy in Ireland
ELT Arrives: the Secondary Mirror Becomes a Giant
ALMA Spots the Most Massive Galaxies from Cosmic Dawn to Cosmic Noon
ESO Science Ambassadors


The Messenger
No. 175 – Quarter 1 | 2019
The 4MOST Issue
Overview and Information for the Call for Proposals
Scientific Operations and Survey Strategy Plan
4MOST Consortium Surveys


The Messenger
No. 174 – December 2018
The SPECULOOS Southern Observatory
ALMA Observations of the Early Universe
The Early Growth and Life Cycle of Galaxies with KMOS3D
Riccardo Giacconi (1931–2018)


The Messenger
No. 173 – September 2018
Service Mode and Visitor Mode at Paranal
Rendezvous with Oumuamua
Massive Star Formation and Evolution in the Galactic Centre
Resolving the Interstellar Medium at the Peak of Cosmic Star Formation


The Messenger
No. 172 – June 2018
Enhanced data discovery services for the ESO Science Archive
Science Verification of HAWK-I using GRAAL adaptive optics
ALMA finds too many massive stars in starburst galaxies
Stellar surface imaging with VLTI and ALMA

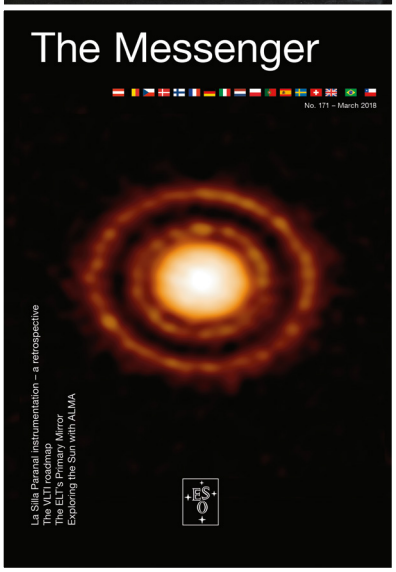
The Messenger
No. 171 – March 2018
La Silla Paranal instrumentation – a retrospective
The VLTI roadmap
The ELT's Primary Mirror
Exploring the Sun with ALMA


The Messenger
No. 170 – December 2017
Paul Hickey in Australia
First Light for GRAVITY
MUSE observes gas stripping in galaxies
Unveiling accretion in a protoplanetary system


Service Mode and Visitor
Rendezvous with Oumuam
Massive Star Formation a
Resolving the Interstellar
Enhanced data discovery
Science Verification of HA
ALMA finds too many mas
Stellar surface imaging wit
La Silla Paranal instrume
The VLTI roadmap
The ELT's Primary Mirror
Exploring the Sun with AL

Personnel Movements

Arrivals (1 October 2020–31 March 2021)

Europe

Brito, Matheus (BR)	Visiting Astronomer Travel Coordinator/ Administrative Assistant
Catricheo, Dusan (CL)	Graphic Designer
del Prado, Miguel (ES)	Software Engineer (ALMA Science Archive)
Fragkoudi, Francesca (CY)	Fellow
Ginolfi, Michele (IT)	Fellow
Greenwell, Claire (UK)	Student
Itrich, Dominika (PL)	Student (ERC-ECOGAL)
Jaworska, Jolanta (PL)	Project and Administrative Assistant
Jenkins, David (UK)	Optical Engineer/Physicist
Kolmeder, Johannes (DE)	Optical Engineer
Law, Chi Yan (CN/HK)	Student
Lotz, Linus (DE)	Software Engineer
Maimone, Maria Chiara (IT)	Student
Molyneux, Stephen (UK)	Student
Muñoz-Mateos, Juan Carlos (ES)	Media Officer
Ortega, Luis (ES)	Contract Officer
Phillips, Judith (DE)	ELT Document Controller
Relat, Marc (DE)	Budget Controller
Schmid, Sebastian (DE)	Optical Engineer
Tychoniec, Łukasz (PL)	Fellow
van der Burg, Remco (NL)	Coordinator of ELT Working Groups
Wallner, Martin (DE)	Head of Creative Team
Wiederer, Thomas (DE)	Payroll Officer

Chile

Abdul-Masih, Michael (US)	Fellow
Alcalde, Belén (ES)	Fellow
Burgos, Pablo (CL)	Software Engineer
Cikota, Aleksandar (HR)	Fellow
Ennis, Ana Inés (AR)	Student
Escorza, Ana (ES)	Fellow
González, Camilo (CL)	Student
Harrington, Kevin (US)	Fellow
Jimenez Gallardo, Ana Maria (ES)	Student
Kurowski, Sebastian (PL)	Student
Müller, Tobias (DE)	ELT AIV Project Manager
Otero, Sofía (CL)	Outreach Officer Chile
Saumann, Francisco (CL)	Deputy Head of Human Resources
Wevers, Thomas (BE)	Fellow

Departures (1 October 2020–31 March 2021)

Europe

Agliozzo, Claudia (IT)	Fellow
Aoki, Misa (JP)	Student
Engler, Byron (NZ)	Student
Kammerer, Jens (DE)	Student
Koch, Franz (DE)	Head of the Mechanical Engineering Department
Lilley, Paul (UK)	Electronics Engineer
Martocchia, Silvia (IT)	Student
Neuville, Hélène (FR)	Contract Officer
Pathak, Prashant (IN)	Fellow
Sanchis Melchor, Enrique (ES)	Student
Stanghellini, Stefano (IT)	Project Manager

Chile

Arriagada, Oriel Alberto (CL)	Electronics Engineer
Jimenez, Nestor (CL)	Telescope Instruments Operator
Kundu, Richa (IN)	Student
Le Gouellec, Valentin (FR)	Student
Montes, Vanessa (CL)	Systems Engineer
Moulane, Youssef (MA)	Student
Moya, María Angélica (CL)	Head of Human Resources Chile
Opitom, Cyrielle (BE)	Fellow
Zúñiga Fernandez, Sebastián (CL)	Student

ESO/B. Tafreshi (twanight.org)

This panorama shows a stunning wash of colour sweeping across the evening sky above the Chajnantor Plateau in northern Chile. Together, the bright Moon and crimson clouds look down upon the 66 antennas of the Atacama Large Millimeter/submillimeter Array (ALMA).

Annual Index 2020 (Nos. 179–181)

Subject Index

Author Index

ESO/Gerhard Hüdepohl (atacamaphoto.com)

As dusk descends on ESO's Paranal Observatory, the four Unit Telescopes that comprise the Very Large Telescope (VLT) shine brightly, taking in the last rays of sunlight as they prepare for the night of work ahead.

ESO's benefits to society in the Member States

From spurring innovation to pushing the boundaries of knowledge, ESO contributes to a better society. Its impact can be measured in five key areas: science and engineering, economy and innovation, talent development, education and outreach, international collaboration and policy. Scan the QR code below to find out more about ESO's impact on society in its Member States.

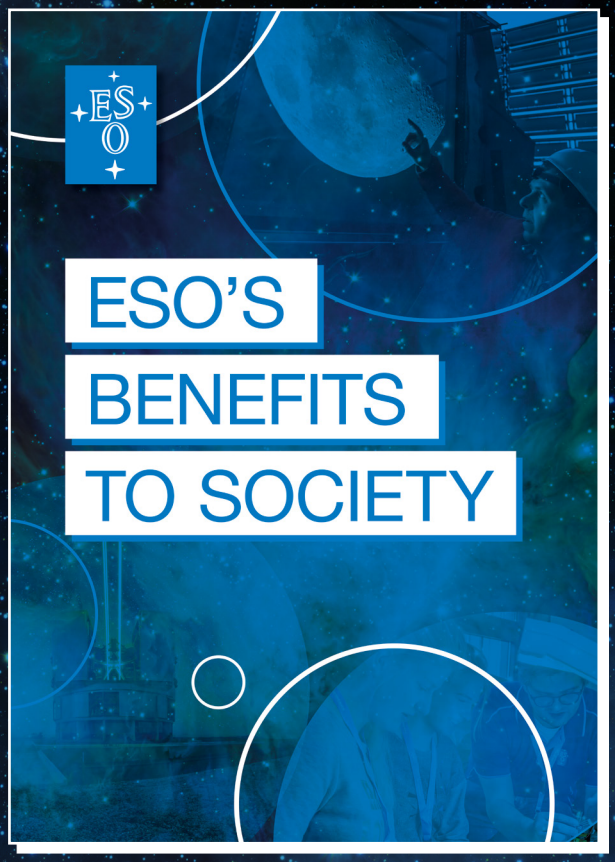

How does ESO impact society?

ESO's benefits to society in the host country Chile

ESO's cooperation with Chile, which hosts the organisation's observatories, started about 60 years ago. During this time, ESO has strongly supported the training of new generations of Chilean astronomers and engineers. This collaboration has also generated commercial opportunities in Chile and enhanced local development. Scan the QR code below to read (in Spanish) about ESO's impact in Chile. An English version will become available via the same link.